LINDSAY A. BROADFIELD

PHD

METFORMIN AND COLORECTAL CANCER

THE EFFECTS OF METFORMIN ON COLORECTAL CANCER GROWTH AND THE INVOLVEMENT OF THE GUT MICROBIOME

By LINDSAY A BROADFIELD, BHSc, MSc.

A Thesis Submitted to the School of Graduate Studies
in Partial Fulfillment of the Requirements
for the Degree of Doctor of Philosophy

McMaster University DOCTOR OF PHILOSOPHY (2018) Hamilton, Ontario (Medical Science)

TITLE: The effects of metformin on colorectal cancer growth and the involvement of the gut microbiome

AUTHOR: Lindsay A. Broadfield, BHSc, MSc

SUPERVISOR: Professor G. R. Steinberg

NUMBER OF PAGES: 238

LAY ABSTRACT

Metformin is the most commonly used type 2 diabetes therapy, and may also reduce colorectal cancer growth. Anti-cancer effects may be caused by: 1) decreased glucose and insulin levels, which support cancer growth; or 2) entry into cancer cells to directly decrease cell growth. The gut microbiome, microorganisms that live symbiotically in the gastrointestinal tract, is also affected by metformin. This thesis aimed to clarify how metformin can inhibit cancer, and if the microbiome is involved. Mice treated with metformin had improved glucose metabolism and decreased colorectal tumor growth; when an antibiotic was introduced, this effect was lost. A fecal microbiome transfer model was used to determine if the microbiome is driving this effect. Mice receiving feces from metformin treated mice also experienced tumor growth inhibition. This suggests that the gut microbiome is involved in the anti-cancer effects of metformin, and is a new potential mechanism of action.

ABSTRACT

Metformin is the most common type 2 diabetes therapy, and may also reduce colorectal cancer growth. Currently, two mechanisms driving reduced cancer growth are considered: 1) Regulation of glucose and insulin levels, which may support cancer growth, and 2) Direct entry into cancer cells to activate the AMP-activated kinase (AMPK) protein, and inhibit cell growth pathways. The gut microbiome is the community of commensal microorganisms in the gastrointestinal tract. It is also affected by metformin, and may elevate production of short-chain fatty acids (SCFAs). Therefore, this thesis aimed to clarify how metformin may inhibit colorectal cancer growth and if the microbiome is involved. The hyperglycemic-responsive, murine-derived MC38 colon cancer cell line was used to test these effects. This model was confirmed to experience growth stimulation caused by high-fat diet (HFD) feeding in mice. Daily i.p. injections of metformin (100mg/kg) had no measurable effect on glucose and insulin sensitivity, or MC38 tumor growth. Oral metformin (250mg/kg) improved glucose tolerance and inhibited MC38 tumor growth in HFD-fed mice. To see if the gut microbiome is required for this effect, the antibiotic ampicillin was used to limit the gut microbiome. The addition of ampicillin blunted metformin's glucose sensitization and tumor inhibition effects. A fecal microbiome transfer model was then used to isolate the role of the microbiome. Conventional mice fed HFD and gavaged with feces from metformin-treated donors experienced no glucose or insulin tolerance improvements. However, tumor growth was decreased by 30%,

and serum SCFAs concentrations were elevated. The SCFA butyrate inhibited *in vitro* MC38 colony growth, but did not activate AMPK. These data suggest that metformin alters the gut microbiome, and fecal transfer from metformin-treated animals can uncouple MC38 tumor growth inhibition from the glucose homeostasis effects of metformin. These novel findings support a new mechanism for metformin to prevent cancer growth and development.

ACKNOWLEDGEMENTS

They say it takes a village to raise a child, and this is also true for graduate students. This thesis would not have been possible without the continued support and encouragement from many people who have surrounded me in the last several years.

First, to my advisor Dr. Greg Steinberg, I thank you for the opportunity to join your lab, as I have learned far more from you and the others you have brought together, than I had ever expected. To Dr. Theos Tsakiridis, my committee member, thank you for your passion for research, for providing key clinical insights, and for allowing me to work on interesting and unique projects outside of my thesis work. To Dr. Paola Muti, my committee member, I thank you for your knowledge on clinical and population based work, for our scientific discussions and musings, and for always being a source of positivity.

To all of the members of the Steinberg lab, both past and present, and my friends outside of our lab: thank you for providing me with a school family; for all the help, advice, discussion, and laughter throughout the years. Working with you all has been one of the greatest pleasures throughout this journey.

To my mother and brother, thank you for your unwavering support throughout all of my education. Your patience and encouragement has, and continues to go a long way.

To Kevin, my husband, you have been my pillar throughout this whole journey. Thank you for supporting me, for learning what a Western blot is and why they have caused me so much frustration, and for never doubting my abilities. Words can't describe how lucky and grateful I am to be your partner, and I can't wait to see what our future holds.

Lastly, this thesis is dedicated to my father, Larry Broadfield. Losing you to the disease that I studied in my PhD, while completing the degree, was the hardest thing I have experienced. I know you always wanted to do a Doctorate and never had the chance. This is for you, dad.

TABLE OF CONTENTS

LIST OF FIGURES

LIST OF TABLES

LIST OF ABBREVIATIONS

ACC: acetyl-CoA carboxylase
ACF: aberrant crypt foci
ACLY: ATP citrate lyase
APC: *adenomatous polyposis coli*
Ato: or butyryl-CoA:acetoacetate-CoA transferase
Buk: butyrate kinase
But: butyryl-CoA:aceteate-CoA transferase
CaMKK: calcium/calmodulin-dependent kinase kinase
cAMP: cyclic AMP
CIMP: CpG island methylator phenotype
CIP: chromosomal instability pathway
CPT-1: carnitine palmitoyltransferase-1
CRC: colorectal cancer
CTP: citrate transport protein
ETC: eletron transport chain
FA: fatty acids
FAP: familial adenomatous polyposis
FAS: fatty acid synthase
FFA: free fatty acids
FFA2: free fatty acid receptor 2
FFA3: free fatty acid receptor 3
FMT: fecal microbiome transfer
FOXO1: forkhead box 01
G6Pase: glucose-6-phosphatase
GF: germ-free
GLP-1: glucacon-like peptide 1
GMB: gut microbiome
GSIS: glucose stimulated insulin secretion
GSK3: glycogen synthesis kinase-3
GTT: glucose tolerance test
HbAIc: hemoglobin A1c
HDAC: histone deacetylase
HFD: high-fat diet
HK: hexokinase
HIF-1: hypoxia induced factor-1
HMG-CoA: β-Hydroxy β-methylglutaryl-CoA
HMGR: HMG-CoA Reductase
IBD: inflammatory bowel disease
IBS: irritable bowel syndrome
IGF-1: insulin-like growth factor-1
IR: insulin resistance
IRS: insulin receptor substrates

ITT: insulin tolerance test
LDA: linear discriminate analysis
LKB1: Liver kinase B1
LPS: lipopolysaccharide
LXR: liver X receptor
MSI: microsatellite instability pathway
mTOR: mammalian target of rapamycin
mTORC2: mTOR complex 2
mTORC1: mTOR complex 1
NAFLD: non-alcoholic fatty liver disease
OCT: organic cation transporter
OXPHOS: oxidative phosphorylation
PDC: pyruvate dehydrogenase complex
PDK1: phosphoinositide-dependent protein kinase 1
PEPCK: phosphenolpyruvate carboxykinase
PGC-1α: Peroxisome proliferator-activated receptor gamma coactivator 1-alpha
PI3K: phosphoinositide-3 kinase
PIP2: phosphatidylinositol-4,5-bisphosphate
PIP3: produce phosphatidylinositol-3,4,5-trisphosphte
PKA: protein kinase A
PKC: protein kinase C
PMAT: plasma membrane monoamine transporter
PRAS40: proline-rich Akt substrate 40
RCT: randomized control trial
REDD: Regulated in development and DNA damage response
SREBP: sterol regulatory binding protein
T2D: type 2 diabetes
TAG: triacylglycerol
TG: triglycerides
TSC2: tuberous sclerosis complex 2
VEGF: vascular endothelial growth factor

DECLARATION OF ACADEMIC ACHIEVEMENT

Contributions to concepts and design of research: Lindsay A. Broadfield, Gregory R. Steinberg, Theos Tsakiridis, Paola Muti.

Contributions to technical assistance of experiments and analysis: Lindsay A. Broadfield, Amna Saigal, Jake C Szamosi.

Contributions to data interpretation: Lindsay A. Broadfield, Gregory R. Steinberg, Theos Tsakiridis, Paola Muti, Amna Saigal, Jake C Szamosi.

LIST OF PUBLICATIONS

Broadfield LA, Marcinko K, Tsakiridis E, Zacharidis PG, Villani L, Lally JSV, Menjolian G, Maharaj D, Mathurin T, Smoke M, Farrell T, Muti P, Steinberg GR and Tsakiridis T. Salicylate enhances the response of prostate cancer to radiotherapy. Prostate Cancer and Prostatic Disease. September 2018. *In submission.*

Lally JSV, Ghoshal S, DePeralta DK, Moaven O, Wei L, Masia R, Erstad DJ, Fujiwara N, Leong V, Houde VP, Anagnostopoulos AE, Wang A, **Broadfield LA**, Ford RJ, Foster RA, Bates J, Sun H, Wang T, Liu H, Ray AS, Saha AK, Greenwood J, Bhat S, Harriman G, Miao W, Rocnik JL, Westlin WF, Muti P, Tsakiridis T, Harwood HJJ, Kapeller R, Hoshida Y, Tanabe KK, Steinberg GR, Fuchs BC. Inhibition of Acetyl-CoA Carboxylase by Phosphorylation or the Inhibitor ND-654 Suppresses Lipogenesis and Hepatocellular Carcinoma. Cell Metabolism. September 20 2018. *E-pub ahead of print*.

Troncone M, Cargnelli SM, Villani LA, Isfahanian N, **Broadfield LA**, Zychla L, Wright J, Pond G, Steinberg GR, and Tsakiridis T. Targeting metabolism and AMP-activated kinase with metformin to sensitize non-small cell lung cancer (NSCLC) to cytotoxic therapy; translational biology and rationale for current clinical trials. Oncotarget. 2017; 8:57733-57754

Villani LA, Smith BK, Marcinko K, Ford RJ, **Broadfield LA**, Green AE, Houde VP, Muti P, Tsakiridis T, Steinberg GR. The diabetes medication Canagliflozin reduces cancer cell proliferation by inhibiting mitochondrial complex-I supported respiration. Molecular Metabolism. 2016; 5:1048-1056

O'Brien AJ, Villani LA, **Broadfield LA**, Houde VP, Galic S, Blandino G, Kemp BE, Tsakiridis T, Muti P, Steinberg GR. Salicylate activates AMPK and synergizes with metformin to reduce the survival of prostate and lung cancer cells *ex vivo* through inhibition of *de novo* lipogenesis. Biochemical Journal. 2015; 469(2):177-187

CHAPTER 1: LITERATURE REVIEW

1.1. Diabetes and Colon Cancer

1.1.1 Diabetes Epidemiology

Type 2 Diabetes (T2D) is one of the greatest health burdens facing the human population. It is characterized by chronically elevated fasting blood glucose (hyperglycaemia) and the gradual desensitization of the insulin-sensitive tissues to insulin signaling, resulting in elevated circulating insulin (hyperinsulinemia). In 2013, 382 million people were living with T2D (Guariguata et al., 2014). In 2035, that number is estimated to climb to almost 600 million people living with T2D globally (Guariguata et al., 2014). In Canada, 7% of Canadians over the age of 12 (2.1 million) were diagnosed with diabetes in 2016, and 22% of the Canadian adult population has pre-diabetes (Government of Canada, 2011; Statistics Canada, 2017). It is also the 7th leading cause of mortality in Canadians, with 1 in 10 deaths of adults on 2008/9 being attributed to diabetes-related comorbidities (Statistics Canada, 2015). These statistics are also reflected by the economic burden that this disease has on the Canadian health care system. By 2022, it is estimated that diabetes will cost the Canadian government over $15 billion in overall healthcare costs related to diabetes (Bilandzic & Rosella, 2017).

1.1.2 Diabetes Pathophysiology and Comorbidities

The World Health Organization defines diabetes as a maintained fasted plasma glucose level of $\geq$ 7.0mmol/L, or 2-hour plasma blood glucose level of

≥ 11.0mmol/L (WHO, 2006). It is a complex, multi-organ disease that develops over time, primarily due to the dysregulation of responses to the hormone insulin. In T2D, insulin-responsive tissues - the liver, skeletal muscle, and adipose tissue - develop insensitivity to insulin, resulting in elevated insulin production to maintain glucose homeostasis (Kahn, Cooper, & Del Prato, 2014). With insulin resistance (IR), elevated hepatic glucose production and decreased glucose uptake by skeletal muscle and adipose tissue work in tandem to promote the hyperglycaemic environment (Fig1.1). As the disease progresses, the pancreatic β-cells that produce insulin eventually decrease insulin output. In 2009, Ralph DeFonzo elaborated on more tissues and organs involved in T2D pathogenesis. He defined the "ominous octet", a list of 8 contributing factors expanded to include: increased glucagon (a hormone with opposing actions to insulin) secretion from pancreatic α-cells, decreased incretin effect, increased lipolysis, increased renal glucose resorption, and the dysregulation of neurotransmitter signaling in the brain (DeFronzo, 2009). This wide range of effects across tissues and organ systems result in a multi-faceted disease that is associated with multiple co-morbidities and complications.

Obesity, another disease with an enormous global burden, is associated with the development of T2D, and is considered a co-morbidity. Estimates suggest that up to 90% of T2D cases are related to elevated weight, and body mass index (BMI, measured as weight (kg) divided by height (m) squared)

(Hossain, Kawar, & El Nahas, 2007). The involvement of body weight on T2D development and pathology is well established, and is the reason why first-line treatment strategies for T2D include lifestyle modifications for weight management (Dorsey & Becker, 2018). Obesity is also associated with elevated circulating free fatty acids (FFA) and triglycerides (TG), which are involved in T2D pathogenesis (discussed in more detail in section 3.2) (Baldeweg et al., 2000). With global rates of obesity increasing and the entanglement of obesity and T2D pathophysiology, T2D rates are also expected to continue rising.

In addition to obesity, other co-morbidities and elevated risk factors for additional complications are associated with T2D. Forty percent of people with T2D have three or more chronic co-morbidities (Lin, Kent, Winn, Cohen, & Neumann, 2015). A recent retrospective analysis identified hyperlipidemia as the most commonly associated condition with T2D, followed by hypertension, obesity, coronary artery disease, chronic obstructive pulmonary disease and chronic kidney disease (Lin et al., 2015). In addition to these diseases the concept of diabetes and cancer being associated have long been noted, with publications discussing the possibility as early as 1934 (Marble, 1934). In 2010, a consensus statement on diabetes and cancer was written and released by experts in both the American Diabetes Association and the American Cancer Society (Giovannucci et al., 2010). It has been identified that T2D and cancer risk is site-specific, with the strongest associations in liver, pancreas, and endometrial cancer (Giovannucci et

al., 2010). Colorectal, breast, and bladder cancer are also positively associated with T2D, though to a lesser degree. T2D and CRC have several common risk factors, including increased age, obesity, smoking, alcohol consumption, and lack of physical activity. In 2005, a meta-analysis of 15 studies showed the presence of T2D increased relative risk of CRC in men and women, with no changes in association due to sex (RR=1.30, 95% CI=1.2-1.4) (Larsson, Orsini, & Wolk, 2005). Results were consistent among studies in North America and Europe, and found diabetes was positively correlated with CRC mortality. The association between T2D and CRC risk was confirmed in updated meta-analyses in 2011 and 2017 (González et al., 2017; Jiang et al., 2011). The most recent update by Gonzalez *et al*. (2017) found CRC risk was estimated to be 27% higher in those with T2D. The data consistency at population level requires a deeper understanding of the pathophysiological and metabolic etiological connection between T2D and subsequent onset of CRC.

1.1.3 Colorectal Cancer Epidemiology and Pathophysiology

Colorectal cancer (CRC) is third most common cancer among men around the world, and accounted for 10% (1.3 million) of all cancer cases globally in 2012 (GLOBOCAN, 2012; Stewart & Wild, 2014). It is also the fourth most common cause of cancer-related deaths in the world (GLOBOCAN 2012, 2018). Higher rates of CRC are seen in developed and highly developed countries, with

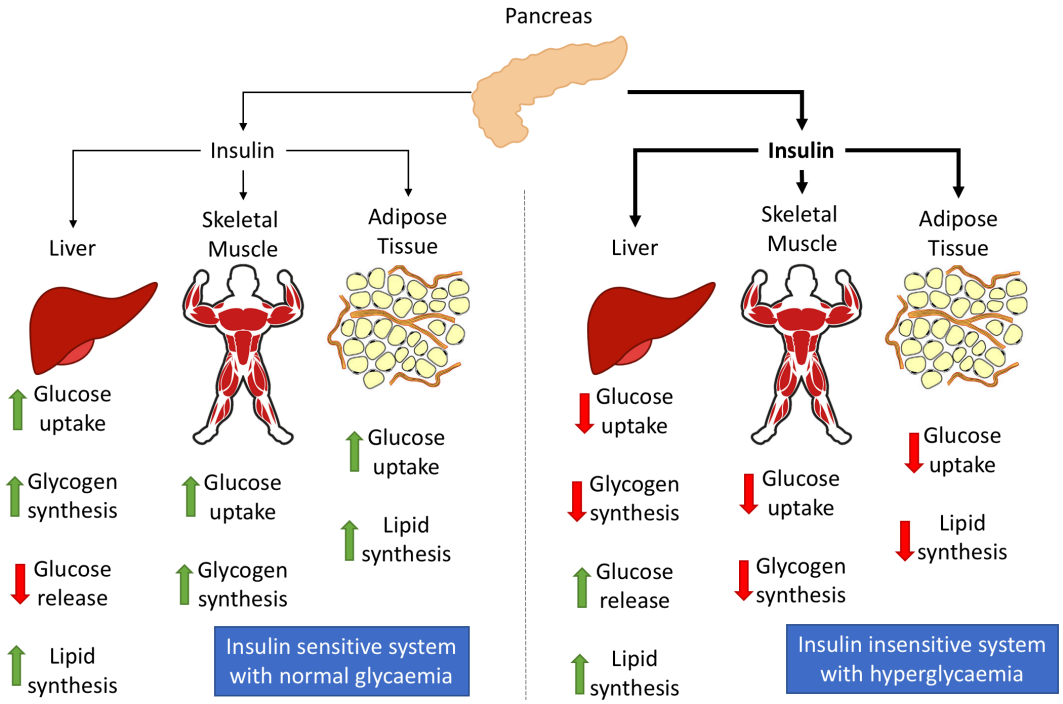

Figure 1.1: Changes in insulin-sensitive tissues with and without insulin resistance.

Insulin is released from the pancreas in response to feeding. In an insulin-sensitive system, this results in glucose uptake into liver, skeletal muscle, and adipose tissue. Glucose is modified to be stored as either glycogen or converted into lipids. In an insulin-insensitive system, liver, muscle and adipose have decreased responsiveness to insulin signaling. This results in decreased glucose uptake and storage in all tissues. In liver, hepatic lipid accumulation contributes to decreased insulin signaling, and further enhances lipid production and storage, and increases hepatic glucose output.

increasing rates in developing countries as populations move towards the consumption of a "Western diet" (Brenner, Kloor, & Pox, 2014). CRC is also the third most common cancer in Canada, and is increasing over time (Ellison & Wilkins, 2012). In 2017, an estimated 16,800 cases were diagnosed, and CRC represents 13% of all cancer cases in Canada (Canadian Cancer Society's Advisory Committee on Cancer Statistics, 2017). It is responsible for 12-13% of all cancer-related deaths among Canadian men and women, with a 64% 5-year survival rate (Canadian Cancer Society's Advisory Committee on Cancer Statistics, 2017).

CRC development was classically described stepwise progression that is clearly defined with activating and inactivating mutations of key genes throughout the adenoma-carcinoma sequence. Normal mucosa changes to have abnormal crypt architecture and morphology, then progresses to low- and high-grade adenomas, and eventually carcinoma and metastatic disease. This process can take a decade to occur, with early mutations in *APC*, and progression through the sequence supported by activating mutations in *KRAS* and inactivating mutations in *TP53* (Cunningham et al., 2010). However, with the advance of genomic sequencing technologies and an increasing understanding of genetic aberrations in carcinogenesis, several alternate pathways have been identified for CRC progression. In a systematic review by Lee *et al.* (2015), three main pathways of genetic mutations are presented as the main mechanisms of CRC development:

the suppressor pathway (classic description of mutations in tumor suppressors and oncogenes; also called the chromosomal instability pathway, CIP), the serrated pathway (also called the CpG island methylator phenotype, CIMP), and the Lynch syndrome pathway (germline mutations in mismatch repair genes; also called the microsatellite instability pathway, MSI). In addition to genetic differences, location of tumor development is important, with differences in genetic landscape and clinical presentation between right/ascending and left/descending CRC tumors (Lee et al., 2015). CRC development in the right ascending colon is associated with poorer survival, larger tumor size, and is driven by genetic and chromosomal instability. Conversely, left descending CRC is associated with familial adenomatous polyposis (FAP), has better survival rates, and smaller tumor sizes (Merlano, Granetto, Fea, Ricci, & Garrone, 2017).

1.1.4 Colorectal Cancer Risk Factors

Several risk factors have been identified for CRC. It occurs more in men, and being male is a risk factor for development. While sporadic formation is most common, familial history of CRC increases risk, with positive first-degree relatives causing the greatest impact on future risk of developing the disease (Taylor, Burt, Williams, Haug, & Cannon-Albright, 2010). In a large twin-study, heritable factors were found to attribute to 35% of risk for developing CRC, and is one of only 3 cancers in the study found to have strong heritability (Lichtenstein et al., 2000). Heritable mutations have been identified, the first being the

adenomatous polyposis coli (APC) gene, the driver gene causing FAP, which can be a precursor to CRC development. In total, 14 genes have been identified as drivers of heritable CRC syndromes, including *KRAS, PTEN, TP53,* and *STK11* (encoding liver kinase B1 (LKB1)) (Peters, Bien, & Zubair, 2016). Inflammatory bowel disease (IBD; including ulcerative colitis and Crohn's disease) is a known risk factor, with increasing risk as disease duration increases (Vetrano & Danese, 2013). IBD shares genetic abnormalities with CRC, including *KRAS* and *TP53*, and results in poorly differentiated tumors (Du, Kim, Shen, Chen, & Dai, 2017; Reynolds, O'Toole, Deasy, McNamara, & Burke, 2017). However, a recent meta-analysis of 81 studies over a wide range of time and geographical locations suggests that CRC incidence in IBD patients is decreasing (Castaño-Milla, Chaparro, & Gisbert, 2014). Non-heritable risk factors are primarily lifestyle-driven, including smoking, consumption of red and processed meats, and high alcohol intake (Chan et al., 2011; Fedirko et al., 2011; Liang, Chen, & Giovannucci, 2009). The presence of obesity and high abdominal adiposity are also associated with elevated CRC risk, and are also driven by lifestyle factors, including diet and physical activity (Dong et al., 2017; Ma et al., 2013). Specifically, a meta-analysis of 21 studies has found that the risk of CRC is reduced by 25% in the most physically active people compared to the least physically active people (Boyle, Keegel, Bull, Heyworth, & Fritschi, 2012). In a recent update of the World Cancer Research Fund's report on diet, nutrition, physical activity and CRC, consumption of whole grains, dietary fiber, dairy

products, and calcium supplements were also found to have strong evidence supporting a reduction in CRC risk (World Cancer Research Fund/American Institute for Cancer Research, 2018). Importantly, these risk factors for CRC closely overlap with those for T2D, suggesting there may be strong associations between disease development and pathologies. One potential mechanism that is continually under investigation is the link between hyperinsulinemia, insulin-like growth factors (IGF) and CRC development (Giovannucci, 2001; M. Pollak, 2012).

1.1.5 Insulin Signaling Pathway

The normal physiological action of insulin is to respond to feeding, with the intent to store energy. It accomplishes this by increasing glucose uptake into liver, skeletal muscle, and adipose tissue. In these tissues, glucose is then stored as either glycogen or triglycerides (TGs). Insulin and the insulin-like growth factor-1 (IGF-1) achieve this through a complex signaling cascade involving several kinases and phosphorylation events. This is initiated by binding to their receptors, the insulin receptor, and IGF-1 receptor. These receptors are tetrameric tyrosine kinase class receptors, with varying subunit isoforms and distribution across tissues, and the ability to form insulin and IGF-1 hybrid receptors (Boucher, Kleinridders, & Kahn, 2014; Siddle, 2011). When insulin or IGF-1 binds, the receptor undergoes conformational change to activate insulin receptor substrates (IRS) within the cell, to then stimulate downstream actions that result in activation

of the P13K-Akt pathway (Fig. 1.2). IRS is an adaptor protein that recruits phosphatidylinositol-3 kinase (PI3K) to the membrane (Copps & White, 2012). This results in phosphorylation of phosphatidylinositol-4,5-bisphosphate (PIP2) to produce phosphatidylinositol-3,4,5-trisphosphte (PIP3), activating 3-phosphoinositide-dependent protein kinase 1 (PDK1) (Alessi et al., 1997). PDK1 recruits Akt to the cell membrane and activates it via phosphorylation at the T308 residue (Vadlakonda, Dash, Pasupuleti, Anil Kumar, & Reddanna, 2013). PI3K activation also results in Akt phosphorylation at the S473 residue via mammalian target of rapamycin (mTOR) complex 2 (mTORC2) phosphorylation and activation (Gan, Wang, Su, & Wu, 2011; Vadlakonda et al., 2013). Activation of the P13K-Akt pathway results in elevated glucose transport (ie. GLUT4 translocation in skeletal muscle) and glycogen synthesis (via glycogen synthesis kinase-3, GSK3), increased protein synthesis through mTOR complex 1 (mTORC1) activation, and elevated lipid synthesis (via SREBP1) (Boucher et al., 2014). While these signaling cascades have normal physiological functions to store excess energy, they are also pathways commonly involved in the growth and promotion of cancer cells.

The role of insulin and IGF-1 signaling in cancer has been an area of great interest, to try and understand the link between diabetes and elevated cancer risk.

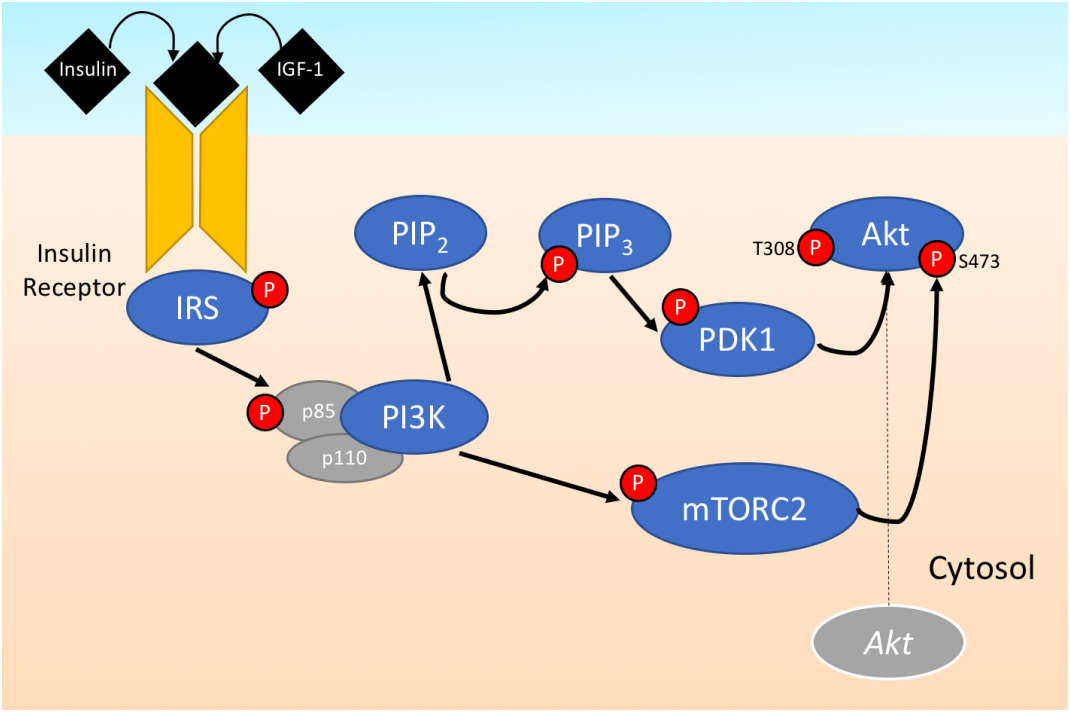

Figure 1.2: Insulin signaling cascade

Insulin or the insulin-like growth factor (IGF-1) bind to their receptor, and activate insulin receptor substrates (IRS) that start the downstream pathways. PI3K is activated by phosphorylation of the p85 subunit, stimulating PIP2 to PIP3 phosphorylation. PIP3 activates 3-phosphoinositide-dependent protein kinase 1 (PDK1), which phosphorylates and sequesters Akt to the plasma membrane, and activates it at the T308 residue. Additionally, PI3K activates mTORC2, which phosphorylates Akt at S473.

Expression of the insulin receptor and IGF-1 receptor have been found in human CRC and immortalized CRC cell lines (Pollak, Perdue, Margolese, Baer, & Richard, 1987; Watkins, Lewis, & Levine, 1990). Additionally, insulin treatment of CRC cells resulted in growth stimulation across a panel of different cell lines from human and mouse sources (Koenuma, Yamori, & Tsuruo, 1989; Watkins et

al., 1990). This was associated with elevated DNA synthesis, and CRC cells with higher metastatic potential had a greater response to insulin than less aggressive cells (Koenuma et al., 1989). The growth stimulatory effect of insulin on pre-clinical models of CRC have also been observed, with insulin and an insulin analog (X10) enhancing CRC allograft growth in mice (Hvid et al., 2012). Insulin has been suggested to also support cancer growth and progression with the finding that it resulted in elevated vascular endothelial growth factor (VEGF), an important factor in angiogenesis and developing blood flow to a growing mass (Warren, Yuan, Matli, Ferrara, & Donner, 1996). Additionally, activation of the insulin signaling pathway was suggested to stimulate the expression of proto-oncogene protein expression in intestinal cells, and that PI3K inhibition prevented these pro-tumorigenic effects (Sun & Jin, 2008). This evidence supports the theory that elevated insulin levels present in T2D can contribute to a pro-growth environment for mutated colon cells to support their proliferation, and progression to carcinoma. However, this may not always be the case. In a large-scale RCT conducted by the ORIGIN trial group, it was found that insulin treatments had no impact on cancer incidence, death from cancer, or cancer at any specific sites, contradicting earlier observational findings that insulin levels and insulin-based therapies increased cancer incidence (The ORIGIN Trial, 2012). Therefore, the role of insulin and CRC growth and development remains murky, and an active area of research.

1.1.6 Metformin Use for T2D Treatment

Metformin is a biguanide isolated from the French lilac plant, *Galega officinalis* (Graham et al., 2011). It is the world's leading T2D therapy, and is part of first line treatment along with lifestyle interventions, as recommended by the American Diabetes Association Standards of Medical Care in Diabetes (2018 version) (Dorsey & Becker, 2018; Maruthur et al., 2016). In patients with T2D, metformin treatment improves measurements of long-term glycaemia (measured by hemoglobin A1C levels), circulating insulin levels, body weight, and even some cardiovascular risk factors (Inzucchi et al., 2015; UKPDS, 1998). Importantly, metformin is well tolerated, effective, and relatively inexpensive compared to newer generation diabetes medications (Inzucchi et al., 2015). Negative side effects associated with metformin treatment are primarily gastrointestinal based, including abdominal discomfort and pain, nausea, vomiting, and diarrhea (Ali & Fonseca, 2012). However, the rates of metformin discontinuation are reportedly quite low, with only 2-3% of patients halting treatment after the first week on immediate-release metformin (Schwartz et al., 2006). Many of these side effects are mitigated with the use of slow- or extended-release formulations. A more serious potential side effect of metformin treatment is the development of lactic acidosis, however this is likely only to occur in critically ill patients that have impaired renal function (Lalau, Arnouts, Sharif, & De Broe, 2015). Ultimately, oral metformin is the first-line antidiabetic therapy prescribed by physicians, with over 80% of patients with T2D being prescribed

metformin in 2013, an increase of almost 30% from the year 2000 (Dorsey & Becker, 2018; Sharma, Nazareth, & Petersen, 2016).

1.1.7 Metformin and Colorectal Cancer

In 2005, Evans and colleagues published the first observational study suggesting metformin may prevent cancer risk (Evans, Donnelly, Emslie-Smith, Alessi, & Morris, 2005). Over the last decade, many studies have been published to further assess metformin's impact on cancer risk, incidence, and mortality rates. Initially positive results were reported in several retrospective analyses, where metformin acted to reduce risk of cancer in specific sites, including CRC and pancreatic cancer, while suggesting insulin or sulfonylurea based therapies increase cancer risk (Currie, Poole, & Gale, 2009; Franciosi et al., 2013; Yang, Hennessy, & Lewis, 2004; Zhang et al., 2011). In a 2013 meta-analysis of 12 observational studies looking at metformin and CRC risk, metformin exposure was associated with a significantly reduced risk (17% lower overall risk or CRC development) (Franciosi et al., 2013). However, when translated to clinical trials, metformin has failed to provide such positive benefits. In several meta-analyses addressing the effects of metformin on cancer, randomized control trials (RCT) showed no impact of metformin on cancer risk or mortality (Franciosi et al., 2013; Thakkar, Aronis, Vamvini, Shields, & Mantzoros, 2013). It is important to note the criticism provided by Suissa and Azoulay (2012) that several retrospective analyses were found to have time-related biases that are possibly painting an

exaggerated positive image of metformin on cancer incidence (Suissa & Azoulay, 2012). When these biases, as well as BMI, were taken into consideration by Gandini *et al*. (2014), positive effects of metformin on cancer incidence were still present, but with a decreased magnitude as previously suggested (Gandini et al., 2014). In a more recent study using a time-varying approach (accounting for duration of metformin exposure), metformin was found to have no effect on CRC or other gastrointestinal cancer risk (De Jong et al., 2017). However, in contrast to this retrospective data, a small RCT on metformin in non-diabetic patients with aberrant crypt foci (ACF), small gastrointestinal lesions that can progress to CRC, metformin exposure was found to decrease average ACF numbers after one month (Hosono, Endo, Takahashi, Sugiyama, Uchiyama, et al., 2010). This study suggests that metformin's impacts on CRC development may take place during early tumorigenesis stages, and not when initiating mutations have already occurred. CRC is typically a slow-growing cancer, and can take five-to-ten years to develop (Simon, 2016). Therefore, clarifying this time-related effect by controlling the point of exposure to metformin at specific stages in carcinogenesis are unlikely to be captured in clinical trials. Collectively, the current data suggest that metformin may have positive effects on preventing CRC, however more robust and long-term RCT will be required to clarify this effect.

1.2. Mechanisms of Metformin action in CRC

Mechanistically, it is not well understood how metformin inhibits CRC growth and development. Currently, two main theories have been posed: 1) metabolic improvements (restoring glycaemia and circulating insulin levels) to reduce a pro-CRC growth environment (systemic/indirect metformin effects), or 2) metformin can directly enter cancer cells, activate the AMP activated protein kinase (AMPK) and inhibit cell growth and proliferation through downstream signaling cascades (direct metformin effects) (Fig. 1.3**)**. Understanding how metformin acts as an anti-cancer agent, and in what metabolic and physiological conditions determine its function is important to understand what patient populations could benefit from metformin treatment, and continues to be an active area of current research and is the focus of the following section.

1.2.1 Metformin Pharmacokinetics

To understand the mechanisms by which metformin may exert positive effects in CRC, it is first vital to understand the pharmacokinetics of the drug. Metformin oral bioavailability is 50-60%, and can be affected by the fed state (Graham et al., 2011; Tucker et al., 1981). Importantly, high-fat and high-caloric food consumption prior to metformin treatment was found to decrease bioavailability by almost 25% (Sambol et al., 1996). In healthy humans, intravenous administration of metformin resulted in rapid uptake and excretion, with quick accumulation of radio-labelled ^{11}C-metformin in the kidneys, ureters,

and bladder (Gormsen et al., 2016). Liver tissue also accumulated metformin rapidly after injection, with decreasing concentration over time. Conversely, oral administration of ^{11}C-metformin first accumulated in the small intestine, and within 10 minutes became present in the bladder (indicative of excretion), with liver accumulation increasing over time (>50 minutes) (Gormsen et al., 2016). Tucker *et al*. (1981) provided data on the peak concentrations of an oral dose of immediate-release metformin, with a 1.5g dose (a typical clinical dose) resulting in plasma concentrations of 3mg/L (~20μM assuming average adult blood volume of 5L) (Tucker et al., 1981).

In the context of pre-clinical studies on metformin and cancer growth, method of administration is not isolated to oral routes, and rarely mimics dosing regimens used in clinical care. In pre-clinical rodent studies, the effects of metformin on various cancer models has primarily involved the delivery of the drug via acute oral (via oral gavage), continuous oral (via dosed drinking water), and acute systemic (intraperitoneal or intravenous injections) methods. This can complicate study-to-study comparison, as tissue distribution and accumulation can change based on method of administration. A handful of studies have been done to look at the variation in metformin tissue distribution between intraperitoneal (i.p.) injection and oral metformin dosing via drinking water. These two methods offer very different tissue exposure to metformin, with i.p. injections causing a

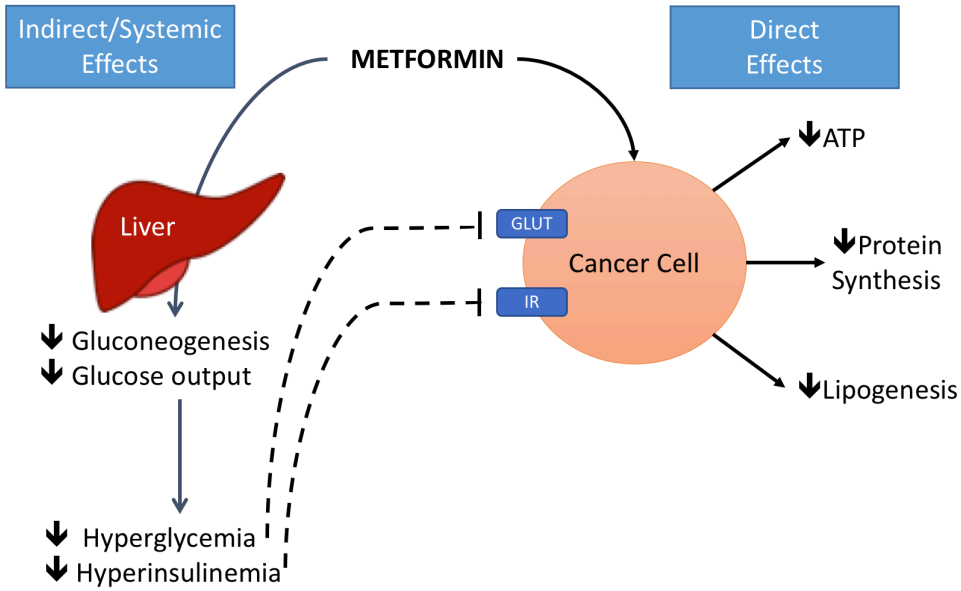

Figure 1.3: Indirect and Direct potential mechanisms of metformin action on CRC

Metformin is proposed to inhibit cancer through two potential mechanisms. Systemic mechanisms involve metformin treating T2D, and normalizing glucose homeostasis and serum insulin levels. This is thought to inhibit cancer cell growth by decreasing glucose available for uptake, and insulin, decreasing pathways involved in cell growth and proliferation. Alternatively, metformin may enter the cancer cells directly, inhibit mitochondrial complex I, and decrease ATP production. This decreased adenylate charge in the cell inhibits multiple pathways involved in supporting a proliferating cell, mostly mediated by activation of AMPK.

high spike in metformin concentration, followed by a rapid decrease, and oral water delivery resulting in lower but more steady state concentration of metformin. Dowling *et al*. (2016) showed i.p. metformin (125mg/mL) resulted in a 0.5-hour peak of 184μM serum concentration of metformin, which had dropped to 42μM by 1-hour post-injection (Dowling et al., 2016). Conversely, the oral delivery group in this study received 5mg/mL (600mg/kg, assuming average mouse weight of 25g, and 3mL/day water consumption), which resulted in a steady-state plasma concentration of 34μM (Dowling et al., 2016). A separate study with the same metformin dose, although delivered to a different mouse strain, resulted in steady state plasma concentration of 10μM, a concentration relatively similar to steady state human circulating concentrations (Memmott et al., 2010). Metformin accumulation in tumor tissues has also been studied with various methods of administration. Accumulation in HCT116 human colon cancer xenografts was measured to be higher after i.p. injection compared to oral dosing (Dowling et al., 2016). However, the oral dosing was respective of a continuous level, whereas the i.p. concentration was measured 0.5-hours post-injection – it is likely that timing plays a role in its elevated concentration. In a parallel study using the same tumour model, oral metformin delivery resulted in similar metformin concentrations in both serum and tumours (3.2-12.4μM) (Chandel et al., 2016). In a separate experiment, equal concentrations (350mg/kg) of oral and i.p. injected metformin were compared, and oral dosing resulted in greater liver and lung cancer A549 tumour xenograft concentrations (Chandel et al., 2016).

The result of these pharmacokinetic studies suggest that to achieve clinically relevant circulating concentrations of metformin, murine dosing should be ~10-fold higher than that of human dosing on a mg/kg basis (~30mg/kg in humans, and 250-350mg/kg in mouse models). Additionally, these studies highlight the importance of not just dose, but also method of administration when studying metformin effects on both metabolism and tumor volumes in mice; with oral metformin dosing resulting in the greatest accumulation of the drug in metabolic and tumor tissues over time. (Summary of metformin concentrations available in Table 1.1).

Reference	Diet	MOA	Dose	Time point	Tissue	Metformin (μM)
Broadfield *et al*. 2018 Thesis (Fig. 3.5 A-B)	45% HFD	i.p.	100mg/kg	2h	serum	23
					liver	3
					MC38 tumor	3
					BAT	3
Chandel *et al.* 2016 Cell Metabolism	not reported	Water	250mg/kg	continuous	plasma	5
					liver	40
Dowling *et al.* 2016 Cell Metabolism	not reported	i.p.	125mg/kg	0.5h	plasma	184
				1h	plasma	42
				0.5h	HCT116 tumor	77
		Water	5mg/mL	continuous	plasma	34
					HCT116 tumor	32
Memmott *et al*. 2010 Cancer Prevention Research	10-16% fat	Water	1mg/mL (120mg/kg)	continuous	plasma	2.7
			5mg/mL (600mg/kg)	continuous	plasma	10
		i.p.	250mg/kg	2h	plasma	24.2

Table 1.1: Metformin concentration in circulation and tissues of mouse models.

1.2.2. Direct effects of metformin on CRC

1.2.2.1 Metformin and Cellular Metabolism in CRC Cells

The demands of a rapidly proliferating cell are different from normal tissue. This concept was conceived early on by Otto Warburg, who described elevated glucose use in cancer cells, despite a decreased efficiency for ATP production, now coined the "Warburg Effect". Altered cellular metabolism became a hallmark of cancer, and elevated glycolysis found to be used by rapidly proliferating cells to produce glycolytic intermediates to feed into additional biosynthetic pathways that support cell growth (Hanahan & Weinberg, 2011). The gut epithelium is the body's most rapidly dividing cell population, renewing itself every 4-5 days in humans and every 1-2 days in mice (Creamer, Shorter, & Bamforth, 1961; Eastwood, 1977). Recent work has shown that in the stem cells which populate the quickly-shed intestinal epithelial cells, the mitochondria plays a critical role in cellular metabolism, differentiation, and programmed apoptosis when cells reach the tip of the microvilli (Rath, Moschetta, & Haller, 2018). In these cells, it is proposed that during active proliferation and differentiation, the cell metabolism shifts from predominantly glycolytic to oxidative, producing high ATP levels from OXPHOS to support the high energy demands of the cells (Rath et al., 2018). It is perhaps this metabolic flexibility that allows CRC cells, once transformed and malignant, to survive in glucose-starvation conditions (Miyo et al., 2016). Understanding how metabolism is changed in CRC has been in recent focus, and the genetic mutations involved in colon epithelial malignant

transformation (eg. *Kras* and *Braf*) have been found to cause metabolic adaptations in CRC cells (Fritsche-Guenther et al., 2018; Miyo et al., 2016; Toda et al., 2016). However, *Kras* mutations have resulted in conflicting results, with some work suggesting it increases glucose uptake and sensitivity (Fritsche-Guenther et al., 2018), while others found it to not be involved in determining CRC cell glucose sensitivity (Miyo et al., 2016). Glutamine uptake appears to be an important mechanism for CRC cell survival, with several CRC cell lines surviving low glucose exposure by increasing glutamine uptake, allowing TCA cycle cycling by converting to α-ketoglutarate (Kim et al., 2018). Altered amino acid metabolism in CRC was also found in a metabolomics analysis of malignant and adjacent normal tissue from 17 patients in a small study (Brown et al., 2016). The metabolic flexibility and adaptation of cancer cells is complex, and more work is needed to understand the changes that occur in CRC cells, and how metabolic therapies can target them.

With an altered metabolism and increased reliance on OXPHOS for survival, targeting mitochondrial metabolism with metformin and subsequent complex I inhibition is appealing (Weinberg & Chandel, 2014). Since metformin requires transport into cells, it is important to note that the organic cation transporter-1 (OCT1) was found in CRC tissue and cell lines, suggesting direct drug exposure is possible in clinical settings (Ballestero et al., 2006; Wheaton et al., 2014). Additionally, the plasma membrane monoamine transporter (PMAT) is

used by intestinal epithelium to absorb metformin, although its expression in CRC tissue and common cell lines has not been investigated (Foretz, Guigas, Bertrand, Pollak, & Viollet, 2014; Zhou, Xia, & Wang, 2007). In several *in vivo* CRC xenograft models, metformin was found to decrease tumor growth of MC38, HCT116, and CT26 cell lines (Algire et al., 2011; Algire, Amrein, Zakikhani, Panasci, & Pollak, 2010; Marini et al., 2016; Mashhedi et al., 2011; Nimri, Saadi, Peri, Yehuda-Shnaidman, & Schwartz, 2015; Wheaton et al., 2014). Metformin has been found to directly interact with CRC cells to alter cellular metabolism, often in the context of low glucose conditions only (Buzzai et al., 2007; Miyo et al., 2016). This was associated with inhibition of complex I, and decreased ATP production and oxygen consumption (Wheaton et al., 2014). The CRC cell line HCT116 lost sensitivity to metformin treatment when transfected to express NDI1, a yeast protein which bypasses the mitochondrial complex I and allows for electron transport chain (ETC) flux and ATP production to continue (Wheaton et al., 2014). Additionally, decreased metformin concentrations were required when mitochondrial membranes were permeabilized, suggesting that a limiting effect of the drug is due to entry to the mitochondria (Wheaton et al., 2014). However, inhibition of the ETC may not be the only mechanism, as work in lung cancer found that metformin directly interacts with the rate-limiting glycolysis enzyme hexokinase (HK) (Salani et al., 2012). This effect was also found in CT26 CRC cells, in which decreased activity, but not expression, of HK was measured (Marini et al., 2016). This study also found that metformin treatment decreased

glucose uptake in CT26 tumor xenografts, although mice were given a high metformin dose of 750mg/kg/day (Marini et al., 2016). This alteration in cellular metabolism activates AMPK in CRC cells, an important regulator of the Warburg effect. Work by Faubert *et al.* (2013) used an AMPK-α knockdown in HCT116 cells, and loss of AMPK function resulted in elevated extracellular acidification and elevated lactate production, ultimately promoting Warburg metabolism (Faubert et al., 2013). Metformin responsiveness is known to vary among cell lines, and this is confirmed in CRC cells. Recent work by Kim *et al*. (2018) showed the differences in metformin responsiveness in 8 CRC cell lines, with only half responding to a high, 10mM dose of the drug (Kim et al., 2018). In a cell line insensitive to low glucose conditions, SW620, metformin only inhibited cell proliferation in glutamine-free media, addressing CRC subpopulations that rely on amino acid metabolism for survival (Kim et al., 2018). Taken together, metformin can directly affect CRC cells, and affects metabolic processes through complex I inhibition and interactions with HK, although in immortalized CRC cell lines supraphysiological concentrations are required for cellular effects.

1.2.2.2 AMPK Structure and Function

One of the well-studied molecular targets of metformin is AMPK. AMPK is a highly conserved protein, and acts as a main metabolic sensor in cells. When activated, AMPK activates catabolic programs to promote energy production while simultaneously inhibiting anabolic processes to limit energy consumption.

It is a heterotrimeric protein, with 3 subunits with distinct functions (Stapleton et al., 1996). The α-catalytic subunit, β-scaffolding and modulator of protein conformation, γ-AMP/energy-sensing subunit act together to respond to various cellular signals (Steinberg & Kemp, 2009). Canonical AMPK activation is achieved allosterically by AMP/ADP and directly phosphorylated by upstream kinases (LKB1, calcium/calmodulin-dependent protein kinase kinase (CaMKK)) (Gowans, Hawley, Ross, & Hardie, 2013; Simon A. Hawley et al., 2005; Shaw et al., 2004). LKB1 is a tumor suppressor protein, and its mutation was found to cause Peutz-Jegher's Syndrome, a disease causing spontaneous cancer formation(Hemminki et al., 1998). Phosphorylation of the threonine-172 (Thr172) residue on the α-subunit activates AMPK, and is achieved with binding of ADP and AMP to 2 of the 4 clefts in the γ-subunit, promoting allosteric T172 phosphorylation >10-fold, while also inhibiting dephosphorylation (Davies, Helps, Cohen, & Hardie, 1995; Hardie, Ross, & Hawley, 2012; Hawley et al., 1995). Conversely, ATP binding promotes dephosphorylation and deactivation when cellular energy is restored (Gowans et al., 2013; Hardie et al., 2012). On the β-subunit, phosphorylation at the serine-108 residue can activate AMPK independent of Thr172 phosphorylation, however when combined with AMP binding and Thr 172 phosphorylation, AMPK activity is >1000-fold (Scott et al., 2014). Once active, AMPK phosphorylates and activates or inhibits several downstream pathways, to promote the restoration of cellular energy. To achieve this effect, AMPK stimulates glucose uptake and inhibits glycogen synthesis,

stimulates β-oxidation and reduces *de novo* lipogenesis, and downregulate protein synthesis pathways (Hardie et al., 2012).

1.2.2.3. Metformin Activates AMPK

Metformin activates AMPK indirectly by inhibiting complex I of the mitochondrial electron transport chain, and decreases cellular energy (El-Mir et al., 2000; Owen, Doran, & Halestrap, 2000). When complex I inhibition occurs, the mitochondrial ETC is halted, and ATP synthase is prevented from producing ATP. Metformin has since been shown to target mitochondrial bioenergetics and decrease flux through the TCA cycle (Andrzejewski, Gravel, Pollak, & St-Pierre, 2014). This changes the cellular adenylate charge in the cell, and AMP levels rise, resulting in allosteric AMPK activation as described above. Upstream kinases are also involved in AMPK activation by metformin, as shown by LKB1-/- mice experiencing blunted hepatic AMPK activation with metformin exposure (Shaw et al., 2005). Additionally, while AMPK activation is the major established mechanism of action, metformin has been shown to have AMPK-independent mechanisms involved in mediating improved metabolism, including altering the cellular energy state, cAMP inhibition, mitochondrial redox status and modulation of the gut microbiome (Foretz et al., 2010; Madiraju et al., 2018; Miller et al., 2013; Shin et al., 2014).

1.2.2.4 AMPK and Fatty Acid Metabolism

Proliferating cells require adequate levels of fatty acids (FA) to produce a variety of metabolic intermediates and building blocks for cellular proliferation. FA can be exogenously taken up from circulation, the preferred method for normal tissue, or can be produced within the cell via *de novo* lipogenesis (Currie, Schulze, Zechner, Walther, & Farese, 2013). In a healthy cell, the glycolysis end-product pyruvate enters the mitochondria for use in the TCA cycle, where the pyruvate dehydrogenase complex (PDC) produces acetyl-CoA. The resulting acetyl-CoA is condensed with oxaloacetate to produce citrate, an important intermediate for FA synthesis (Akram, 2014). The citrate transport protein (CTP) moves citrate back to the cytoplasm, where it is cleaved by ATP citrate lyase (ACLY) into acetyl-CoA. It is then carboxylated to malonyl-CoA by acetyl-CoA carboxylase (ACC), the rate-limiting enzyme in the *de novo* lipogeneis pathway. The FA synthase (FAS) enzyme condenses malonyl-CoA in seven serial condensations, and an addition of acetyl-CoA creates palmitate (Röhrig & Schulze, 2016). Palmitate can undergo a series of desaturations and elongations to form various FA with varying carbon chain lengths and double bonds, providing a range of FA for a variety of cellular uses.

AMPK is tightly tied to FA synthesis, both in biological function and its historical discovery (Fig 1.4). The discovery that β-Hydroxy β-methylglutaryl-CoA (HMG-CoA) reductase (HMGR) kinase and the ACC kinase co-purified

with AMPK, and all had similar deactivation kinetics in response to the adenine nucleotide AMP, resulted in the naming of AMPK in 1989 (Carling, Clarke, Zammit, & Hardie, 1989). AMPK negatively regulates *de novo* FA synthesis by phosphorylating ACC at the critical serine 79 residue (Ha, Daniel, Broyles, & Kim, 1994). This occurs acutely when AMPK is activated, and ACC phosphorylation is often used as a readout of AMPK activation. ACC inhibition results in decreased malonyl-CoA, decreasing the pool available for allosteric inhibition of carnitine palmitoyltransferase 1 (CPT1), and increasing mitochondrial β-oxidation and ATP production from FA (Cook, Otto, & Cornell, 1983). This is a classic example of how AMPK decreases anabolic processes and upregulates catabolic processes to restore cellular energetics. AMPK is also a direct inhibitor of the sterol regulatory element binding protein -1c and -2 (SREBP-1c, -2) (Li et al., 2011). SREBPs regulate the expression of lipid synthesis enzymes, including FAS, ACC, and HMGR, the rate-limiting step in cholesterol synthesis (Rawson, 2003). Therefore, AMPK is an important regulator of lipid metabolism which may have important implications for the growth and proliferation of CRC.

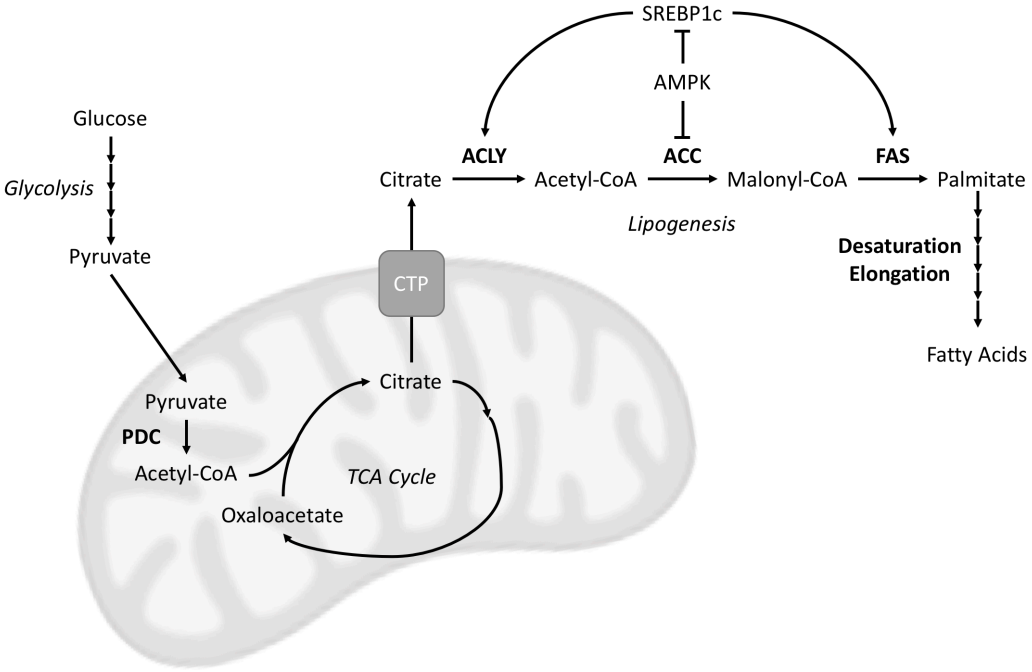

Figure 1.4: Fatty Acid Synthesis and AMPK Interactions.

AMPK is involved in regulating fatty acid synthesis in multiple direct and indirect ways. Glucose metabolism to pyruvate via glycolysis enters the mitochondria and enters the tricarboxylic acid cycle (TCA) cycle via conversion to acetyl-CoA by the pyruvate dehydrogenase complex (PDC). Oxaloacetate and acetyl-CoA by citrate synthase. Citrate transfer protein (CTP) moves citrate into the cytoplasm, where it is converted to acetyl-CoA by ATP citrate lyase (ACLY), then malonyl-CoA by acetyl-CoA carboxylase (ACC), the rate-limiting step in lipogenesis. Fatty acid synthase (FAS) generates palmitate from maolonyl-CoA, producing the back bone of lipid molecules. A series of desaturations and elongations can generate a range of fatty acid carbon chain lengths. AMPK regulates this pathway by phosphorylating and inhibiting ACC activity, and by inhibiting the transcription factor SREBP1c, which regulates the expression of ACLY and FAS.

1.2.2.5 Metformin Effects on Lipid Metabolism in CRC

Elevated lipid metabolism is a known occurrence in cancer growth and progression, as lipids are required for the generation of plasma membrane lipids and production of signaling molecules required for replicating cells (Röhrig & Schulze, 2016). In cancer cells, the role of the mitochondria in metformin-mediated changes in lipid production was found to be critical, and that the loss of functional mitochondria caused reduced metformin response, and allowed maintenance of lipid synthesis via glutamine carboxylation and support of the TCA cycle, an effect found to occur independent of AMPK (Griss et al., 2015). Lipid synthesis is important to CRC cells, with HCT116 cells having elevated FAS expression and associated lipogenic rates (Zhan et al., 2008). When FAS or ACC were inhibited with siRNA silencing (resulting in approximately 80% and 70% reduction in protein expression of FAS and ACC, respectively), decreased cell viability and increased apoptosis was measured (Zhan et al., 2008). Inhibition of fatty acid synthesis with the ACC inhibitor TOFA stimulated apoptosis in HCT-8 and HCT-15 CRC cells (Wang, Xu, Sun, Luo, & Liao, 2009). Despite this evidence that lipid synthesis is important in CRC cells, limited studies observing the effects of metformin on lipid metabolism in CRC cells exist. In work by Sanchez-Martinez *et al*. (2015) (Sánchez-martínez et al., 2015), over-expression of lipid metabolism genes responsible for acetyl-CoA synthetase and stearoyl-CoA desaturase drove epithelial-mesenchymal transition, a hallmark of malignant progression and invasion ability, and was reverted with metformin treatment and

AMPK activation. In the MC38 murine CRC cell line, metformin treatment reduced FASN expression in tumor tissue in mice on HFD (Algire et al., 2010). This effect was associated with AMPK activation, and SREBP-1 downregulation via mTORC1 inhibition (Algire et al., 2010). Given the well-established connections between metformin-mediated AMPK activation and inhibition of lipogenic pathways, further work in this area in CRC is warranted.

1.2.2.6 AMPK and the mTOR Protein Synthesis Pathway

The mTOR protein complex is an evolutionarily conserved protein complex that is involved in regulating cell growth, proliferation, and promotion through cell cycle (Foster & Fingar, 2010). It upregulates anabolic processes, and downregulates catabolic processes, opposing the actions of AMPK. Two different complexes exist, the rapamycin-sensitive mTORC1, and the rapamycin-insensitive mTORC2. These are regulated by two distinct proteins, the regulatory-associated protein of mTOR (Raptor, regulates mTORC1) and rapamycin insensitive companion of mTOR (Rictor, regulates mTORC2) (Foster & Fingar, 2010). These two complexes have distinct cellular interactions and outcomes. mTORC1 responds to growth signaling and nutrients to increase cell growth and proliferation, whereas mTORC2 is involved in regulating actin cytoskeletal organization and mediating Akt signaling (Jacinto et al., 2004; Yao et al., 2017). When a cell experiences insufficient nutrients or growth signaling, mTOR activity

is blunted until energy and nutrient restoration occurs (Shimobayashi & Hall, 2014).

mTORC1 activation by extra- and intracellular signaling, indicating energy and nutrient abundance, results in two unique and distinct mechanisms to promote cell growth, involving the ribosomal protein S6 kinase (S6K) and the transcriptional repressor 4EBP1 (Fig. 1.5). Protein translation is promoted when mTORC1 phosphorylates and activates S6K on its T189 residue (Hong, Zhao, Lombard, Fingar, & Inoki, 2014). Active S6K has a wide range of targets (reviewed by (Tavares et al., 2015)), but most notably phosphorylates and activates the ribosomal S6 protein, which elevates ribosome biogenesis transcription, and increasing overall protein synthesis (Chauvin et al., 2014). Transcriptional repression by 4EBP1 is reversed with mTORC1 activation, which results in hyperphosphorylation of 4EBP1. Hyperphosphorylated 4EBP1 dissociates with the eIF4E, the rate-limiting protein of the cap-binding protein complex involved in transcription regulation (Mamane et al., 2004). eIF4E activation is associated with increased transcription of several genes involved in cancer growth and progression, including cyclin-D1 (cell cycle) and the vascular endothelial growth factor (VEGF; angiogenesis for tumor growth promotion) (Rosenwald et al. 1995, Graff and Zimmer 2003).

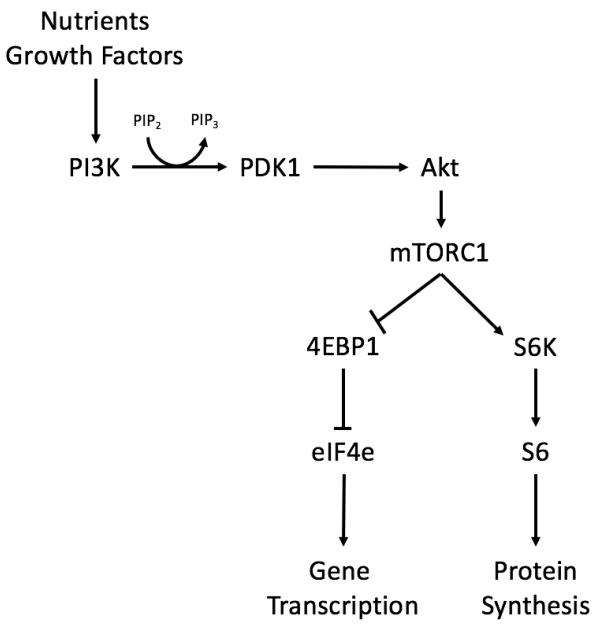

Figure 1.5: mTORC1 Protein Synthesis Pathway

The mTORC1 pathway is activated by various signals including nutrients and growth factors (such as insulin). When receptors are bound and activated to their respective ligands, PI3K is activated, PIP2 phosphorylated to PIP1, and PDK1 is activated. This phosphorylates and activates Akt, which in turn phosphorylates and activates mTORC1. mTORC1 controls protein synthesis at two levels. 1), it inhibits the transcriptional regulator 4EBP1, to lift its inhibition of the transcription factor eIF4e, allowing gene transcription to occur; 2) S6 kinase (S6K) and ribosomal S6 proteins are activated by mTORC1 to stimulate protein translation.

As mentioned, AMPK and mTOR signaling pathways result in opposing effects on anabolic and catabolic pathways. Therefore, it comes as no surprise that they negatively regulate one another. Early work connecting AMPK and mTOR signaling was through the findings that AMPK enhances the tuberous sclerosis

complex 2 (TSC2) activity, which inhibits the mTORC1 activator and GTPase, Rheb (Corradetti, Inoki, Bardeesy, DePinho, & Guan, 2004; Hahn-Windgassen et al., 2005; Inoki, Zhu, & Guan, 2003). Rheb is also modulated by Akt, but rather to activate mTORC1 signaling (Sato, Nakashima, Guo, & Tamanoi, 2009). Akt also activates mTORC1 signaling by restoring cellular energy levels, decreasing AMPK activation and its inhibitory effects on mTORC1 (Hahn-Windgassen et al. 2005). TSC2-deficient cells remain sensitive to decreased energy, leading to the finding that AMPK also inhibits mTORC1 signaling by directly phosphorylating Raptor (Ser792), resulting in binding of the cytosolic anchor protein 14-3-3, and mTORC1 inhibition (Gwinn et al., 2008). Conversely, Akt phosphorylates the mTOR inhibitor, proline-rich Akt substrate 40kDa (PRAS40), to reduce the association of 14-3-3, allowing mTORC1 activity to continue (Vander Haar, Lee, Bandhakavi, Griffin, & Kim, 2007). Therefore, mTORC1 activation is alternately regulated by inhibitory AMPK and stimulatory Akt signaling via TSC2 and association with 14-3-3 (Fig 1.6).

1.2.2.7 Metformin Effects on the mTOR Pathway in CRC

The PI3K/Akt/mTOR pathway is upregulated in CRC, and its activation promotes cancer cell growth and proliferation (Francipane & Lagasse, 2013). Early studies on the mTOR pathway in CRC found over 30% of CRC tumors had

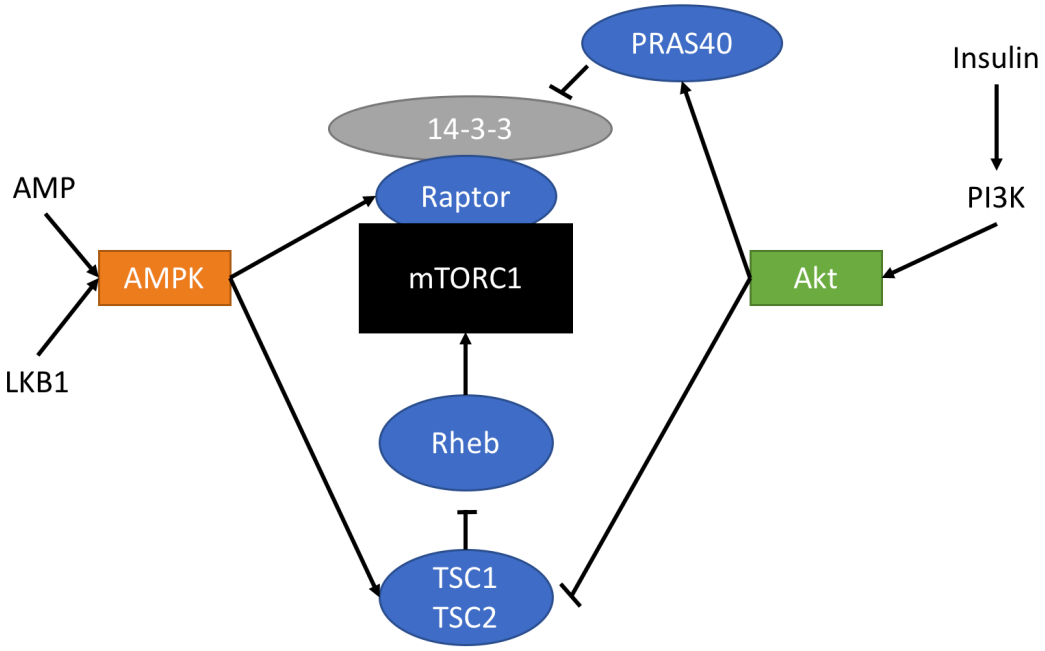

Figure 1.6: mTORC1 Regulation by AMPK and Akt.

AMPK and Akt have opposing effects on mTORC1 regulation, and subsequently protein synthesis. AMPK inhibits mTORC1 via two known mechanisms: 1) activating TSC2, which is an mTORC1 activator, and 2) phosphorylation of Raptor, causing 14-3-3 to bind and inhibit mTORC1 activation. Conversely, Akt stimulates mTORC1 activation via two known mechanisms: 1) inhibiting TSC2, allowing Rheb to activate mTORC1, and 2) phosphorylation of PRAS40 to decrease association with 14-3-3, allowing mTORC 1 activation.

PI3K mutations, and were associated with late-stage disease (Samuels et al., 2004). More recent work suggested that mTOR should be considered a proto-oncogene in CRC, with findings that it promotes tumorigenecity (Murugan, Alzahrani, & Xing, 2013). Targeted inhibition or silencing of mTORC inhibits

CRC cell growth in *in vivo* and *in vitro* models, identifying it as a potential for targeted molecular medicine (Gulhati et al., 2009; Roulin, Cerantola, Dormond-Meuwly, Demartines, & Dormond, 2010). However, mTOR inhibitors in cancer have been largely unsuccessful, with resistance to treatments frequently occurring (Francipane & Lagasse, 2013; Wang & Zhang, 2014). Findings have associated *KRAS* mutations with incomplete inhibition of 4EBP1, suggesting a mechanisms of resistance to targeted therapies (Ducker et al., 2014). Since metformin and AMPK activation can inhibit mTOR signaling through two different mechanisms affecting mTORC1 activation (See section 2.5), it poses a potential mechanism for how metformin can inhibit CRC growth. Indeed, in CRC developmental models using $Apc^{Min/+}$ mice, decreased intestinal polyp size with metformin treatment was associated with elevated AMPK activation decreases in mTOR signaling (Tomimoto et al., 2008). Interestingly, overall polyp numbers were not different between control and metformin treated mice, just polyp size, and no differences in proliferation or apoptosis markers were measured with metformin treatment (Tomimoto et al., 2008). Confirming the role of AMPK activation in the inhibition of CRC tumorigenesis, a chemically-induced model treated with the AMPK activator berberine resulted in reduced tumor burden, and inhibition of the mTOR signaling pathway including p70S6K, S6K, and 4EBP1 (Li et al., 2016; Li et al., 2015). In work by Cufi *et al*. (2013), the role of PI3K mutations in CRC response to metformin was studied, with the findings that xenografts from SW48 CRC cells with the PI3KCA activating mutation *H1047R* conferring insulin-

resistance responded to metformin treatment (Cufí et al., 2013). Recently, work on CRC cell lines found that metformin had differential effects on AMPK activation, and inhibited mTOR signaling regardless of AMPK activation status (Mogavero et al., 2017). In the HT29 cell line, AMPK activation and mTOR inhibition was found, however mTOR inhibition without AMPK activation was found in HCT116 cells, providing support that mTOR activation by metformin may have AMPK-independent mechanisms (Mogavero et al., 2017). Some reports suggest that this is mediated through the hypoxia-induced factor-1 (HIF-1) target REDD1 (REgulated in Development and DNA damage response) or through inhibition of RAG GTPases involved in mTOR activation (Kalender et al., 2010). Additionally, both cell lines experienced decreased IGF1R activation, suggesting metformin can also decrease insulin receptor function independent of AMPK activation (Mogavero et al., 2017). Together, these results suggest metformin can act on the mTOR pathway and inhibit *in vivo* tumor growth independent from changes in circulating insulin. While mTOR inhibition may be a direct effect of metformin on cancer cell growth inhibition, mTOR signaling may also result from its effects on improving circulating insulin levels, indirectly decreasing the upstream activators of the PI3K/Akt/mTOR pathway. However, this effect is likely not to be interfering in models absent of altered metabolism, as no changes in glucose and insulin levels are found in non-diabetic mouse models treated with metformin (Algire et al., 2011; Algire et al., 2010; Li et al., 2015; Tomimoto et al., 2008).

In summary, multiple potential mechanisms exist to characterize how metformin may directly interact with cellular bioenergetics and processes. These effects may be mediated through the inhibition of mitochondrial complex I, and subsequent activation of AMPK. Within the context of rapidly proliferating cancer cells, AMPK-mediated inhibition of both *de novo* lipogeneis and mTOR protein synthesis pathways are suggested to be involved in the mechanism of cancer growth inhibition (Fig1.7).

1.2.3 Metformin as an Indirect Anti-Cancer Agent

As mentioned, it is not currently understood whether direct or indirect mechanisms are driving metformin's anti-cancer effects. While direct mechanisms have been discussed, there remains the possibility that the act of treating the altered metabolism present with T2D is decreasing a systemic environment rich in growth factors that may stimulate tumor growth and development. Metformin-mediated changes in metabolism primarily occur in the liver, and involve regulation of glucose production and lipid accumulation. In this section, the effects of metformin on metabolism, and how this may be linked to decreased CRC, are discussed.

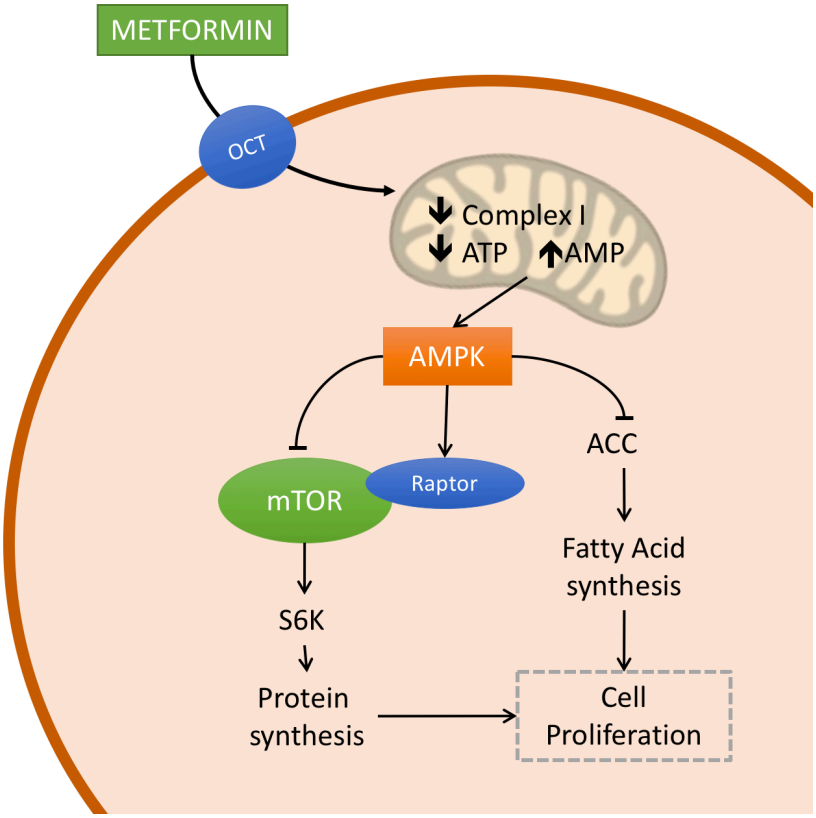

Figure 1.7: Metformin and AMPK inhibit protein synthesis and lipid synthesis

Metformin enters cells via organic cation transporters (OCT), or other cation transporters, and inhibit mitochondrial complex I. This causes a change in the adenylate charge in the cell, with decreased ATP and increase ADP/AMP. This causes allosteric activation of AMPK. Active AMPK downregulates anabolic processes and upregulates catabolic processes to restore cellular energy levels. Protein synthesis and lipid synthesis are both inhibited by AMPK, by inhibition of mTOR and ACC. This decreases cellular intermediates required for a proliferating cell.

1.2.3.1 Metformin Regulates Hepatic Glucose Metabolism

The strong connections between T2D and CRC suggest that defects in glucose homeostasis may be an important driver of disease development. The liver is the primary organ regulating glucose homeostasis. Normal circulating glucose levels in humans has a range of 4-7mM (Saltiel & Kahn, 2001). The liver balances hormone and neural signals in response to the fed or fasted states to maintain glycaemia. After feeding, the liver is responsible for dispersing up to 65% of the glucose load (Moore et al., 2012). With an increase in circulating glucose levels, pancreatic beta cells are stimulated to release insulin, and decrease glucagon levels. In the liver, insulin binding to its receptor on hepatocytes stimulates GLUT2 co-localization to the insulin receptor on the membrane, allowing for glucose entry to the cell (Eisenberg et al., 2005). During these times of excess glucose, hepatic glucokinase phosphorylates glucose, and is branched together to be stored as glycogen. In addition to glucose transporter translocation, insulin signaling in the liver acts to decrease transcription of gluconeogenic enzymes, ensuring both aspects of hepatic glucose output are inhibited (Saltiel & Kahn, 2001). In fasted states, the liver breaks down glycogen, comprised of branched glucose molecules, in a process called glycogenolysis. Glucagon is released during fasting to activate protein kinase A (PKA), ultimately leading to the phosphorylation and activation of glycogen phosphorylase (Jiang & Zhang, 2003). Glycogen phosphorylase releases one glucose molecule from the branches of glycogen, which is modified to glucose-6-phosphate, an intermediate for entry

into glycolysis. When hepatic glycogen stores are depleted, the liver continues to provide glucose via gluconeogenesis, where glucose is produced from alternative sources, such as pyruvate. Gluconeogenesis is a highly regulated process, with transcriptional regulation through cAMP activation and its response factor CREB. The recruitment of co-activators CBP and TORC2 are translocated to the nucleus, activating the transcription factor PGC-1α to regulate the gluconeogenic enzymes glucose-6-phosphatase (G6Pase), and the rate-limiting phosphenolpyruvate carboxykinase (PEPCK) (Herzig et al., 2001; Puigserver et al., 2003; Yoon et al., 2001). Insulin is a negative regulator of these events, with insulin-stimulated Akt activation inhibiting PGC-1α and subsequent downstream effects (Puigserver et al., 2003). Hepatic control of glucose homeostasis is vital to whole-body metabolism, and is a dynamic process responding to various hormonal- and nutrient-based inputs.

The mechanism of how metformin regulates glucose metabolism continues to be an area of active research. Initially, the glucose normalization effects of metformin were thought to be due to altered glucose usage and uptake in skeletal muscle (Klip & Leiter, 1990). However, it was later found that decreased hepatic gluconeogenesis and subsequent glucose output was the likely mechanism altering glucose homeostasis in T2D (Hundal et al., 2000). The important role of the liver in metformin's actions were solidified when high levels of a cation transporter responsible for metformin uptake into cells, OCT1, was

found on hepatocytes, and its deletion limited metformin effects on lowering blood glucose and activating AMPK (Shu et al., 2007). Metformin-mediated AMPK activation is one of the best studied mechanisms of hepatic glucose regulation, with findings by Zhou et al. (2001) showing metformin activated AMPK to decrease glucose production in human hepatocytes (Zhou et al., 2001). Subsequent studies established that the genetic deletion of LKB1, effectively eliminating AMPK activity in the liver, prevented metformin-mediated glucose improvements in HFD-fed mice (Shaw et al., 2005). Molecular mechanisms mediating these effects include decreased PEPCK and G6Pase gene expression with AMPK activation by metformin and subsequent reductions in hepatic gluconeogenesis and hepatic glucose output (He et al., 2009; Koo et al., 2005; Madsen, Bozickovic, Bjune, Mellgren, & Sagen, 2015; Shaw et al., 2005). However, AMPK-independent effects of metformin action on hepatic glucose metabolism have also been found, linked to the overall decrease in cellular energy with metformin treatment (Foretz et al., 2010). Recent work has shown metformin decreases cAMP levels with glucagon, causing decreased PKA activity, resulting in decreased glucose output (Miller et al., 2013). Additionally, metformin can reduce glucose production by altering the cellular redox state via direct inhibition of glycerolphosphate dehydrogenase (Madiraju et al., 2014). While more work is required to clarify these and other mechanisms, altering hepatic gluconeogenesis and glucose output is a major mechanism of metformin's actions, and AMPK activation is in part responsible for these effects.

1.2.3.2 *Metformin Effects on Hepatic Lipid Production and Insulin Sensitivity*

Several factors are involved in the gradual development of insulin resistance. Fat accumulation and hepatic insensitivity are two main causes of insulin resistance, and link elevated adiposity to insulin resistance and T2D development. Lipotoxicity and elevated ectopic lipid accumulation is known to cause insulin resistance, however the mechanisms remain poorly understood (Unger, 2003). FA have been associated with direct effects on the pancreatic β-cells, with acute exposure stimulating, and chronic exposure decreasing, glucose-stimulated insulin secretion (Lewis, Carpentier, Adeli, & Giacca, 2002; Nolan, Madiraju, Delghingaro-Augusto, Peyot, & Prentki, 2006). While seemingly contradictory, elevated insulin secretion is a hallmark of pre-diabetes and T2D, and decreased insulin secretion with disease progression is well known to occur. At the level of the liver, hepatic lipid accumulation, and not visceral adiposity, was associated with insulin resistance in the liver (Fabbrini et al., 2009). As the liver is responsible for most endogenous glucose production, altering its metabolism has large potential repercussions on whole-body metabolism. Multiple mechanisms have been observed to play a role in altered insulin signaling in liver, creating a complex and multi-faceted picture to insulin resistance development. In a seminal review by Samuel and Shulman (2012), five potential and integrated mechanisms of hepatic insulin resistance were discussed (Samuel & Shulman, 2012). These mechanisms include protein kinase Cε (PKCε) activation by diacylglycerols from intracellular triacylglycerol (TAG)

stores to interfere with insulin receptor signaling, ceramide-mediated Akt2 sequestration by PKC-ε, impaired Akt2 activation decreasing insulin-mediated glycolysis and the gluconeogenic transcription factor forkhead box 01 (FOXO1) inhibition, and Akt2 activation of SREBP-1c to modulate genes involved in lipid synthesis (Samuel & Shulman, 2012). Together, these mechanisms result in impaired insulin signaling, elevated lipid synthesis, increased gluconeogenesis and glucose output from the liver, further potentiating the whole body metabolic imbalance if left unchecked.

As previously discussed, AMPK plays an important role in mediating metformin's effects on liver metabolism. Metformin-mediated AMPK activation was found to phosphorylate and inhibit ACC to reduce FA synthesis and increase β-oxidation, and decrease lipogenic enzyme expression via SREBP1c (Zhou et al., 2001). In the first study on metformin and insulin signaling in human hepatocytes, metformin was found to elevate insulin receptor activation, IRS-2, GLUT1 translocation to the plasma membrane, and 2-deoxyglucose uptake (Gunton, Delhanty, Takahashi, & Baxter, 2003). With the connection between hepatic lipid content and insulin resistance, the lipogenic ACC enzyme became a target of interest. Early work on the role of ACC in insulin sensitivity showed surprising results that ACC2-/- mice experienced elevations in both lipid and carbohydrate oxidation, and that the loss of the enzyme protected animals from developing HFD-induced insulin insensitivity (Choi et al., 2007). ACC was found to be

important in mediating metformin actions, with the development of a transgenic mouse model with mutations on the phosphorylation sites of both ACC isoforms, the ACC-double knock-in (ACC-DKI) mouse (Fullerton et al., 2013). With the loss of the AMPK phosphorylation site and thus inability to inhibit ACC activity, ACC-DKI mice fed a control high-carbohydrate diet developed non-alcoholic fatty liver disease (NAFLD), insulin resistance and hyperglycemia due to elevated hepatic glucose production. When fed a high-fat diet, these differences between genotypes were eliminated. However, when these mice fed a high-fat diet were treated with metformin, mice lacking the AMPK phosphorylation sites on ACC were unresponsive to the suppressive effects of metformin to lower liver lipogenesis, liver lipids and insulin resistance; effects that were required for reducing blood glucose (Fullerton et al., 2013). These data indicated that metformin induced reductions in blood glucose in obese mice fed a high-fat diet involves activating AMPK and the suppression of lipogenesis.

Alternative mechanisms involving AMPK to improve insulin sensitivity with metformin treatment have also been proposed. Recent work looking at the role of glucagon found that metformin reduces PKA activity, decreasing an inhibitory phosphorylation at AMPK-Ser173 and elevating the activating phosphorylation at AMPK-Thr172, resulting in decreased cAMP levels and improved insulin sensitivity (Aw, Sinha, Xie, & Yen, 2014; Miller et al., 2013) Metformin has also been found to alter lipogenic and cholsterogenic gene

expression. AMPK activation by metformin decreases *Srebp-1c* promoter activity by 75%, likely through direct interactions with liver X receptor and its ligands (Yap, Craddock, & Yang, 2011). Recent work using a microarray analysis found that while several metabolic genes were altered with metformin treatment in hepatoma cells, genes involved in lipid synthesis were overrepresented (Madsen et al., 2015). Therefore, while the mechanisms mediating hepatic insulin resistance continue to be resolved, current evidence suggests that metformin can improve insulin sensitivity through changes in fat metabolism in the liver. These findings in combination to the hepatic glucose homeostasis effects of metformin show that it acts on multiple aspects of the multifaceted mechanisms involved in insulin resistance and T2D.

1.2.3.3 Potential systemic effects of metformin on CRC

Given the connections between T2D and cancer incidence, the effect of metformin on CRC may be due to its ability to reduce circulating glucose and insulin. While this is a potential theory, current studies in human populations have not yet looked at metformin and CRC risk in individuals without metabolic disease (Chang et al., 2018). However, a small clinical trial on non-diabetic patients with pre-CRC polyps, ACF, found metformin decreased polyp formation, suggesting the possibility that CRC prevention with metformin could occur independently of alterations in glucose and insulin levels (Hosono, Endo, Takahashi, Sugiyama, Sakai, et al., 2010). In pre-clinical studies using the ACF

mouse model, $Apc^{Min-/+}$, a similar effect was found, with metformin-mediated decreases in polyp size, but not polyp number, in a metabolic-independent manner (Tomimoto et al., 2008). Interestingly, mutations in the *Apc* gene were found to directly upregulate expression of GSK-3, which can inhibit AMPK by binding to AMPK-β, and prevent AMPK activation (Suzuki et al., 2013; Valvezan, Zhang, Diehl, & Klein, 2012). This suggests an interaction between *Apc* mutations and downregulation of AMPK and its catabolic outcomes, possibly limiting inhibitions on cell growth and proliferation pathways. Additionally, this suggests that metformin may interact with early initiation stages of CRC development that occur independent from metabolic changes. While HFD feeding has been found to enhance ACF development in the $Apc^{Min/+}$ model, to date no studies have directly studied the role of HFD on the inhibitory effects of metformin (Park, Kim, Seo, Kim, & Sung, 2016). Similar protective effects of metformin have been found in chemically-induced models of CRC development in mice and rats, on chow diets (Takahashi, Hosono, Endo, & Nakajima, 2013; Viktoria et al., 2017). In a study on rats with chemically induced diabetes (via Streptozotocin) and colon carcinogenesis (via dimethylhydrazine), metformin inhibited ACF and tumor formation; however this study did not compare metformin effects on rats with carcinogen exposure only, failing to provide a control to test the effect of metformin on this model with and without T2D (Jia et al., 2015). Some work has been done to address this issue, with metformin showing effectiveness against tumor initiation in mice with chemically induced T2D, CRC, and exposure to

HFD (Zaafar, Zaitone, & Moustafa, 2014). In this study, metformin was also effective against carcinogen-induced cancer in non-diabetic mice. These models of CRC prevention suggest that metformin may be acting in a direct manner rather than due to systemic metabolic effects - however this cannot be ruled out without the correct experimental designs to ask this question.

While evidence for the systemic effects of metformin on CRC initiation are lacking, evidence exists that improvements in metabolic outcomes drive tumor inhibition in tumor allograft models. Using the MC38 murine colon cancer cell line, work by Algire et al. (2010, 2011) found that MC38 allograft growth in C57BL6 mice was stimulated by HFD feeding, and inhibited with metformin treatment (Algire et al., 2011; Algire et al., 2010). Importantly, this effect was found only in HFD-fed animals, with no changes in tumor volume growth measured in chow-fed animals on metformin treatments. When AMPK signaling was measured in these tumors, metformin elevated AMPK phosphorylation regardless of diet, suggesting that the treatment regimen was activating tumor AMPK, but potentially not to sufficient levels to inhibit tumor growth (Algire et al., 2010). Additionally, when LKB1 was knocked down in MC38 cells using shRNA, metformin treatment inhibited tumor growth in mice on chow diet. This suggests that the loss of the major upstream kinase of AMPK enhanced MC38 sensitivity to metabolic alterations with metformin treatment. Further work on this cell line found that metformin treatment decreased insulin receptor signaling and

glucose uptake in tumor tissue, an effect found in HFD-fed mice only, and associated this with decreased serum insulin levels (Mashhedi et al., 2011). Supporting these outcomes in non-CRC cancer models, Iversen et al. (2017) found that metformin tissue distribution of metformin using i.p. injections (commonly used in pre-clinical studies) was insufficient to affect tumor cell bioenergetics (Iversen et al., 2017). The authors make the important note that high metformin concentrations commonly used in *in vitro* studies are not translatable to physiological conditions, and that changes in cell bioenergetics and cell growth outcomes are likely linked to the presence of transporters on the cell membrane allowing metformin uptake (Iversen et al., 2017). Systemic effects of metformin on tumor growth appear to be likely involved in the anti-cancer effects of the drug, however, isolating out these effects are difficult, and rely on multiple variables including cellular uptake of metformin and tumor cell sensitivity to insulin and glucose conditions.

In summary, evidence exists that the systemic effects of metformin on normalizing glucose and insulin metabolism in the context of T2D may be the mechanism inhibiting tumor growth in models of established CRC. Conversely, in pre-cancerous models using ACF and polyp formation via genetic mouse models or chemically-induced carcinogenesis, metformin may have preventative effects independent from metabolic alterations. Further work is required in this area to clarify the roles of metformin in prevention and treatment models of CRC.

1.3. The Gut Microbiome as a Mechanism of Metformin's Systemic Effects

1.3.1 The Gut Microbiome as a Mediator of Health and Disease

The gut microbiome (GMB) is the varied and diverse community of microorganisms including bacteria, viruses, and fungi residing in the gastrointestinal tract. The human GMB has a collective genome considered to be 100-fold greater than that of the human genome (which contains up to 20,000 protein-coding genes) (Qin et al., 2010). Over the last decade, the presence of commensal bacteria in the human gastrointestinal tract has been linked to cancer, obesity and diabetes, non-alcoholic fatty liver disease and steatosis, irritable bowel syndrome, anxiety, and depression (Lee & Hase, 2014; Wang & Jia, 2016). These disease states are often associated with altered GMB diversity, commonly described as "dysbiosis". Dysbiotic microbiome profiles have been linked to glucose homeostasis and insulin sensitivity. The importance of understanding the GMB and its involvement in disease states was further established in 2008, with the formation of the NIH Human Microbiome Project. This consortium of scientists focused on characterizing the human GMB, technologies used to observe, study, and measure the GMB, and studying the relationship between the GMB and human disease. The efforts of the Project culminated in the first milestone publication where two publications were released to describe the healthy human microbiome (Microbiome Project Consortium, 2012, 2013). The wide range of diseases that appear to be affected by GMB alterations points to the complexity of the symbiotic relationship between host and microbiome.

Numerous interactions have been observed between the GMB and disease states, not limited to the involvement of metabolism, the immune system, and cell receptor and signaling interactions through metabolite production (Gilbert et al., 2016). Importantly, the GMB has been associated with response to metformin treatment, and is a potential mediator of metformin's anti-cancer effects (Buse et al., 2016; Wu et al., 2017).

1.3.2 Gut Microbiome and T2D

With the advent of studying the GMB as a mediator of human health and disease, studies on how obesity affects the GMB were of great interest. Early studies in germ free (GF) mice highlight the importance of an in-tact GMB, and showed drastic changes with GMB conventionalization. GF mice exposed to diluted cecal contents from conventionally raised wildtype mice experienced close to 60% increase in fat content within two weeks, along with elevated blood glucose and insulin resistance (Bäckhed et al., 2004). These results occurred with a simultaneous decrease in food consumption and increased metabolic rate, suggesting that either the host or the conventional GMB had great impacts on energy production. It is now well understood that human physiology relies on the presence of commensal bacteria to ferment indigestible polysaccharides into metabolites, such as short-chain fatty acids (SCFAs) and branched chain amino acids (BCAA), that are then absorbed and used by the host as a source of energy (Gijs den Besten et al., 2013).

In obesity, changes in microbe populations across various studies support a shift in the ratio of *Baceriodetes*:*Firmicutes* (Bäckhed et al., 2004; Ley et al., 2005; Turnbaugh et al., 2006). In the *ob/ob* mouse model, decreases of up to 50% of the *Bacteroides* populations and decreases in *Firmicutes* populations were measured in fecal samples (Turnbaugh et al., 2006). In humans, *Bacteroidetes* and *Firmicutes* are the predominant species of GMB genomes (Ley et al., 2005; Ley, Turnbaugh, Klein, & Gordon, 2006; Schwiertz et al., 2009). Interestingly, the ratio of *Bacteroides:Firmicutes* was found to be shifted back in obese humans when exposed to low fat or low carbohydrate diets, correlating to a decrease in body weight (Ley et al., 2006). In T2D and insulin resistance, changes in GMB taxa and diversity has also been found. A metagenome-wide association study of people with T2D in China found that those with the disease had a mild dysbiosis in their GMB, and this was associated with a decrease in butyrate-producing species (Qin et al., 2012). In this study, T2D was associated with enrichment of *Akkermansia, Bacteroides,* and *Clostridium*, and controls were enriched in *Clostridiales, Eubacterium, and Roseburia* (Qin et al., 2012). In humans with insulin resistance, an altered GMB was present, and enriched for taxa that produce branched chain amino acids (BCAA) (Pedersen et al., 2016). Changes in BCAA producing populations was associated with increased circulating BCAA and metabolites, and two main species were suggested to be involved in this outcome: *Prevotella copri* and *Bacteroides vulgates* (Pedersen et al., 2016). The

contribution of *P. copri* to developing insulin resistance was confirmed when it was found to induce this effect in mice (Pedersen et al., 2016). To test if metabolic changes could be induced by GMB transfer, a study by Kootte *et al*. (2017) conducted a fecal transfer in human males with metabolic syndrome, finding improved insulin sensitivity at 6 weeks after FMT (Kootte et al., 2017). However, this effect did not persist to 18 weeks after FMT, although changes in SCFA metabolites were measureable in circulation (Kootte et al., 2017). These studies confirmed that GMB plays a role in obesity and T2D pathology, and suggest some functional outcomes of a dysbiotic microbiome in these disease states, including metabolism of SCFA and BCAA.

1.3.3 Gut Microbiome and Colorectal Cancer

Early work on the influence of the gut microbiome in CRC development found that germ-free rats exposed to various colon carcinogens experienced less tumor formation than conventional rats, suggesting a role of the gut microbiome in CRC development (Reddy et al., 1975; Reddy, Narisawa, & Weisburger, 1976). Recently, an expert opinion was published identifying critical research gaps in CRC, and the role of the gut microbiome was identified as a key area requiring research focus (Lawler et al., 2018). Inflammation has been associated with CRC development, and it is thought that host-microbiome interactions affecting inflammation are a potential carcinogenic mechanism. Several studies have found that interactions between microbes and inflammation in intestinal epithelial cells

can enhance development of CRC (Arthur et al., 2015; Arthur et al., 2012; Hu et al., 2013; Wu et al., 2013). In work by Hu et al. (2013), wildtype mice had elevated CRC development by simply being co-housed with a mouse model of inflammation and CRC development, an affect that was associated with activation of interleukin-6 (IL-6) (Hu et al., 2013). Specific taxa have been identified to potentially increase risk of CRC development, including *E. Coli NC101*, *Streptocuccus bovis/gallolyticus*, and *Bacterodies fragillis* (Abdulamir, Hafidh, & Bakar, 2011; Arthur et al., 2012; Boleij, Van Gelder, Swinkels, & Tjalsma, 2011; Goodwin et al., 2011). High-throughput sequencing found *E. Coli NC101* was elevated in patients with irritable bowel syndrome and CRC, and that this bacteria contained a protein, polyketide synthase (pks), that had genotoxic effects (Arthur et al., 2012). Additionally, infection with *S. Bovis/gallolyticus* was found to increase risk of CRC, with up to 60% of infected patients also having CRC (Boleij et al., 2011). Therefore, it is possible that some potentially carcinogenic species occur, and that they may be related to CRC development, providing a negative link between GMB and cancer.

Changes in the composition and diversity of the gut microbiome with the presence of CRC has recently become an area of interest. In the last 5 years, several groups have been working to characterize these changes, and propose potential biomarkers within the gut microbiome of animals and individuals with CRC (Yu et al., 2017). While several studies have suggested there is no change in

overall community diversity in stool from healthy controls compared to CRC cases (Vogtmann et al., 2016; Weir et al., 2013; Wu et al., 2013), there are still notable changes in specific taxa and functional outcomes from the microbiome population. Taxa changes associated with the presence of CRC include decreases in butyrate-producing populations, including *Faecalibacterium*, *Roseburia,* and *Clostridia*, and butyrate levels in fecal material (Ahn et al., 2013; Baxter, Zackular, Chen, & Schloss, 2014; Ohigashi et al., 2013; Wu et al., 2013). Additionally, taxa noted to be elevated with CRC presence include *Fusobacterium* and *Porphymonas* (Feng et al., 2015; Weir et al., 2013; Wu et al., 2013). In a human to mouse fecal transplant study, using fecal samples from 3 CRC patients and 3 healthy controls, germ-free mice were inoculated with human fecal samples and underwent a carcinogen-induced cancer model to induce CRC formation (Baxter et al., 2014). This work showed no changes in tumor burden in animals inoculated with CRC fecal samples, however there were distinct changes in microbial composition over time and disease progression. Understanding changes in GMB composition in the context of CRC and environmental factors linked to CRC development have been considered, with recent work revealing that red meat consumption was associated to a more hostile gut environment (Feng et al., 2015). Additionally, location of the malignant tissue in the colon has been suggested to cause differential effects on the microbiome, with recent work showing proximal CRC had altered bacterial biofilm structures, whereas distal tumors were largely void of these changes (Dejea et al., 2014). In terms of the GMB as a potential

biomarker for CRC presence and development, a recent metagenome-wide association study found that combining GWAS data with the commonly used fecal occult blood test improved sensitivity of CRC detection by 45% (Zeller et al., 2014). Additionally, Yu et al. (2015) found 20 microbial gene markers that were changed with CRC presence compared to controls, and validated these markers across ethnicities, suggesting that there may be universal signatures of CRC that are measurable through microbiome sequencing (Yu et al., 2017). Taken together, the current surge of interest and research in the microbiome as a biomarker appears promising, however much work is yet to be done in validation of across different ethnicities and populations. Additionally, the development of sequencing technologies and analysis methods continue to be developed, and further discoveries in this field are expected to continue as researcher have improved methods to measure and analyze the GMB and its functional outcomes.

1.3.4 Short Chain Fatty Acid Production in the Gut Microbiome

SCFAs are produced by bacterial fermentation of insoluble fibres and starches consumed in the diet (Cummings, Pomare, Branch, Naylor, & Macfarlane, 1987). The three SCFAs are acetate, propionate, and butyrate, containing two-, three-, and four-carbons in their molecular backbone, respectively. Acetate is a common anion used in multiple biochemical reactions, which is often used in the form of acetyl-CoA, and is also the starting point for butyrate production (Duncan et al., 2004). Acetate is the least studied SCFA for

metabolic and health benefits, likely due to how integrated it is in biological functions. However, recent work has suggested that acetate from colonic bacterial fermentation is involved in modulating metabolism through elevated glucose-stimulated insulin secretion (Perry et al., 2016). Conversely, butyrate is the most commonly studied SCFA, and is the primary source of energy for colonic epithelial cells (Clausen & Mortensen, 1995). Its synthesis can result from 4 different sources, however is primarily produced from acetyl-CoA (~80% of butyrate production) and lysine (~11% of butyrate production) (Vital, Howe, & Tiedje, 2014). These two synthesis pathways converge at crotonoyl-CoA, which is then oxidized by butyryl-CoA dehydrogenase (Bcd) to produce butyryl-CoA. At this point, butyryl-CoA can be phosphorylated to butyryl-phosphate, and finally butyrate by butyrate kinase (Buk) (Fig. 1.8). Alternatively, buturyl-CoA can be directly converted to butyrate by butyryl-CoA:aceteate-CoA transferase (But) or butyryl-CoA:acetoacetate-CoA transferase (Ato), with the latter suggested to be the route utilized by the majority of colonic bacteria (Louis & Flint, 2009). It has been noted that butyrate production is not isolated to a specific phylum of bacteria, and are rather a functional group within the gut (Barcenilla et al., 2000; Louis & Flint, 2009). Propionate has fewer known biological functions, however may be involved in metabolism through interactions in the liver and with lipid metabolism (Hosseini, Grootaert, Verstraete, & Van de Wiele, 2011). Propionate can be produced from multiple sources, with precursor molecules originating from fermentation, biosynthetic pathways, and amino acid catabolism (Gonzalez-

Garcia et al., 2017). All the pathways converge on a final step, with the conversion of propionyl-CoA to propionate via propionate-CoA transferase. SCFAs produced by fermentation in the gut have a variety of functions in the body, and changes in bacteria responsible for producing these metabolites may have roles in the pathophysiology of various diseases including T2D and CRC.

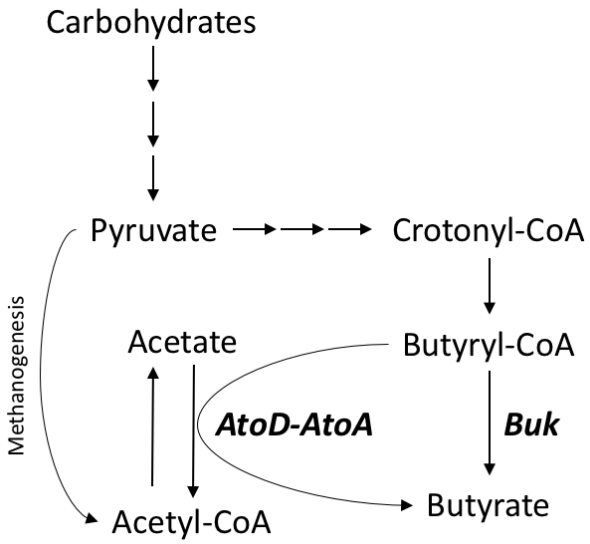

Figure 1.8: The butyrate synthesis pathway

Butyrate is synthesized by bacteria that break down complex carbohydrates. The majority of butyrate is produced via pyruvate conversion to acetyl-CoA, which is then converted to butyryl-CoA. Butyrate kinase (Buk) and butyryl-CoA:acetoacetate-CoA transferase α and β subunits (AtoD and AtoA) catalyze the final step to produce butyrate.

1.3.4.1 SCFA, Metabolism, and T2D

Diets high in fibre have long been associated with lower body weight and serum insulin levels (Ludwig et al., 1999) and as such the role of SCFAs on metabolism and T2D has been an area of interest. As mentioned, butyrate is the primary source of energy for healthy colonocytes, and is oxidized to acetyl-CoA in the mitochondria (Clausen & Mortensen, 1995; Roediger, 1980). SCFAs also provide building block metabolites for glucose and fat, with propionate being integrated into 69% of whole-body glucose production, and acetate and butyrate being incorporated into fat and cholesterol synthesis in the liver (den Besten et al., 2013). In humans, elevated acetate, but not butyrate or propionate, was negatively associated with serum insulin and visceral adipose in young women with obesity (Layden, Yalamanchi, Wolever, Dunaif, & Lowe Jr., 2012). Conversely, people with obesity were found to have elevated total SCFA levels, with propionate found to be significantly higher in obesity (Schwiertz et al., 2009). Several pre-clinical studies have attributed butyrate supplementation to decreased body weight and improved insulin sensitivity, effects that have been associated with activation of AMPK in the liver, and the promotion of oxidative metabolism (Gao et al., 2010; Layden et al., 2012; Mollica et al., 2017). Early work suggested that the three SCFAs have different fates in metabolism, with propionate inhibiting hepatic lipogenesis and cholesterol synthesis, whereas acetate is used as a metabolic building block for fat synthesis (Demigné et al., 1995). The authors posed that this fits with the benefits seen in a high-fibre diet, where elevated propionate may

preferentially impair hepatic lipogenesis, and the effects were seen at concentrations of propionate found in portal circulation. Additionally, activation of hepatic AMPK by SCFAs was found to protect against obesity in HFD-fed mice in a PPARγ-dependent manner (den Besten et al., 2015). This effect was found to be driven by adipose tissue, with PPARγ adipose-specific knockout mice experiencing no improvements in body weight and insulin sensntivity as compared to a liver-specific PPARγ knockout. In skeletal muscle, butyrate was associated with elevated AMPK activation and muscle-synthesis proteins, and maintained muscle mass despite HFD-feeding (Gao et al., 2010). Therefore, evidence suggests that SCFA production by the gut microbiome is associated with several improvements of metabolism, and that part of these effects are mediated on insulin-sensitive tissues.

One of the classic mechanisms attributed to butyrate, is its actions as a histone deacetylase (HDAC) inhibitor. HDAC inhibition has been linked to insulin sensitivity, through interactions with PPARγ and its coactivator PGC-1α, increasing energy expenditure (Ye, 2013). HDAC inhibition by butyrate was found to affect 2% of mammalian genes, and that one of the genes inhibited by butyrate through this mechanism encodes for the p21Waf1/Cip1 cyclin-dependent kinase inhibitor (Davie, 2003). Recent work has provided some controversy on the benefits of butyrate as an HDAC inhibitor, with the findings that the true impact of butyrate on colon health is through its use as an energy source for

colonic cells (Donohoe et al., 2011). Another potential mechanism for SCFA effects on metabolism is through mediating gut inflammation and the integrity of the intestinal barrier. Several studies have found that SCFA regulate tight-junction proteins, helping to regulate the intracellular movement of metabolites and microbes between the intestinal lumen and portal vein circulation (Cani, Bibiloni, Knauf, Neyrinck, & Delzenne, 2008; Peng, Li, Green, Holzman, & Lin, 2009; Wang, Wang, Wang, Wan, & Liu, 2012). For example, inflammatory stimulation by lipopolysaccharide (LPS) was found to be modulated by butyrate treatment, an effect that was associated with maintaining Akt and mTOR activity (Yan & Ajuwon, 2017). Additionally, Arpaia *et al.* (2013) found that regulatory T cells, which have key functions in regulating gut inflammation, experience extra-thymic regulation with butyrate and propionate treatment (Arpaia et al., 2013). Importantly, propionate does not share the same HDAC inhibitory capabilities of butyrate, suggesting that these effects are independent of HDAC inhibition. Another mechanism by which SCFA may impact metabolism involves the discovery that the previously orphaned short-chain fatty acid receptors FFA2 and FFA3 bind to SCFA (Ulven, 2012). FFA2 is found on several immune cells, and is associated with neutrophil response. Propionate and butyrate also inhibit intestinal gluconeogenesis, an effect attributed to binding to FFA3, an effect that was lost in mice that lack the ability to undergo gluconeogenesis in the intestines (De Vadder et al., 2014). Therefore, SCFA have a wide range of mechanisms that affect host metabolism, including interactions with insulin-sensitive tissues, gene regulation,

modulation of inflammatory responses, and binding to their recently discovered receptors.

1.3.4.2 SCFA Effects on CRC

As discussed above, decreased numbers of SCFA-producing taxa and fecal butryate levels have been associated with CRC presence and development (Baxter et al., 2014; Daniel, Ball, Besselsen, Doetschman, & Hurwitz, 2017; Ohigashi et al., 2013; Weir et al., 2013). The ability for SCFAs to prevent CRC cell growth can be attributed to several potential mechanisms: altering cellular bioenergetics, inhibition of histone deacetylases, and altering apoptosis and autophagy pathways in the cells (Archer et al., 2005; Donohoe et al., 2014; Hinnebusch, Meng, Wu, Archer, & Hodin, 2002; Tang, Chen, Jiang, & Nie, 2011). Since butyrate is the primary source of energy for colonocytes, its use in malignant cells is suggested to change due to the Warburg effect. Donohoe *et al.* (2014) suggest that elevated uptake of glucose, driven by the Warburg effect, allows butyrate to avoid oxidation for energy production and accumulate in the cell to inhibit HDAC (Donohoe et al., 2014). This dual action potential of butyrate was confirmed in earlier work by the same group, showing colonocytes isolated from germfree mice existed in an energy-deprived state, and that butyrate treatment rescued the cells by providing energy, rather than acting as an HDAC inhibitor (Donohoe et al., 2011). Additionally, more recent work has suggested that butyrate effects may be mediated by the concentration of butyrate. Yan et al. (2017) showed that 1mM

butyrate increased ATP levels, whereas 0.1mM butyrate activated AMPK, suggesting energy stress in the cells (Yan & Ajuwon, 2017). The ability for butyrate to act as an HDAC inhibitor is well known, and has been previously discussed. In colon cancer cells, this mechanism has been shown to occur as well, with histone hyperacetylation by butyrate causing both autophagy and apoptosis (Archer et al., 2005; Hinnebusch et al., 2002; Tang et al., 2011). CRC cell growth and differentiation are inhibited by butyrate treatment, and evidence suggests this is due to p21, as HCT-116 CRC cells with depleted p21 failed to respond to butyrate treatments (Hinnebusch et al., 2002). When butyrate affects p21 expression, it can inhibit the expression of the cell cycle promoter cyclin B1, by interacting with the cyclin B1 promoter; an effect that was found to require prolonged HDAC inhibition (Archer et al., 2005). Another potential mechanism, is the role of butyrate as a mediator of tight junction permeability in the gut. Gut barrier dysfunction elevates inflammation and potential for harmful bacteria to enter the circulation. This has also been linked to the development of cachexia, the wasting of skeletal muscle and body-wide energy dysregulation that can occur in late-stage cancer, in a genetic model of CRC (Puppa et al., 2011). Butyrate has been found to improve intestinal barrier function by improving tight-junction assembly (Peng et al., 2009; Yan & Ajuwon, 2017). Additionally, these functions were found to be mediated by AMPK activation, as downregulation of AMPK impaired the assembly of tight-junction protein formation (Zhang, Li, Young, & Caplan, 2006). Butyrate elevates RNA and protein expression of the tight-junction

proteins claudin-2 and claudin-4, while also decreasing phosphorylation of Akt and the downstream mTOR target, 4EBP1 (Yan & Ajuwon, 2017). Taken together, butyrate has multiple potential functions in CRC cells, with its effects dependent on its concentration and the energy status of the cell it is interacting with. Overall, evidence suggests that butyrate may inhibit CRC cell growth and proliferation through multiple complementary mechanisms.

1.3.5 Metformin Impacts on the Gut Microbiome

The impact of metformin on the gut microbiome is a recent area of research. As metformin is absorbed in the small intestine, but is only 40-50% bioavailable, drug exposure to microbial populations in the gut will occur (Buse et al., 2016; Wilcock & Bailey, 1994). Initial studies on metformin effects on the microbiome, published in 2014, observed changes in C57BL/6 mice fed 60% HFD treated with 300 mg/kg/day metformin (Lee & Ko, 2014; Shin et al., 2014). Both studies found similar effects on the microbiome with metformin treatment, including a restoration of decreased *Bacteroidetes* populations (Lee & Ko, 2014; Shin et al., 2014). Additionally, changes in amounts of *Akkermansia muciniphila* were noted in both studies, as this species is known to have metabolic effects in the HFD-setting (Everard et al., 2013; Lee & Ko, 2014; Shin et al., 2014). Additionally, inferred metagenomic analysis found that metformin treatment in HFD-fed animals increased several metabolic pathways, including propionic synthesis (Lee & Ko, 2014). These early reports showed that metformin exposure

drastically changed the makeup of the gut microbiome in HFD-fed animals, and was found to have a greater impact than switching animals back to chow diet (H. Lee & Ko, 2014). The role of intestinal inflammation was also considered, however not found to be involved in the metformin-mediated changes in metabolism in the mice (Shin et al., 2014). The next step in support for the role of the gut microbiome in mediating metformin's effects came from Forslund *et al*. (2015), where the bacterial metagenome from multinational studies on metformin use in diabetes were analyzed (Forslund, Hildebrand, Nielsen, & Falony, 2015). Study populations in Denmark (MetaHIT study), Sweden, and China were used, and metformin was the only T2D therapy to modulate the gut microbiome (Forslund et al., 2015). Additionally, this study confirmed the functional changes in SCFA-producing pathways, including both butyrate and propionate synthesis. However, studying the metagenome in microbiomes from groups from the 3 different countries highlighted inconsistencies in expected trends, such as the abundance of *Akkermansia* taxa. In a separate study, 16S rRNA sequencing of fecal samples from a population of Columbians with T2D with and without metformin treatment, the increases of *Akkermansia muciniphila* were confirmed, as well as changes in SCFA synthesis pathways (De La Cuesta-Zuluaga et al., 2017). Further confirmation that the microbiome is associated with metformin-mediated metabolic improvement came from Wu *et al*. (2017), who found that fecal transfer from treatment-naive T2D patients put on metformin for 4 months into germ-free mice fed HFD improved glucose sensitivity (Wu et al., 2017). This

is an important experiment, as the effects of metformin on the microbiome were isolated, as the fecal recipient mice were not treated with metformin directly. Additionally, elevated *Akermansia muciniphila* was found, however it did not correlate with long-term glucose regulation, as measured by HbA1c (Wu et al., 2017). A summary of taxa changes with metformin exposure is summarized in Table 1.2. Taken together, this recent and growing body of evidence supports the role of the gut microbiome on metformin's metabolic effects, and that this may in part be due to changes in SCFA production.

1.3.6 Models to Study the Gut Microbiome

Several experimental protocols can be used to study the gut microbiome, with various benefits and downfalls. One method to study the effects of the gut microbiome on various outcomes is through "knocking out" the bacterial load and diversity by treating animals with antibiotics, such as ampicillin. Ampicillin is in the penicillin class of antibiotics, and acts against Gram-positive and some Gram-negative bacteria. It is a cell wall inhibitor, preventing bacterial cell wall synthesis and results in cell lysis, and reduces bacteria numbers and genomic load in the gut microbiome (Membrez et al., 2008). Studies addressing the effects of antibiotics on gut microbiome and host metabolism often use combinations of antibiotics, to achieve maximal depletion of bacterial load, however treatment with antibiotics has been found to often improve glucose and insulin metabolism (Fujisaka et al., 2016). In obese *ob/ob* mice, the combination of ampicillin and norfloxacin

resulted in decreased fasting blood glucose and glucose tolerance, after a 2-week intervention (Membrez et al., 2008). This was associated with decreased hepatic glycogen stores, and glucose-stimulated insulin secretion. In other studies testing antibiotic effects on gut microbiome and metabolism, the role of host genetics (ie. mouse strains) is suggested to play a large role in determining if animals have a metabolic or inflammatory response to antibiotic exposure (Fujisaka et al., 2016; Rune et al., 2013). Recent work by Fujisaka *et al*. (2016) showed that C57BL/6J mice were more responsive to diet-induced obesity with 60% HFD exposure, and that antibiotic treatments resulted in improved glucose metabolism and insulin signaling compared to two other mouse strains, the 129J and 129T mouse lines (Fujisaka et al., 2016). In other work on the C57BL/6J mouse line, it was suggested that early exposure to ampicillin affected glucose metabolism, but exposure during adulthood resulted in no impact on host metabolism, including fasting insulin levels (Rune et al., 2013). Taken together, the use of antibiotics in a pre-clinical model is useful for decreasing the bacterial load in a biological system, but may cause metabolic changes.

To isolate the effects of the gut microbiome on various experimental outcomes, the use of fecal microbiome transfer (FMT) models has been employed. The experimental designs involving FMT vary, depending on source of

Taxa Level	Name	Study Conditions
Taxa Increased with Metformin Exposure		
Phylum	*Verrucomicrobia*	C57BL/6 mice fed 60% HFD and 300mg/kg/day metformin oral gavage(Shin et al., 2014)
Family	*Escherichia*	Treatment-naïve T2D patients on placebo or 1.7g/d metformin (Wu et al., 2017) Multinational metagenomic dataset; controls, T2D, and T1D (Forslund et al., 2015)
	Lactobacillaceae	Upper instine of Sprague-Dawley rats on HFD with 200mg/kg metformin intestinal infusion (Bauer et al., 2018)
Genus	*Blautia*	Treatment-naïve T2D patients on placebo or 1.7g/d metformin (Wu et al., 2017) Wistar Rats on 60% HFD with 200mg/kg/day metformin oral gavage (Zhang et al., 2015)
	Butyricoccus	Wistar Rats on 60% HFD with 200mg/kg/day metformin oral gavage (Zhang et al., 2015)
	Phascolarctobacterium	Wistar Rats on 60% HFD with 200mg/kg/day metformin oral gavage (Zhang et al., 2015)
	Lactobacillus	Wistar Rats on 60% HFD with 200mg/kg/day metformin oral gavage (Zhang et al., 2015) Upper instine of Sprague-Dawley rats on HFD with 200mg/kg metformin intestinal infusion (Bauer et al., 2018)
	Allobacterium	Wistar Rats on 60% HFD with 200mg/kg/day metformin oral gavage (Zhang et al., 2015)
	Bifidobacterium	Treatment-naïve T2D patients on placebo or 1.7g/d metformin (Wu et al., 2017)
	Shewanella	Treatment-naïve T2D patients on placebo or 1.7g/d metformin (Wu et al., 2017)
	Parasutterella	Wistar Rats on 60% HFD with 200mg/kg/day metformin oral gavage (Zhang et al., 2015)
	Prevotella	T2D patients on metformin or other treatments (De La Cuesta-Zuluaga et al., 2017)
	Megasphaera	T2D patients on metformin or other treatments (De La Cuesta-Zuluaga et al., 2017)
	Klebsiella	Wistar Rats on 60% HFD with 200mg/kg/day metformin oral gavage (Zhang et al., 2015)
Species	*Akkermansia muciniphilia*	C57BL/6 mice fed 60% HFD and 300mg/kg/day metformin oral gavage (Lee & Ko, 2014) Treatment-naïve T2D patients on placebo or 1.7g/d metformin (Wu et al., 2017) Multinational metagenomic dataset; controls, T2D, and T1D (Forslund et al., 2015) C57BL/6 mice fed 60% HFD and 300mg/kg/day metformin oral gavage (Shin et al., 2014) T2D patients on metformin or other treatments (De La Cuesta-Zuluaga et al., 2017)
	Bliophila wadsworthia	Treatment-naïve T2D patients on placebo or 1.7g/d metformin (Wu et al., 2017)
Taxa Decreased with Metformin Exposure		
Genus	*Intestinibacter*	Treatment-naïve T2D patients on placebo or 1.7g/d metformin (Wu et al., 2017) Multinational metagenomic dataset; controls, T2D, and T1D (Forslund et al., 2015)
Genus	*Anaerotruncus*	C57BL/6 mice fed 60% HFD and 300mg/kg/day metformin oral gavage (Shin et al., 2014)
	Clostridium XIVa	Wistar Rats on 60% HFD with 200mg/kg/day metformin oral gavage (Zhang et al., 2015)
	Flaconifractor	Wistar Rats on 60% HFD with 200mg/kg/day metformin oral gavage (Zhang et al., 2015)
	Lachnospiracea_incertae_sedis	Wistar Rats on 60% HFD with 200mg/kg/day metformin oral gavage (Zhang et al., 2015)
	Clostridium XI	Wistar Rats on 60% HFD with 200mg/kg/day metformin oral gavage (Zhang et al., 2015)

Table 1.2: Changes in microbiome taxa in animals and humans with metformin treatment.

the donor material (human vs. animal) and the model used for receiving the fecal material (gnotobiotic vs conventional). It is important to note that the role of diet is very strong in these models, with recent work finding fat content in the diet can have large impacts on microbiome composition independent of metabolic changes (Dalby, Ross, Walker, & Morgan, 2017). Some studies rely on the coprophagic behaviour in mice, and simply place fecal material from donor cages into the recipient cages, and allow recipient mice to consume the donor fecal materials freely (Kulecka et al., 2016). A more tightly controlled method is to collect fresh fecal material, dilute with saline, and gavage fecal contents into recipient mice; this method maintains the bacterial colonies as close to what is present in the recipient mice by avoiding freeze-thaw cycles, and limiting death of the predominantly anaerobic bacterial populations present in feces due to exposure to air (Bäckhed et al., 2004; Zhou et al., 2017). Gnotobiotic and germ-free animals provide a unique opportunity to colonize sterile animals with the donor microbiome, or isolate out individual microbes of interest (Grover & Kashyap, 2014). However, these models have been long known to have altered metabolism prior to inoculation with donor material, and underdeveloped immune and endocrine systems (Grenham, Clarke, Cryan, & Dinan, 2011). When donor material is introduced to germ free animals, the maturation of these systems could be impacted by the differences in microbial composition between treatment groups, and results should be interpreted within this context (Chung et al., 2012; Ericsson & Franklin, 2015). A benefit to germ-free and gnotobiotic animal models

is that there is no resistance to colonization of new bacterial populations by endogenous communities, resulting in higher rates of colonization by the donor fecal materials (Ericsson & Franklin, 2015). Overall, fecal microbiome transfer is a common method to isolate out the effects of the gut microbiome on outcomes in research animals.

1.4. Summary

In summary, T2D and CRC share several similar risk factors, including obesity and decreased activity. Metformin treatment is frequently used for T2D treatment, and is associated with decreased CRC risk. The mechanisms involved in this effect remain unclear, but are previously suggested to be mediated by either 1) systemic/indirect effects by treating metabolic alterations present in T2D that could promote malignant cell growth, or 2) direct effects by entering the CRC cells and altering cellular bioenergetics, lipid metabolism, and protein synthesis. Here, it is proposed that the GMB may also be playing a role in mediating metformin's anti-cancer effects. GMB dysbiosis is present in both T2D and CRC, and current work suggests similar functional changes are associated with both diseases, such as changes in SCFA metabolism. Importantly, metformin appears to modulate the dysbiotic microbiome, and restore taxa that produce SCFAs (Fig. 1.9). This leads to several questions regarding whether metformin exposure to the GMB is driving changes in CRC growth and development seen in pre-clinical models, and whether it is dependent on changes in metabolism as well. This is an

exciting intersection between T2D, CRC, and the GMB, an area not previously explored.

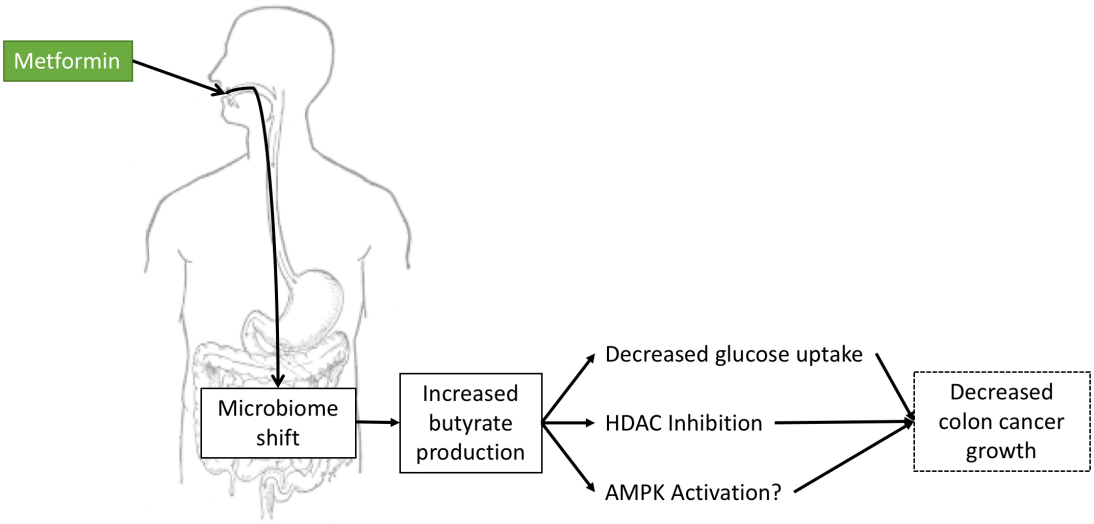

Figure 1.9: Proposed effects of metformin on the gut microbiome that may mediate metformin's anti-cancer effects.

Metformin causes changes in the gut microbiome, which have been linked to functional changes such as short-chain fatty acids, including butyrate. Butyrate mediates gut epithelial health by providing epithelial cells with energy and promoting immune functions that support gut health. Butyrate has several proposed functions that can decrease CRC growth, including modulating glucose uptake into cells, inhibiting histone deacetylases to affect gene expression, and potentially activating AMPK.

1.5. Thesis Objective and Hypothesis

Current evidence exists for metformin to inhibit CRC by acting directly on the tumor and/or indirectly by altering glucose homeostasis/insulin sensitivity. A potential third, yet to be examined, mechanism involves metformin modulation of the gut microbiome. Therefore, the overall objective of this thesis was to test if metformin inhibited CRC growth through direct or indirect mechanisms to, and to examine the potential role of the GMB in mediating these effects.

1.5.1 Aim 1: Confirmation of elevated colorectal cancer growth via diet-induced obesity

Confirmation that the MC38 murine colon cancer mouse model is important to study the role of metabolic effects of metformin-mediated inhibition of CRC. Therefore, aim 1 compared the effects of i.p. injected metformin in chow- and 45% HFD-fed mice on glucose and insulin sensitivity and tumor growth.

Hypothesis: HFD-feeding will stimulate MC38 tumor allograft growth compared to chow-fed controls, and metformin treatment via i.p. injection will inhibit this growth stimulatory effect.

1.5.2 Aim 2: Oral metformin and antibiotic treatment effects on metabolism and colorectal cancer growth

To begin testing the role of the gut microbiome, oral metformin treatments are required to ensure metformin-GMB interactions. The antibiotic ampicillin was added to limit the effects of the microbiome.

Hypothesis: Oral metformin will improve glucose and insulin sensitivity and decrease tumor growth compared to untreated controls, and ampicillin (and thus decreased microbiota load) will blunt this effect.

1.5.3 Aim 3: Isolating the role of the gut microbiome in metformin's anticancer effects using fecal transfer

Antibiotics can significantly decrease the bacterial load in the GMB, however resistant bacteria remain. Therefore, aim 3 isolated out the effects of metformin on the GMB, metabolism, and CRC growth, using a fecal transfer model. Additionally, the role of butyrate and SCFA were considered as potential metabolites involved in metformin's anti-cancer effects.

Hypothesis: Fecal transfer from diet-induced obese mice treated with oral metformin to treatment-naïve diet-induced obese mice will improve glucose and insulin sensitivity and decrease MC38 tumor volume growth compared to control

mice receiving fecal transfer from un-treated obese mice, and these effects will be associated with changes in SCFA production.

Chapter 2: Methods

2.1 Animal Models and Treatments.

Wild-type C57-B6 mice were bred in house (study 1) or ordered in at 6 weeks of age from Jackson Laboratories (studies 2 and 3). At 6 weeks of age, animals in diet-induced obesity groups were given 45% high-fat diet (D12451, Research Diets, Cedarlane), and allowed to feed *ad libitum* for 12 weeks; chow animals remained on standard diet (17% kcal from fat; Diet 8640, Harlan Teklad) for the duration of the study. After 12 weeks of HFD-feeding, animals were weight matched into groups. For study 1, mice received daily i.p. injections of saline (control) or 100mg/kg metformin for 4 weeks. For study 2 and 3 (donor mice only), mice were given 250mg/kg metformin in drinking water for 4 weeks. Dosage was calculated weekly to adjust for changes in body weight and water consumption over time. For study 2, 1g/L ampicillin (Sigma Aldrich) was dissolved in drinking water. All control and treated waters were stored at 4°C until use. Body weight was measured weekly, and maintained on at 12-hour light/dark schedule, with ambient room temperatures of 23-24°C, bedding and enrichment, and had *ad libitum* access to drinking. A whole-body composition analyzer was used to measure total adipose content. The Minispec LF90II (Brucker, Milton, ON) was used for measuring body composition, using the Minispec Plus and Opus programs (Brucker, Milton, ON). Percent body fat was calculated as g adipose / g bodyweight (measured at time of scan) * 100. All experimental procedures and protocols were conducted in accordance with approval from the McMaster Animal Research Ethics Board.

2.2 Glucose and Insulin Tolerance Testing.

Glucose and insulin tolerance tests (GTT and ITT) were conducted to assess glucose and insulin sensitivity. Mice were fasted 6 hours in a quiet room, and baseline blood glucose was measured by creating a small tail nick on the last 1-2cm of the tail to draw a drop of blood to measure glucose using a glucometer (Aviva glucometer, Roche). After baseline measurement, animals were weighed to give an accurate dose of glucose or insulin, on a per kilogram basis. In GTT, chow-fed animals received 2g/kg glucose and HFD-fed animals received 1g/kg glucose. In ITT, chow-fed animals received 1U/kg human insulin, and HFD-fed animals received 0.6U/kg insulin. Following i.p. injection of glucose/insulin, blood glucose was measured at 20, 40, 60, 90, and 120 minutes post-injection using the tail nick to draw a drop of blood. Blood glucose values were averaged for each treatment group, and area under the curve was calculated as the average blood glucose * 120 minutes.

2.3 Fasted Serum Glucose and Insulin.

Mice were fasted overnight from 7PM-7AM (dark/feeding cycle for mice), and 150µL of blood was collected by facial bleed (study 1) or tail vein (studies 2 and 3). Blood glucose was measured using Aviva glucometers prior to collection. Collected blood was allowed to clot at room temperature for 30 minutes to remove clotting factors. Samples were spun at 14,000rpm for 10 minutes in a centrifuge pre-cooled to 4°C. Serum was removed and stored at -80°C until use.

Serum insulin was measured in samples with only 1 freeze-thaw cycle, using a commercially available insulin ELISA kit (Millipore). Curve fitting of the output data was conducted using 4-parameter logistic regression analysis on free software available at elisaanalysis.com.

2.4 MC38 Tumor Allograft Model.

MC38 murine colon cancer cells were provided by Dr. Pollak (McGill University). Cells were maintained in DMEM (Gibco) media with 10% fetal bovine serum (Gibco) and 1% anti-anti solution (Gibco). MC38 cells were maintained in an incubator at 37°C and 5% CO_2. Mice were anaesthetized using isofluorane, shaved on their hind flank, and injected with $2.5x10^5$ cells in 100µL warm PBS. A 25G needle was used for injections to avoid disrupting cells during injection. MC38 allografts had 100% successful grafting for all experiments. When tumours were palpable (3-4 days post-injection), tumour volume measurements were conducted every other day using a Vernier hand caliper. Tumour volume was calculated using the formula $0.5(length * width^2)$.

2.5 Cell Culture and Clonogenic Assays.

MC38 cells were grown in 25mM glucose DMEM or 5mM glucose DMEM for two weeks prior to seeding. Metformin (Sigma Aldrich) and sodium butyrate (Sigma Aldrich) were made fresh prior to each experiment, and were solubilized into water for treatments. Clonogenic assays in MC38 cells were

conducted by seeding 200 cells per well into a 12-well plate, and allowed to adhere overnight. Treatments were applied in triplicate the following day, and cultures were monitored daily. Once cells had proliferated and produced colonies (approximately 5 days), cells were washed with PBS and stained with 0.5% crystal violet stain in 40% ethanol (Sigma Aldrich). Once dried, colonies containing more than 50 cells were counted using a grid mounted under the 12-well plate to ensure accuracy.

2.6 Fecal Microbiome Transfer.

Recipient cages (n=2-3 per cage) corresponded to specific donor cages (n=2-3 per cage) and recipients and donors were matched for the duration of the experiment (no mixing of donor/recipient cages after protocol start). Donor animals were on water treatments for 24-hours prior to fecal transfer initiation. Fecal material was collected for fecal microbiome transfer. Feces were collected fresh from donor cages prior to dilution (1:10 wt/vol) in 0.9% saline solution. Feces and saline were combined in conical tubes and vortexed until homogenous (approximately 5 minutes, maximum vortex speed), and centrifuged for 30 seconds at 2000rpm. Resulting supernatant was collected into new tubes, and 200µL were gavaged into recipient mice, 3 times weekly. Fecal transfer continued throughout metabolic testing and tumor engraftment and growth (approximately 6-7 weeks).

2.7 Tissue Collection.

For acute *in vivo* metformin signaling experiments, animals were fasted overnight (7PM-7AM), and allowed to re-feed for 2 hours (7AM-9AM), after which they were injected i.p. with saline control or 100mg/kg metformin. 1- or 2-hours post-injection, mice were injected i.p. with a mixture of ketamine and xylazine for anesthetic. Tumor tissue was taken first, while tissue was still being perfused. Tumors were quickly weighed (<1 minute), then cut in half for snap freezing in liquid nitrogen, and to be fixed in 10% buffered formalin. Following tumor extraction, the abdomen was opened to allow for snap-freezing liver tissue using specially designed tongs chilled in liquid nitrogen; this process ensures maintenance of AMPK phosphorylation in liver tissue. All frozen tissues were stored at -80°C, and fixed tissues were kept in 10% buffered formalin for 24-48 hours before being stored in 70% ethanol.

2.8 Western Blotting.

For *in vitro* protein analysis, cells were seeded into 6-well plates were allowed to adhere overnight, and treated the following day. Once the time point was reached, cells were washed with ice cold PBS, lysed with cell lysis buffer (5mM Hepes, 150mM NaCl, 100mM NaF, 1M Na-Pyrophosphate, 0.5mM EDTA, 250M sucrose, 1mM DTT, 1mM Na3VO4, 1% Triton-X, 1% protease inhibitor tablet), immediately snap frozen with liquid nitrogen, and stored at -80°C. The following day, plates thawed on ice, wells were scraped with a cell

scraper, and samples were transferred to 1.5mL tubes. Samples were spun in a pre-chilled centrifuge for 10 minutes at 10,000rpm at 4°C. The resulting supernatant was collected into a fresh tube. For *in vivo* protein analysis, tumor and liver samples were isolated from mice, and snap frozen in liquid nitrogen, as described above. Tumor samples were powdered by hand on liquid nitrogen and dry ice using a pre-chilled mortar and pestle. Tumor powder was then lysed by adding approximately 20mg of sample to cell lysis buffer, physically agitated by a hand homogenizer. Similarly, liver samples had a small section chipped off (~20mg tissue), placed into ice cold lysis buffer, and agitated using a hand homogonizer. Homogenates were then allowed to rotate for 45 minutes at 4°C, frozen over night at -80ºC, then thawed on ice and centrifuged for 10 minutes at 10,000prm at 4°C, and the resulting supernatant was collected into a fresh tube. Protein concentration was determined using BCA protein assays (Pierce), and samples were made for even loading volumes. 10-40µg of MC38 cell protein and 5-10µg of tumor and liver protein was loaded onto 7.5% or 10% acrylamide gels were used to resolve out respective proteins. PVDF or nitrocellulose blotting membrane was used to probe for proteins. Antibodies used included (Cell Signaling catalogue number in brackets): AMPKα (Cat. No. 2352), pAMPKα-T172 (Cat. No. 2535), ACC (Cat. No. 3676), pACC-S79 (Cat. No. 3661), P70S6K (Cat. No.9202) , pP70S6K-T389 (Cat. No. 9205), Raptor (Cat. No. 2280), pRaptor-S792 (Cat. No. 2083), pAkt-S473(Cat. No. 4058), pAkt-T308 (Cat. No. 4056), and β-actin (HRP conjugated, Cat. No. 5125). All primary antibodies and

secondary HRP-linked antibodies were sourced from Cell Signaling (Danvers, MA). Blots were quantitated using Image J Software (NIH, La Jolla, CA).

2.9 Quantitation of Metformin.

Serum was analyzed using 40µL mixed with 600 µL of a mixture of 31.6% MeOH / 36.3% ACN in H_2O (LC/MS grade solvents pre-equilibrated at -20^oC) for metabolites extraction. A 5µL aliquot of 12.5µM $^2H_6$-metformin (CDN Isotopes, Quebec Canada) internal standard was added to each sample. Extracts were partitioned into aqueous and organic layers following dichloromethane (DCM) treatment and centrifugation. Aqueous supernatants were dried by vacuum centrifugation with sample temperature maintained at -4°C (Labconco, Kansas City MO, USA). Dry samples were resuspended in 100µL of 50% ACN in H_2O and a volume of 5µL was injected for LC-MS/MS analysis. Metformin values are reported in µM. Frozen tissues were crushed at liquid nitrogen temperature using a mortar and pestle to a fine powder. Approximately 10 mg (+/- 10%) of the tissue was weighed and 1800µL of of 31.6% MeOH / 36.3% ACN in H_2O was added to the sample. Three 2.8 mm pre-washed ceramic beads were added to each tissue sample. Each sample was thoroughly homogenized 45 seconds at 50 Hz bead beating (SpeedMill Plus, Jena Analytics) four times with a cooling time of 1 minute between sessions. Extracts were partitioned into aqueous and organic layers following DCM treatment and centrifugation. Aqueous supernatants were dried by vacuum centrifugation with sample temperature maintained at -4°C

(Labconco, Kansas City MO, USA). Dry samples were suspended in 95µL of 50% ACN in H_2O, a 5µL aliquot of 12.5µM $^2H_6$-metformin internal standard was added to each sample and a volume of 5µL was injected for LC-MS/MS analysis. Metformin values are reported in pmol/mg of tissue.

Briefly, data were collected in positive electrospray ionization mode using an Agilent 1290 ultra-high pressure HPLC coupled to a 6540 Q-TOF mass spectrometer (Agilent Technologies). Gas temperature and flow were set at 325°C and 9 L/min respectively, nebulizer pressure was set at 45 psi, capillary voltage was set at 4000V and fragmentor was set at 140V. Ions used for reference mass correction were 922.0098 and 149.02332. MS/MS spectra were acquired on both metformin and $^2H_6$-metformin using 4 different collision energies (10, 20, 30 and 40V) to confirm compounds identity in samples extracts compared to authentic standards spectra. Metformin was separated from other analytes by reverse phase chromatography using a Pursuit PFP 2mm by 150mm, 3uM column coupled to a guard column (Agilent Technologies). Separation was achieved using binary solvent gradient of solvent A consisting of 0.05% formic acid in water and solvent B consisting of acetonitrile. The gradient consisted of 3 minutes at 100% A followed by a 5-min plateau at 100% B followed by re-equilibration at 100% A for 6 minutes. Ratios of endogenous metformin (m/z: 130.1087) to the internal standard (m/z: 136.1461) were compared to an external calibration curve with linear limits of detection from metformin standard sample

concentrations of 9.76E-9M to 8.00E-5M. Quality control and background quality control ($^2H_6$-metformin internal standard in water) samples run every 5 experimental samples. Blanks were run after QC samples and before the next experimental sample set. Five quality control samples (6.25E-7M of metformin and $^2H_6$-metformin solution) that were in the same concentration range as the experimental samples, where metformin was detected, gave an overall average variance from the expected concentration (average measured-expected/expected *100) of 11%.

2.10 16S rRNA Sequencing.

Fecal samples were collected between 7-9AM on the day prior to sacrifice. Fecal pellets were stored in autoclaved tubes at -80°C. A commercially available kit was used for DNA extraction (Zymo Research, Cat. No D6012). 16S rRNA amplification and sequencing was conducted in the McMaster Farncombe Institute Genomics Facility. Purified DNA was used to amplify the v3 region of the 16S rRNA gene by PCR. 50 ng of DNA was used as template with 1U of Taq, 1x buffer, 1.5 mM MgCl2, 0.4 mg/mL BSA, 0.2 mM dNTPs, and 5 pmoles each of 341F (CCTACGGGAGGCAGCAG) and 518R (ATTACCGCGGCTGCTGG) Illumina adapted primers, as described in Bartram *et al.* (2011)(Bartram, Lynch, Stearns, Moreno-Hagelsieb, & Neufeld, 2011). The reaction was carried out at 94°C for 5 minutes, 25 cycles of 94°C for 30 seconds, 50°C for 30 seconds and 72°C for 30 seconds, with a final extension of 72°C for

10 minutes. Resulting PCR products were visualized on a 1.5% agarose gel. Positive amplicons were normalized using the SequalPrep normalization kit (ThermoFisher#A1051001) and sequenced on the Illumina MiSeq platform at the McMaster Genomics Facility. Resulting sequences were run through the sl1p pipeline as described in Whelan *et al*. (2017) (Whelan & Surette, 2017).

2.11 Analysis of 16S rRNA Sequencing.

All microbiome analysis was conducted in R (version 3.4.4) (R Core Team, 2013). Data were curated using the phyloseq package (version 1.22.3) (McMurdie & Holmes, 2013) and all microbiome figures were plotted using ggplot2 (version 3.0.0) (Gómez-Rubio, 2017). OTUs were filtered to remove all non-bacterial reads and any OTUs present only once in the data set. Bray-Curtis distances were calculated using the distance() function in phyloseq, and PCoA plots were generated using phyloseq and ggplot2. To generate taxa bar charts, data were organized using the following tidyverse (Wickham, 2017) packages: dplyr (version 0.7.6), tidyr (0.8.1), and rlang (0.2.0). The plots were generated using ggplot2. Colour palettes used in the figures came from the RColorBrewer package (1.1.2) (Neuwirth, 2014). PERMANOVA tests were conducted using the vegan package (2.5.2). Butyrate pathway genes were identified using PICRUSt (Langille et al., 2013) and exploratory analysis of differential expression of genes of interest was modeled using the DESeq2 package (version 1.18.1) (Love, Huber, & Anders, 2014). Hypothesis testing of differential abundance of genera, families,

and phyla previously shown to change with metformin administration was also conducted using DESeq2. Exploratory analysis of OTUs contributing to the separation of metformin-treated and control mice was conducted using LEfSe (Segata et al., 2011) with all default parameters. Linear models of Shannon and Simpson diversity were fit using lm() in R.

2.12 Statistical Analysis.

Unless stated otherwise, all data is presented as mean with SEM. Data were analyzed and plotted in GraphPad Prism 6 (La Jolla, CA), except for 16S rRNA analysis, analyzed as described above. Depending on experimental design, t-tests, 1-way and 2-way ANOVA were used to test for significant variation, and post-hoc Tukey test or Fisher LSD was used to test for differences between groups. Significance was determined at $p<0.05$.

Chapter 3: Results

3.1 Effect of 100mg/kg metformin on metabolism in chow- and HFD-fed mice.

Previous reports have shown that the anti-tumor effects of metformin on the MC38 colon cancer cell line are only observed on the background of diet-induced obesity (Algire et al., 2010). Therefore, study 1 was conducted to confirm stimulatory effects of HFD on metabolism and MC38 allograft growth, glucose and insulin sensitivity and tumor growth was measured in chow- and HFD-fed C57BL6 mice treated with metformin (Fig 3.1A, B). In chow animals, bodyweight was not affected by control or metformin i.p. injections (Fig. 3.2A). Similarly, no changes in percent body fat were detected (Fig. 3.2B). Glucose tolerance was not different between control and metformin treatment; however, insulin tolerance was improved by metformin treatment (Fig. 3.2 C-F). In mice fed 45% HFD for 12 weeks, metformin treatment had no effect on body weight or adiposity after 4 weeks of treatment (Fig 3.3A, B). Additionally, no differences in glucose or insulin tolerance were detected between control and metformin-treated mice (Fig 3.3 C-F). HFD-fed animals were given different doses of both glucose and insulin compared to chow mice for tolerance testing (2g/kg vs 1g/kg glucose and 0.6U/kg vs 1U/kg insulin for chow and HFD-fed mice, respectively). This suggests that HFD-fed animals did have significant glucose and insulin intolerance compared to chow controls, evident by the similar GTT AUC values achieved despite a doubled dose of glucose for HFD-fed mice (1459 ±127 mM•min vs 1614 ± 314 mM•min in chow- and HFD-fed animals, respectively, Fig 3.2D, 3.3D). Similarly, 6-hour fasted blood glucose was elevated in HFD-fed

mice compared to chow-fed mice (Fig. 3.4A). Fed insulin was measured in blood collected after a 12-hour fast, and a 2-hour re-feeding period. HFD-fed mice had a strong tendency for elevated insulin, with a mean concentration of 5.79ng/mL compared to 1.14ng/mL in HFD and chow mice (p=.0515), respectively (Fig. 3.4B). Metformin treatment tended to lower serum insulin levels in HFD-fed animals, however this was not a statistically significant effect (p=0.3286).

3.2 Effect of diet and metformin treatment on MC38 colon cancer allografts.

HFD feeding has been shown to stimulate MC38 murine colon cancer allograft growth (Algire et al., 2011; Algire et al., 2010). This effect is confirmed in the current data, with HFD mice experiencing significantly elevated tumor growth compared to chow mice (Fig. 3.4C). By endpoint, HFD control mice had tumor volumes over 2-fold higher than chow controls (520.6mm^3 vs 237.2mm^3, respectively) (Fig. 3.4D). Despite the growth stimulation caused by HFD, there were no observable differences in either HFD or chow-fed mice receiving metformin injections. To examine the potential relationship between circulating glucose and insulin levels on tumor volumes, correlations were calculated. 6-hour fasted blood glucose has a significant positive correlation with tumor volume (R^2=0.2482, 95% CI: 0.1294 to 0.7148; Fig. 3.4E), but 12h-hour fasted blood glucose does not (R^2 = 0.1452, 95% CI: -0.1413 to 0.7158). Similarly, fed serum insulin was not correlated to tumor volume (R2=0.0052,

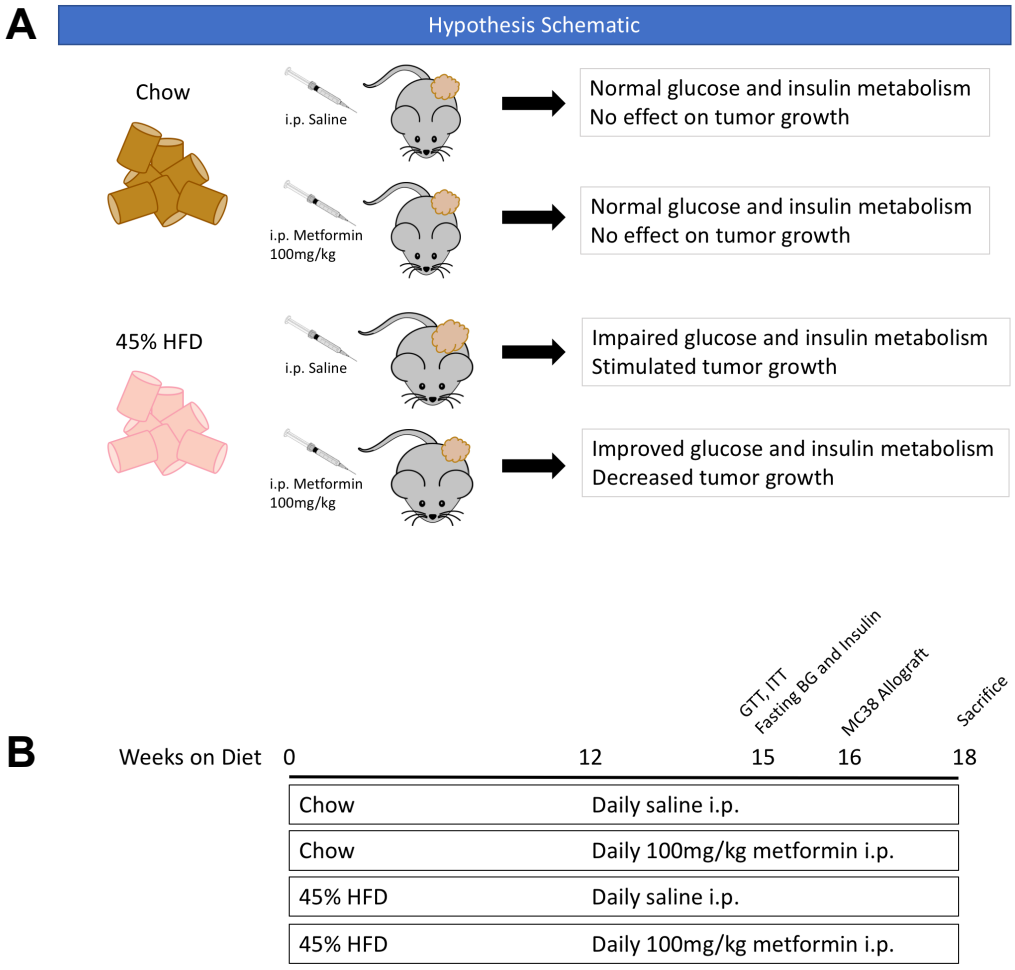

Figure 3.1: Hypothesis schematic and experimental timeline for study 1: Effect of daily 100mg/kg i.p. metformin in mice fed chow and HFD.

A) Hypothesis schematic depicting hypothesized outcomes in the treatment groups. B) Study timeline.

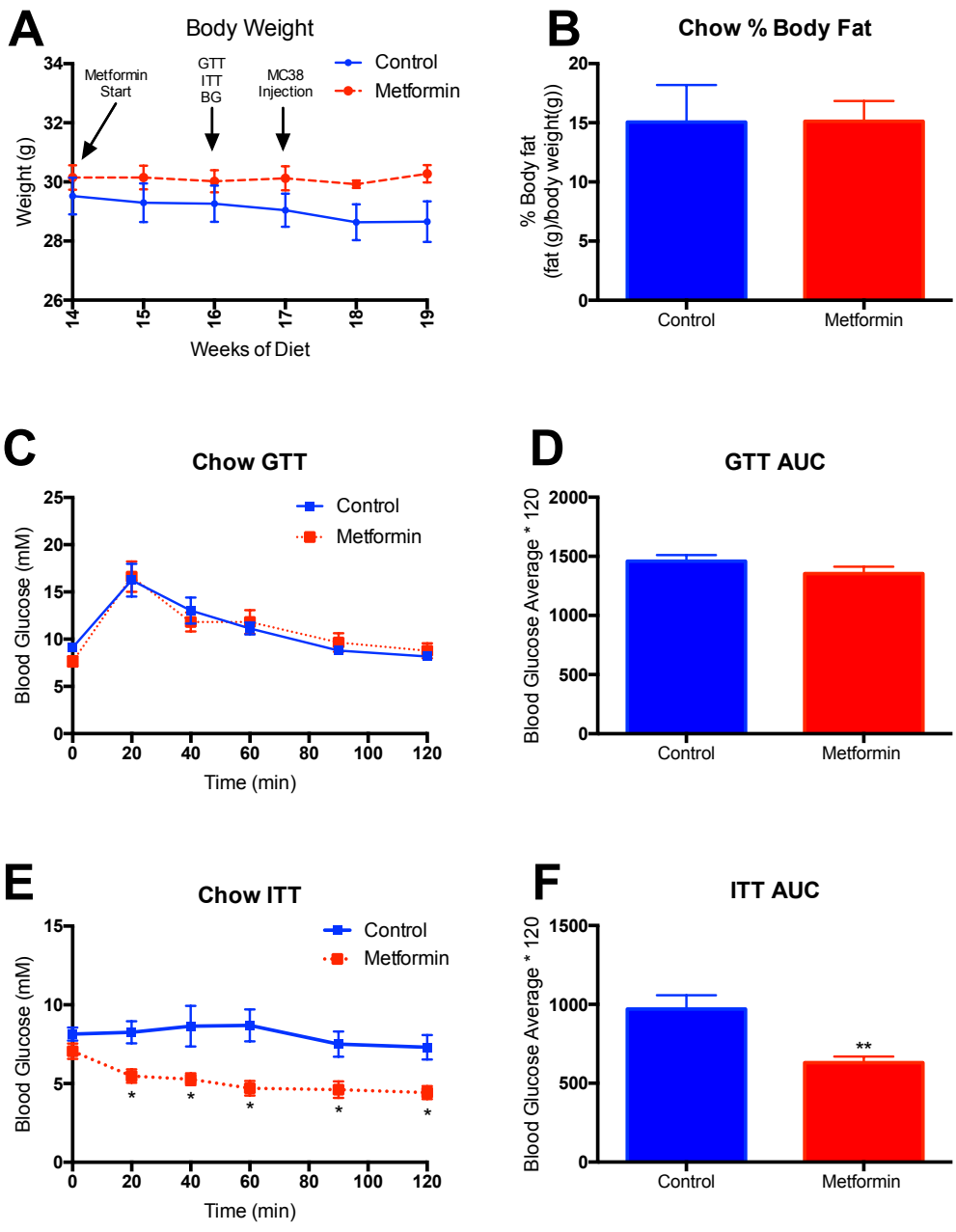

Figure 3.2: Metabolic effects of daily 100mg/kg i.p. metformin injections in mice on chow diet.

Figure 3.2: Metabolic effects of daily 100mg/kg i.p. metformin injections in mice on chow diet. Body weight was monitored during the treatment period (A). Percent adiposity was measured using a Whole-Body Composition Analyzer, and percent adiposity calculated as adipose mass(g)/total animal mass(g) (B). Glucose tolerance testing was conducted using 2g/kg body weight D-glucose, injected after a 6-hour fast (B). Area under the curve was calculated as average blood glucose * 120 minutes (C). Insulin tolerance testing was conducted using 0.6U/kg bodyweight insulin, injected after 6-hour fast (E). Area under the curve was calculated (F). Sample size is n=4-5 per group. 2-way repeated measures ANOVA with post-hoc Tukey testing and unpaired t-tests were used to test for differences between groups, with $p<0.05$ considered significant.

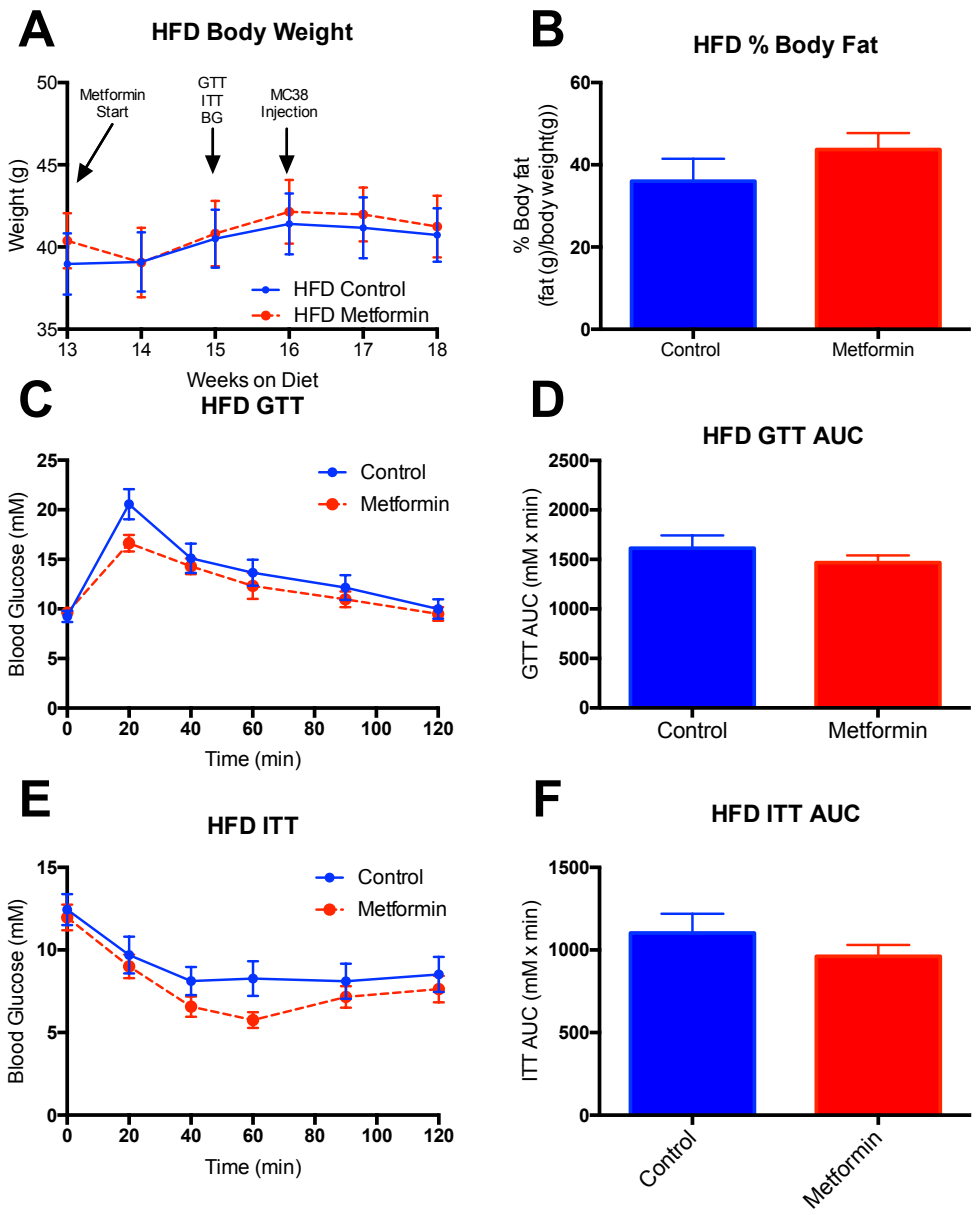

Figure 3.3: Metabolic effects of daily 100mg/kg i.p. metformin injections in mice on 45% HFD.

Figure 3.3: Metabolic effects of daily 100mg/kg i.p. metformin injections in mice on 45% HFD. Body weight was monitored for the duration of treatments (A). Percent adiposity was measured using a Whole-Body Composition Analyzer, and percent adiposity calculated as adipose mass/total animal mass (B). Glucose tolerance testing was conducted using 2g/kg body weight D-glucose, injected after a 6-hour fast (C). Area under the curve was calculated as average blood glucose * 120 minutes (D). Insulin tolerance testing was conducted using 1U/kg bodyweight insulin, injected after 6-hour fast (E). Area under the curve was calculated (F). Sample size is n=4-11 per group. 2-way repeated measures ANOVA with post-hoc Tukey testing and unpaired t-tests were used to test for differences between groups, with $p<0.05$ considered significant.

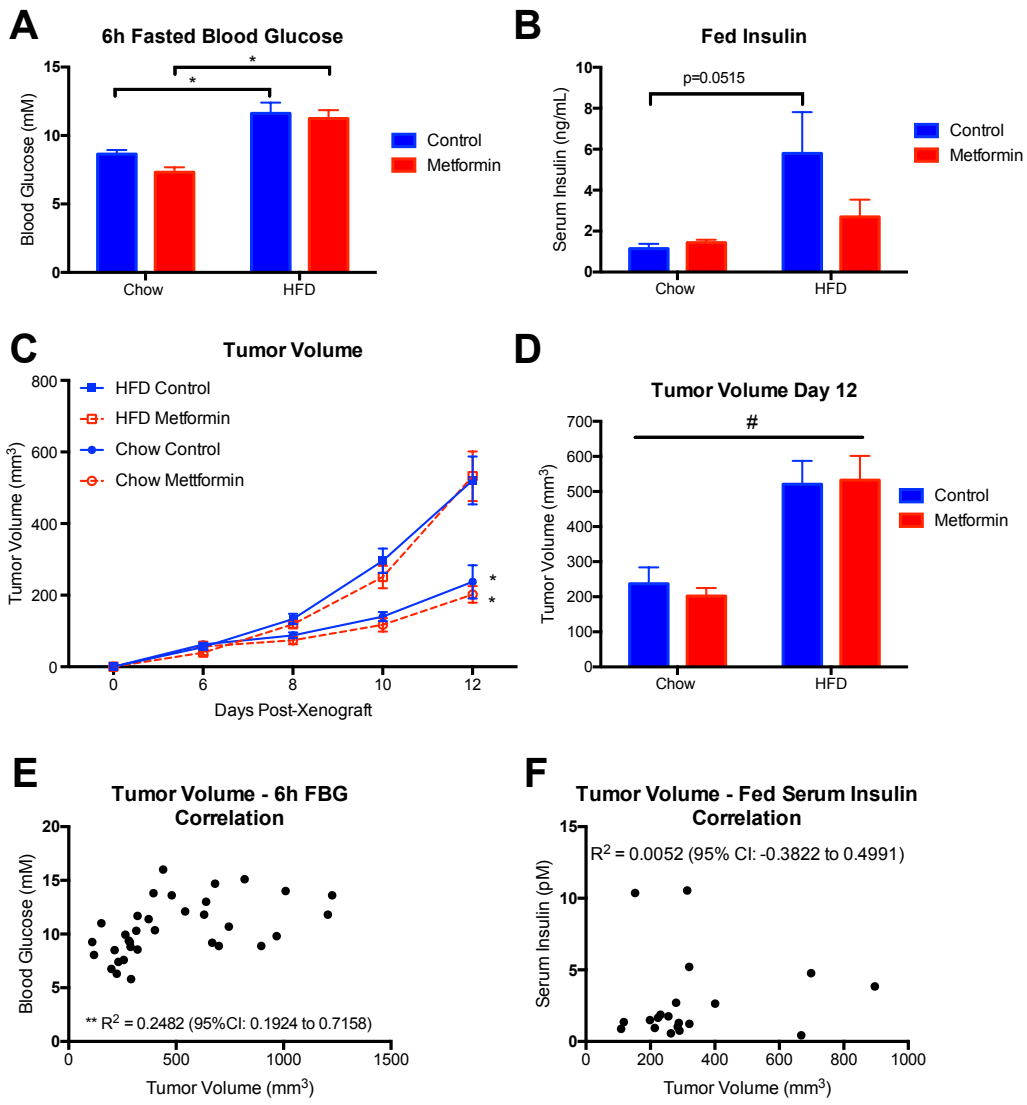

Figure 3.4: Effect of 100mg/kg i.p. metformin injections on glucose, insulin, and MC38 allograft growth in chow and 45% HFD-fed mice.

Figure 3.4: Effect of 100mg/kg i.p. metformin injections on glucose, insulin, and MC38 allograft growth in chow and 45% HFD-fed mice. Blood glucose was measured after 6-hours of fasting (A). Fed insulin was measured in serum taken after 12-hour fast followed by a 2-hour re-feed (B). After 4 weeks of treatments, animals were injected s.c. on the flank with $5x10^5$ MC38 cells. Tumor volume was measured every other day once tumors were palable (C), and final volumes on day 12 are plotted (D), with * indicating significant differences between Chow-Control vs HFD-Control, and Chow-Metformin vs HFD-Metformin, and # indicating an overall diet effect on tumor growth. Pearson correlation calculations were run on all chow and HFD animals, with matched tumor volumes and 6-hour fasted blood glucose (FBG)(E) or to fed serum insulin concentrations (F). Sample size is n=4-18 for each group. Repeated measures 2-way ANOVA were run on time-linked measurements, and 2-way ANOVA on all other grouped analyses, with post-hoc Tukey test were used to test for differences, with $p<0.05$ considered significant.

95% CI: -0.3822 to 0.4991; Fig. 3.4F). These data confirm the stimulatory effects that HFD feeding has on MC38 tumor growth.

3.3 Metformin concentration in tissues with i.p. administration.

Metformin is a cation, and requires transporters to be brought into the cell. As such, to consider the direct effects of metformin on tumor growth, it must first be transported into the cancer cell. We measured the concentration of metformin in serum, tumor, liver, brown adipose tissue (BAT) and gastrocnemius skeletal muscle 2-hours after an i.p. injection of 100mg/kg metformin (Fig. 3.5A,B). Serum metformin after 2-hours was 23μM, similar to what has been reported in the literature with comparable metformin delivery (Chandel et al., 2016; Memmott et al., 2010). Metformin concentrations in liver and MC38 allograft tumor tissue 2-hours after i.p. injection were 30.6 and 26.1pmol/mg (approximately 3.1 and 2.6μM), respectively. Additionally, a correlation calculation between tumor metformin concentrations and tumor volumes was conducted, and was found to not be significant ($R^2 = 0.7681$, 95% CI: -0.9918 to 0.02583).

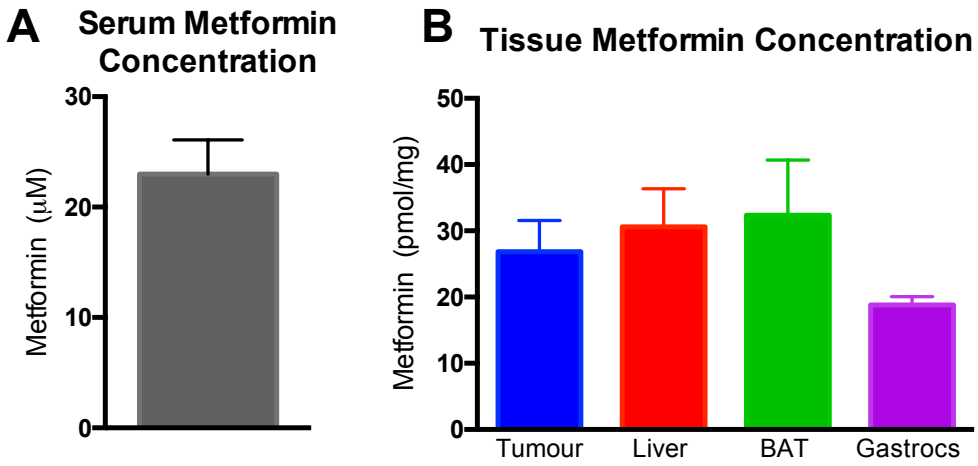

Figure 3.5: Metformin concentration in serum and tissues with daily 100mg/kg i.p. metformin injections.

Metformin concentration was measured in serum (A) and tissues (B) of HFD-fed mice at experimental endpoint. Samples (n=5) were taken 2-h post injection of 100mg/kg i.p. metformin and measured using LC-MS analysis.

3.4 AMPK and mTOR signaling in MC38 allograft tumors in mice on 45% HFD.

AMPK activation in MC38 allograft tumors has been previously reported with both oral and i.p. administration of metformin, however the conditions (ie. timing post-treatment) in which tumor tissue was collected were unclear (Algire et al., 2011; Algire et al., 2010). In our chronically-treated animals, tumor tissue was removed 6 hours after the last injection of metformin, and immunoblotting was used to assess signaling changes in the AMPK and mTOR pathways. At this time point, there were no detectable changes in AMPK or ACC phosphorylation status, as measured by pAMPK-T172 and pACC-S79 (Fig. 3.6A-C). ACC is used as a read-out of AMPK activation, as it can account for both allosteric and covalent mechanisms of AMPK activation in the cell, in addition to its inhibitory effects on *de novo* lipogenesis (Ford et al., 2015). mTOR protein synthesis pathway signaling was also assessed, by measuring the phosphorylation of the down-stream protein kinase p70S6K-T389, and the AMPK-specific phosphorylation of Raptor-S792. At these two points in the mTOR signaling cascade, chronic metformin resulted in no significant changes in phosphorylation states of p70S6K or Raptor (Fig. 3.6D-F) Immunoblotting of the activation of protein kinase B (Akt) protein was also conducted. Akt phosphorylation occurs at two sites, and is a result of the insulin signaling cascade. The T308 site is activated by phosphoinositide-dependent protein 1 (PDK1), and the S473 site is activated by

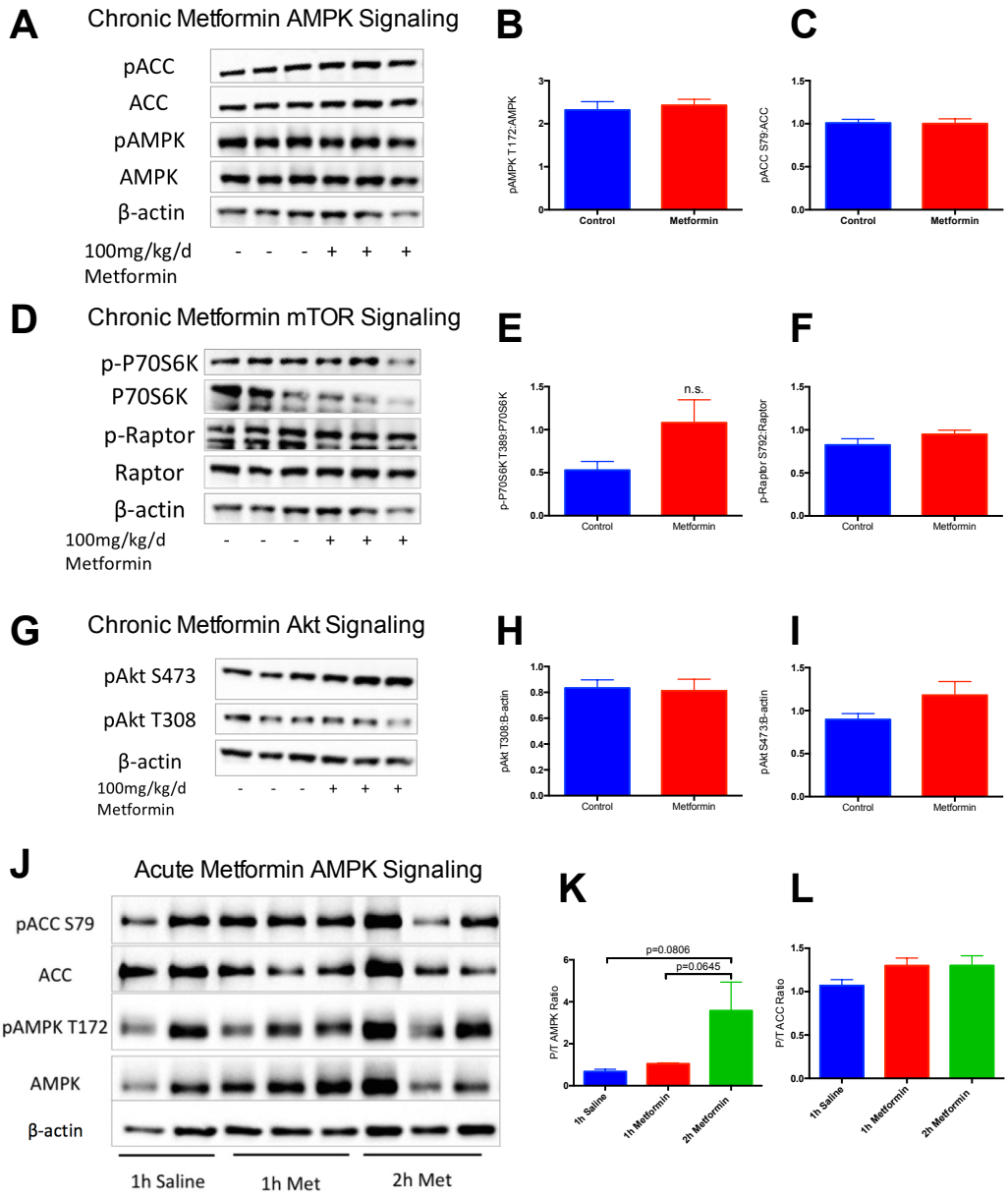

Figure 3.6: Chronic and acute effects of 100mg/kg i.p. metformin on signaling pathways.

Figure 3.6: Chronic and acute effects of 100mg/kg i.p. metformin on signaling pathways. Tumor allografts grown in 45% HFD-fed mice were chronically treated with i.p. injections of vehicle or 100mg/kg metformin. Chronically-treated tumors were collected 6-hours post-injections, and were snap frozen in liquid nitrogen and processed for Western blotting. 10μg per well of protein was loaded for blots, of which A), D) and G) are representative. Densitometry for phosphorylated over total AMPKα T175 (B), ACC S79 (C), P70S6K T389 (E), Raptor S792 (F) and pAkt S473 (H) and pAkt T308 (I) were normalized to β-actin or their non-phosphorylated control. Acute *in vivo* AMPK pathway signaling was measured in MC38 allograft tissue 1 or 2 hours post-i.p. injection of metformin (100mg/kg). Sample size is n=3-6 for each treatment group. Student's t-test and 1-way ANOVA with post-hoc Tukey's tests were run to test for statistical differences at $p<0.05$.

mTORC2 (Mackenzie & Elliott, 2014). In MC38 tumor allografts chronically exposed to metformin, levels of phosphorylation at either residue was not affected (Fig. 3.6G-I). Knowing that metformin has a relatively short half-life (5-6 hours)(Wilcock & Bailey, 1994), we conducted acute metformin exposure experiments to assess effect of i.p. metformin on MC38 tumor allograft signaling 1- or 2-hours post-injection. In these animals, there was a trend to elevated AMPK phosphorylation, at the 2-hour time point compared to both saline control, and 1-hour metformin samples (Fig. 3.6 J,K). Phosphorylation of ACC was also measured, and was comparable between vehicle and metformin treated mice (Fig. 3.6 L).

3.5 Direct effect of metformin on MC38 cell growth and AMPK signaling.

To better understand how the MC38 murine colon cancer cell line responds to metformin, we assessed *in vitro* clonogenic growth and associated changes in AMPK signaling with metformin. Recent work has shown that cancer cell lines have varied responses to glucose availability in culture due to changes in oxidative phosphorylation capacity, and that this can affect response to biguanides (Birsoy et al., 2014). Therefore, MC38 cells were grown in normal 25mM (high) glucose DMEM, and 5mM low-glucose DMEM (a concentration closer to physiological concentrations). The effect of glucose concentration in the media had no measurable effect on metformin response, resulting in IC_{50} concentrations of 2.0mM and 2.4mM in high- and low-glucose media, respectively (Fig. 3.7A).

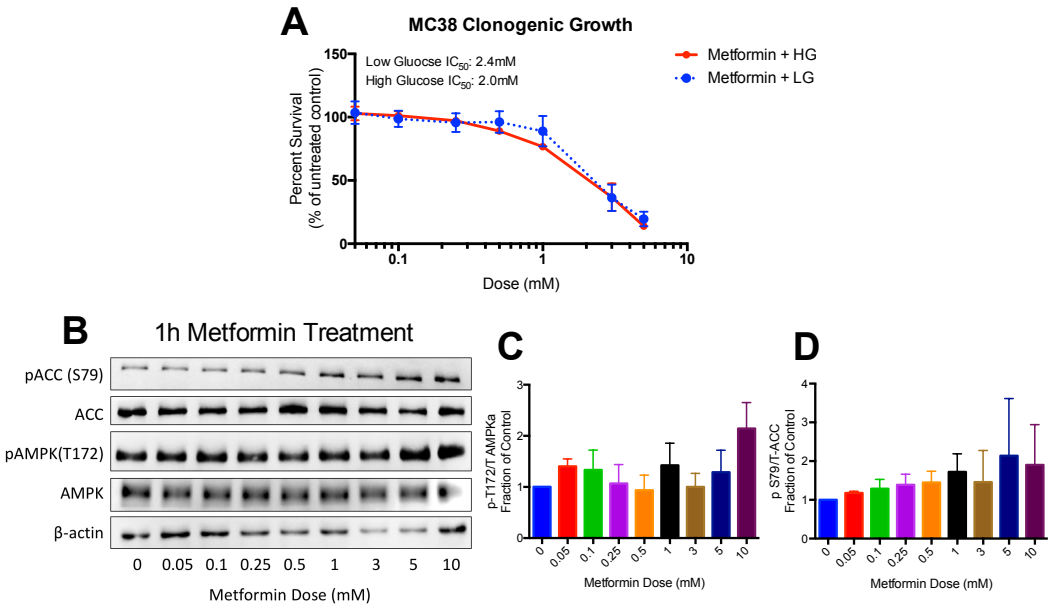

Figure. 3.7: In vitro effects of metformin on growth and AMPK signaling in MC38 murine colon cancer cells.

Clonogenic growth was assessed by seeding 200 cells/well in 12-well plates in low (5mM) and high (25mM) glucose media, treated with metformin (0.05-5mM), and allowed to grow for 5 days when colonies of >50 cells had grown. Colonies were stained with crystal violet, counted, normalized to untreated control (100%) and used to calculate IC_{50} concentrations, after performing a log(x) transformation and running non-linear regression analysis (A). AMPK signaling was measured in MC38 cells grown in low-glucose media treated with metformin for 1 hour (B-D), and densitometry was measured. 1-way ANOVA tests were run to determine statistical significance of the treatments at $p<0.05$, and sample size is n=3-4 for each experiment.

AMPK signaling was measured in MC38 cells grown in low-glucose media after an acute 1-hour treatment to a range of metformin doses. At this time point, there were no measurable changes in AMPK or ACC phosphorylation (Fig 3.7 B-D).

3.6 Oral metformin treatment improves metabolic outcomes in 45% HFD-fed mice and is blunted by ampicillin exposure.

Since i.p. injections of metformin were unable to elicit measurable changes in MC38 tumor growth in HFD-fed mice, we questioned if it was due to the systemic delivery of the drug. Oral metformin deliver in mouse models has been shown to reduce MC38 tumor growth, as well as other cancer cells (Algire et al., 2010; Cufí et al., 2013; Lau et al., 2014). Additionally, recent evidence suggests that the gut microbiome is involved in mediating the glucose-sensitizing effects of metformin, an effect which would be bypassed with i.p. or i.v. injections (Wu et al., 2017). Therefore, we treated C57BL/6J mice on 45% HFD with 250mg/kg metformin in drinking water, with and without ampicillin treatment (1g/L). The presence of ampicillin in drinking water is known to decrease the overall numbers of bacteria in the gut microbiome (Membrez et al., 2008). The hypothesis of this study was that oral metformin dosing would lower blood glucose, serum insulin and tumor growth compared to control, and that ampicillin would blunt these effects (Fig. 3.8 A). This was conducted using the same feeding and treatment timeline as the i.p. metformin study (Fig. 3.8 B). Animal weights were tracked throughout the study, and metformin treated animals

had slightly lower body weights after treatment initiation (Fig. 3.9A). Antibiotic addition to drinking water may affect how much water the animals consume, so this was measured. Mice in the metformin and ampicillin group consumed less water (Fig. 3.9B). However, this is not expected to impact metformin exposure, as metformin water was adjusted weekly to reflect changes in bodyweight and water consumption, maintaining a dose of 250mg/kg. Glucose tolerance testing confirmed oral metformin's effectiveness to improve glucose clearance, and the presence of ampicillin impaired this effect (Fig. 3.9C**)**. However, ampicillin on its own was found to have glucose sensitizing effects alone and with metformin at the 40-minute time point. Oral metformin treatment resulted in a significant decrease in the rate of change of glucose in the blood (as measured by the AUC), and ampicillin alone and with metformin had no measurable differences from control (Fig. 3.9D). At the time of the GTT, body weights were not significantly different, suggesting the improvement in glucose tolerance is likely not related to reduced body weight. (Fig 3.9E) Insulin sensitivity was also tested, and due to variation at baseline, analyzed relative to the percent of baseline. Oral metformin resulted in the greatest decrease in blood glucose in response to insulin, and was significantly lower than metformin + ampicillin treated mice (Fig. 3.8F). However, the overall results of this test resulted in no detectible difference between groups (Fig 3.9G). Body weights at the time of ITT testing were not different between groups (Fig. 3.9H). Fasting blood glucose was not different between groups, however when calculating the difference (delta) in fasting blood

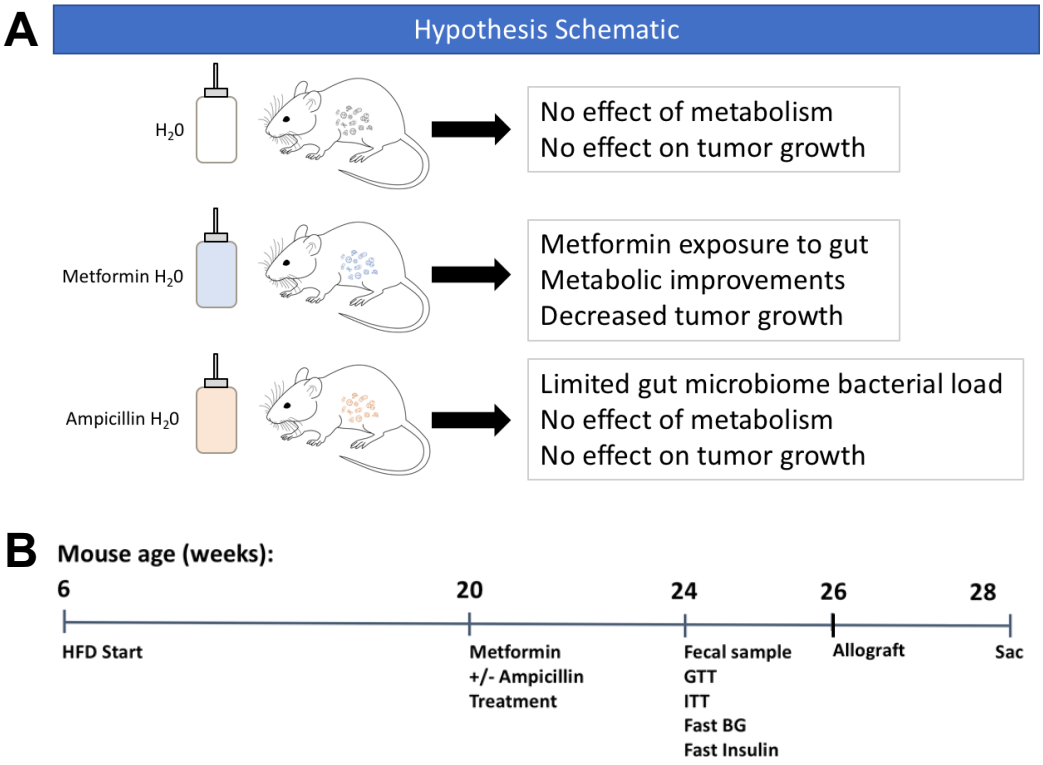

Figure 3.8: Hypothesis schematic and design for study 2: The effects of oral metformin on colon cancer in mice on HFD.

A) Hypothesis schematic depicting hypothesized outcomes in the treatment groups. B) Study timeline.

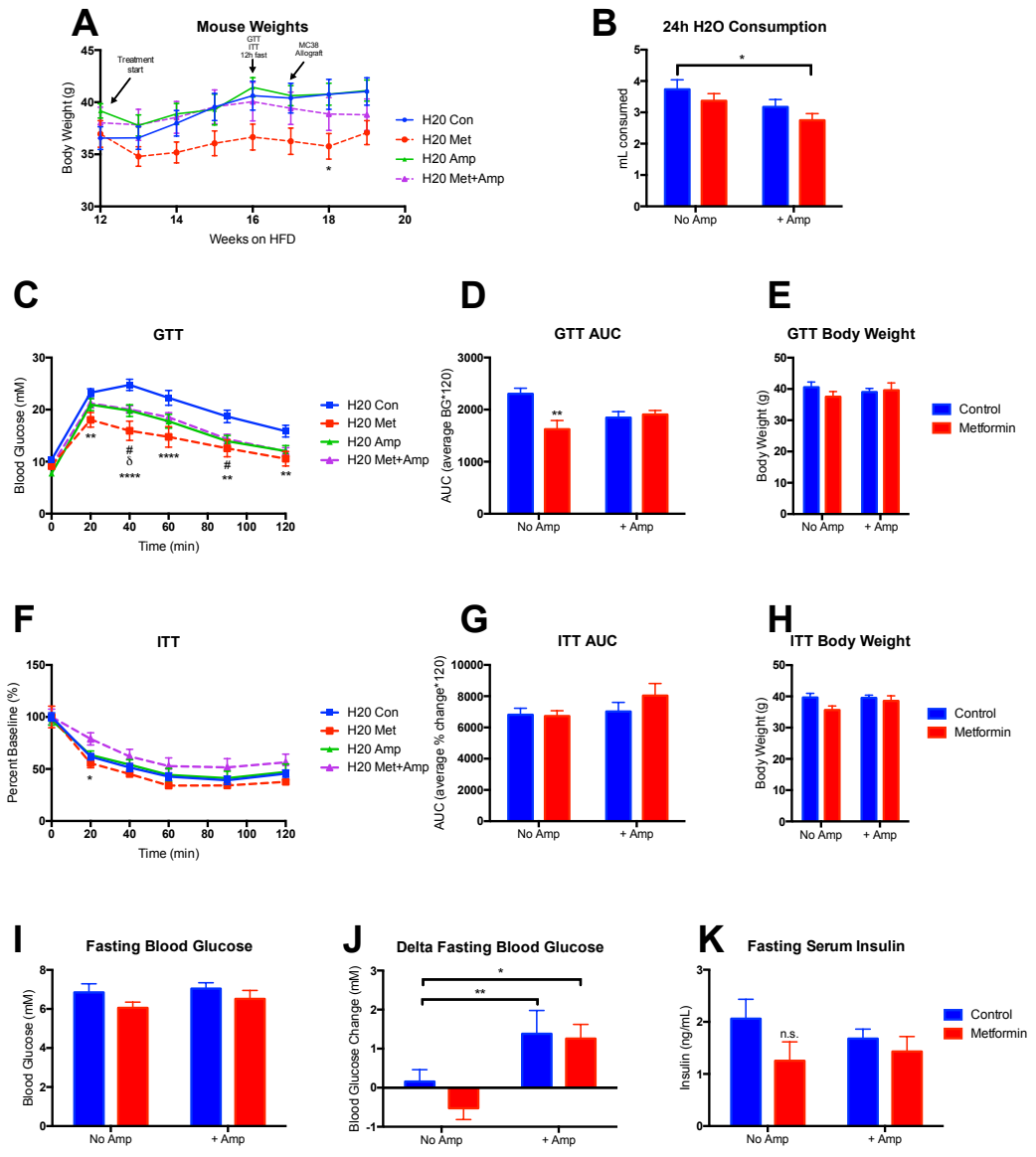

Figure. 3.9: Effect of oral metformin and ampicillin on metabolic outcomes.

Fig. 3.9: Effect of oral metformin and ampicillin on metabolic outcomes.

A) Mouse body weight during weeks of HFD feeding. B) 24h water consumption. Glucose tolerance tests were conducted by fasting mice for 6h, and injected with 2mg/kg glucose (C), and blood glucose measured over time. * indicates differences between H20 Con and H20 Met, # indicates differences between H20 Con and H20 Amp, and δ indicating H20 Con and H20 Met+Amp differences. Area under the curve was measured by calculating the average blood glucose * 120 minutes (D), and bodyweight on the day of the GTT is plotted (E). Similarly, insulin tolerance (ITT) was measured, using 1U/kg insulin (F), with * indicating differences between H20 Met and H20 Met+Amp. Area under the curve was also calculated (G), and body weight on the day of ITT (H). Fasted blood glucose, delta blood glucose (baseline blood glucose – 4-weeks treated blood glucose) and serum insulin were measured after mice were fasted overnight for 12 hours (K). Sample size is n=5-12 per group. Repeated measures (for time-sensitive measurements) and non-repeated measures 2-way ANOVA were used test for differences, with post-hoc Tukey or Sidak testing to detect differences between groups, and significance determined at $p<0.05$. * $p<0.05$, ** $p<0.01$.

glucose before and after treatments, ampicillin exposure elevated blood glucose over 4 weeks of treatments (Fig. 3.9 I,J). Fasting serum insulin was also measured, with no measurable effect of metformin or ampicillin treatments (Fig. 3.9K).

3.7 Oral metformin inhibits MC38 tumor allograft growth in mice fed 45% HFD and is impaired by ampicillin exposure.

After the metabolic findings showing ampicillin treatment impairs the metabolic effects of metformin in HFD-fed mice, we continued to study how these treatments affect the growth of a colon cancer allograft. Oral metformin was found to significantly inhibit MC38 tumor growth (32.5% decrease compared to controls), and this effect was lost with the presence of ampicillin in the system (Fig 3.10A). By endpoint measurement, there were no detectible differences between both ampicillin and ampicillin + metformin groups compared to control, but metformin alone significantly decreased tumor volume (Fig. 3.10B). At endpoint, tumour weights were also measured, and an overall effect of metformin was detected among the 4 groups (Fig. 3.10C). To test for a relationship between tumor volume and metabolic outcomes, we calculated correlation statistics between tumor volume and 6-hour and 12-hour fasted blood glucose, and fasted serum insulin. 6-hour fasted blood glucose was correlated with tumor volume by end-point (R^2=0.1109, 95% CI: 0.04732 to 0.5684; Fig. 3.9D) but 12-hour fasted blood glucose was not (R^2=0.02004, 95% CI: -0.1551 to 0.4148). Fasted serum

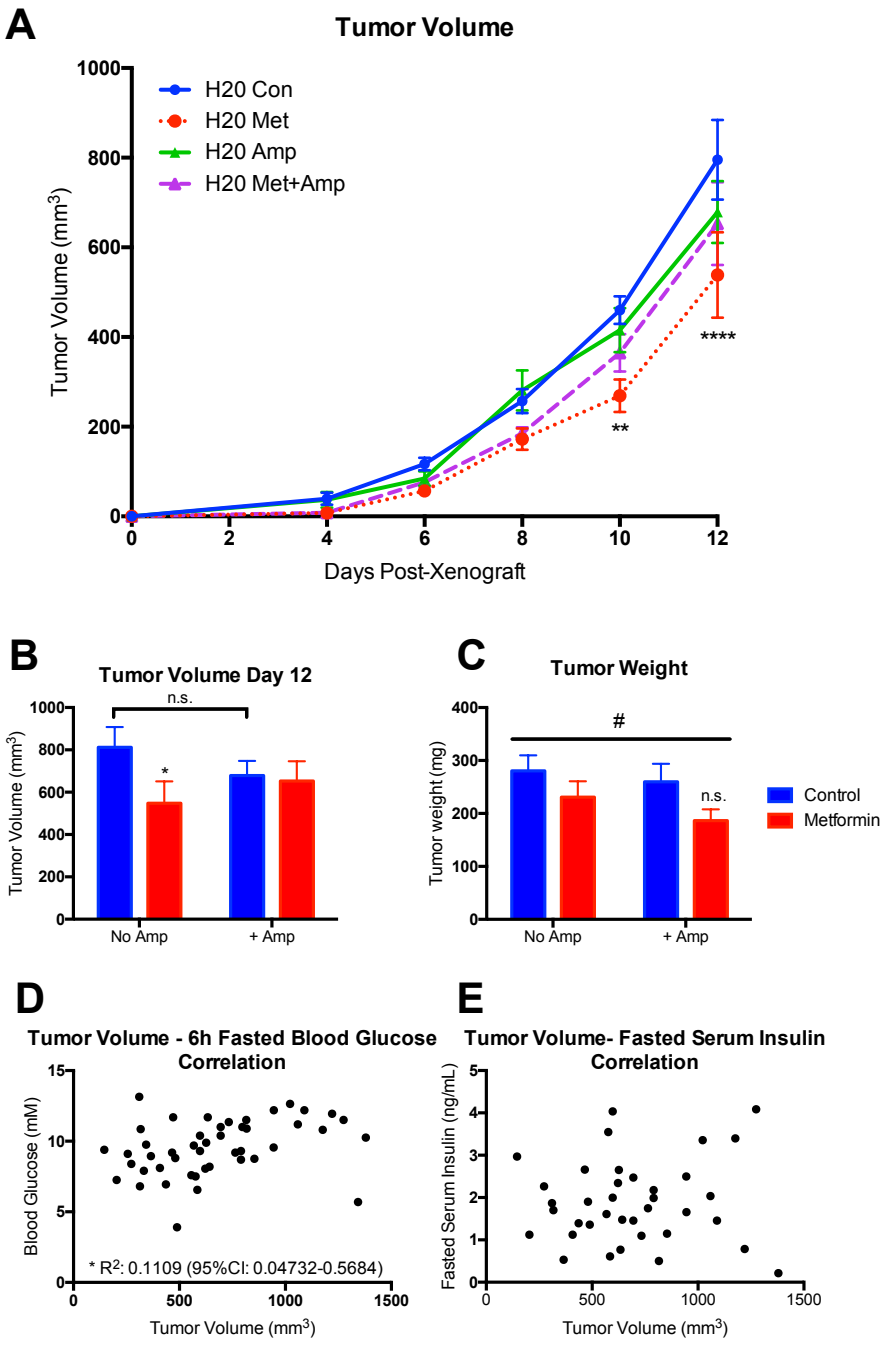

Figure 3.10: Effect of oral metformin and ampicillin on MC38 tumor growth.

Fig 3.10: Effect of oral metformin and ampicillin on MC38 tumor growth. After 4 weeks of treatments, mice were injected s.c. with $2.5x10^5$ MC38 cells. Once tumors were palpable, tumor volume measurements were taken every other day (A), with * indicating differences between H20 Con and H20 Met. Endpoint tumor volume (B), tumor weight (C), and body weight (D) were measured after removal, with # indicating an overall metformin effect. Pearson correlation calculations were run on matched tumor volumes to 6-hour fasted blood glucose (E) or to fasted serum insulin concentrations (F). Sample size is n=5-12 per group. 2-way ANOVA with post-hoc Tukey test or Fisher LSD testing was used, with $p<0.05$ considered significant.

insulin was also not correlated to tumor volume (R2=0.00342, 95% CI: -0.2707 to 0.3754; Fig 3.10E).

3.8 Fecal microbiome transfer from metformin-treated mice on HFD to HFD-fed mice does not affect metabolic outcomes.

With the findings that ampicillin treatment blunted some of the effects of oral metformin treatment to lower blood glucose and tumor volumes, designing a study to isolate the effects of metformin on the gut microbiome became an area of focus. To test the microbiome effects alone, we conducted a fecal microbiome transfer (FMT) study in C57B6/J mice on 45% HFD. Our hypothesis was that the microbiome is a key factor in metformin's metabolic and anti-cancer effects, and that these effects will be transferrable via FMT (Fig. 3.11A). FMT has been used in recent years to gain a better understanding of the role of the microbiome on a variety of effects, including metformin's effects on glucose homeostasis in people with type 2 diabetes (Bauer et al., 2018; Kulecka et al., 2016; Lundberg, Toft, August, Hansen, & Hansen, 2016; Wu et al., 2017; Zhou et al., 2017). In this study, the same feeding and treatment timeline was used as in the previous studies, and mice were separated into donor mice (receiving control or 250mg/kg metformin water) or microbiome recipient (MB) mice, receiving a dilution of fecal material from donors (Fig. 3.11B). Body weight was measured for the duration of the study, and was not different between control MB or metformin MB groups (Fig. 3.12A). Similarly, after 4 weeks of gavage from control or

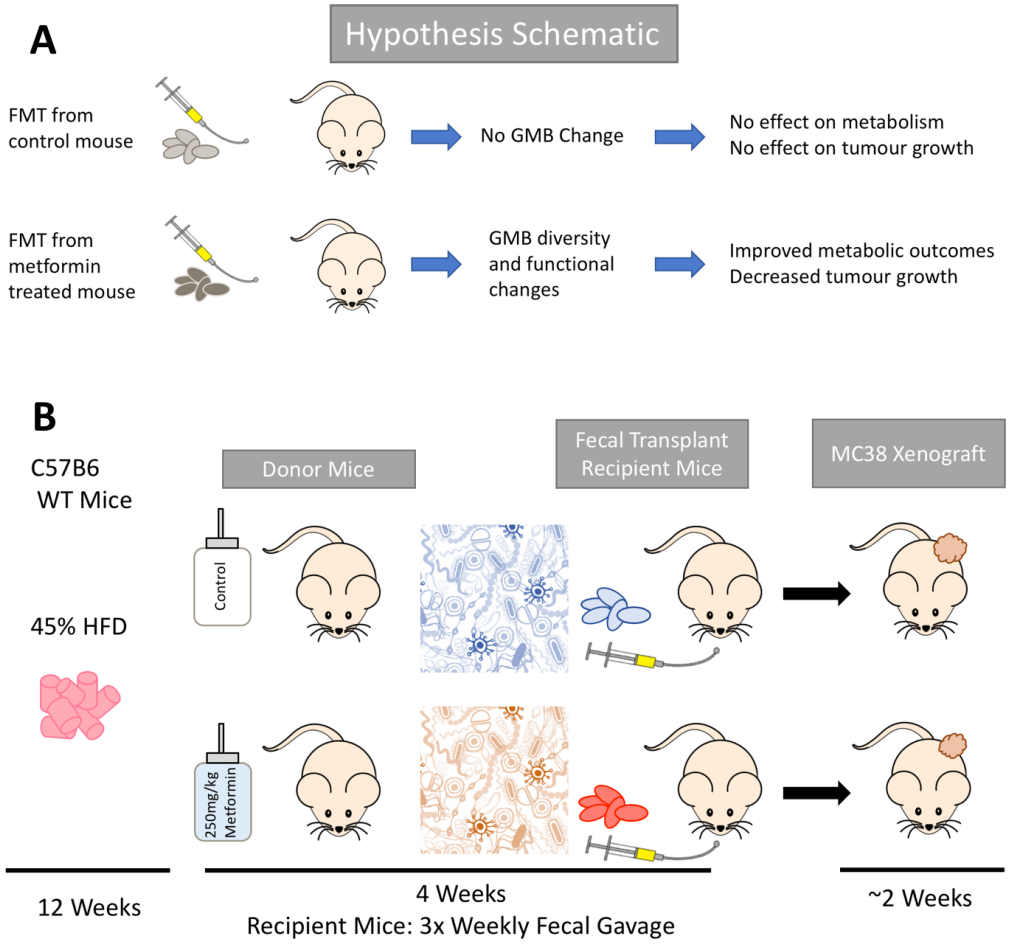

Figure 3.11 – Hypothesis schematic and study timeline for study 3: The role of the gut microbiome on metformin's anti-cancer effects

A) Hypothesis schematic depicting hypothesized outcomes in the treatment groups. B) Study timeline.

metformin treated donors, there was no measurable change in % body fat (Fig. 3.12B). Interestingly, there was no treatment effect on either glucose or insulin tolerance testing, comparing control MB to metformin MB animals (Fig. 3.12 C-F). Fasting blood glucose and serum insulin were also measured, and found to not be different between control MB and metformin MB mice (Fig. 3.12G,H).

3.9 Fecal microbiome transfer from metformin treated mice inhibits colon cancer allograft growth.

To test if FMT from metformin-treated mice affects colon cancer growth, control MB and Metformin MB mice were injected with MC38 colon cancer cells. Metformin MB mice experienced significant tumour growth inhibition, with a ~30% decrease in growth compared to HFD control by day 12 (Fig 3.13A, C). This effect is mirrored by a reduced rate of growth, as measured by the AUC, and a strong trend towards a decreased *ex-vivo* tumor volume (measured after tumor tissue is removed from the animal) (Fig. 3.13 B, D). Similar to previous experiments, 6-hour fasting blood glucose significantly correlated with tumor volume (R^2=0.1473, 95% CI: 0.04657-0.6424), despite no significant changes in 6-hour fasted blood glucose levels between control MB and metformin MB groups (9.6mM and 10.1mM in control MB and metformin MB animals, respectively; Fig. 3.13E). Neither 12-hour fasting blood glucose or fasting serum insulin was not correlated to tumor volume, similar to results in studies one and

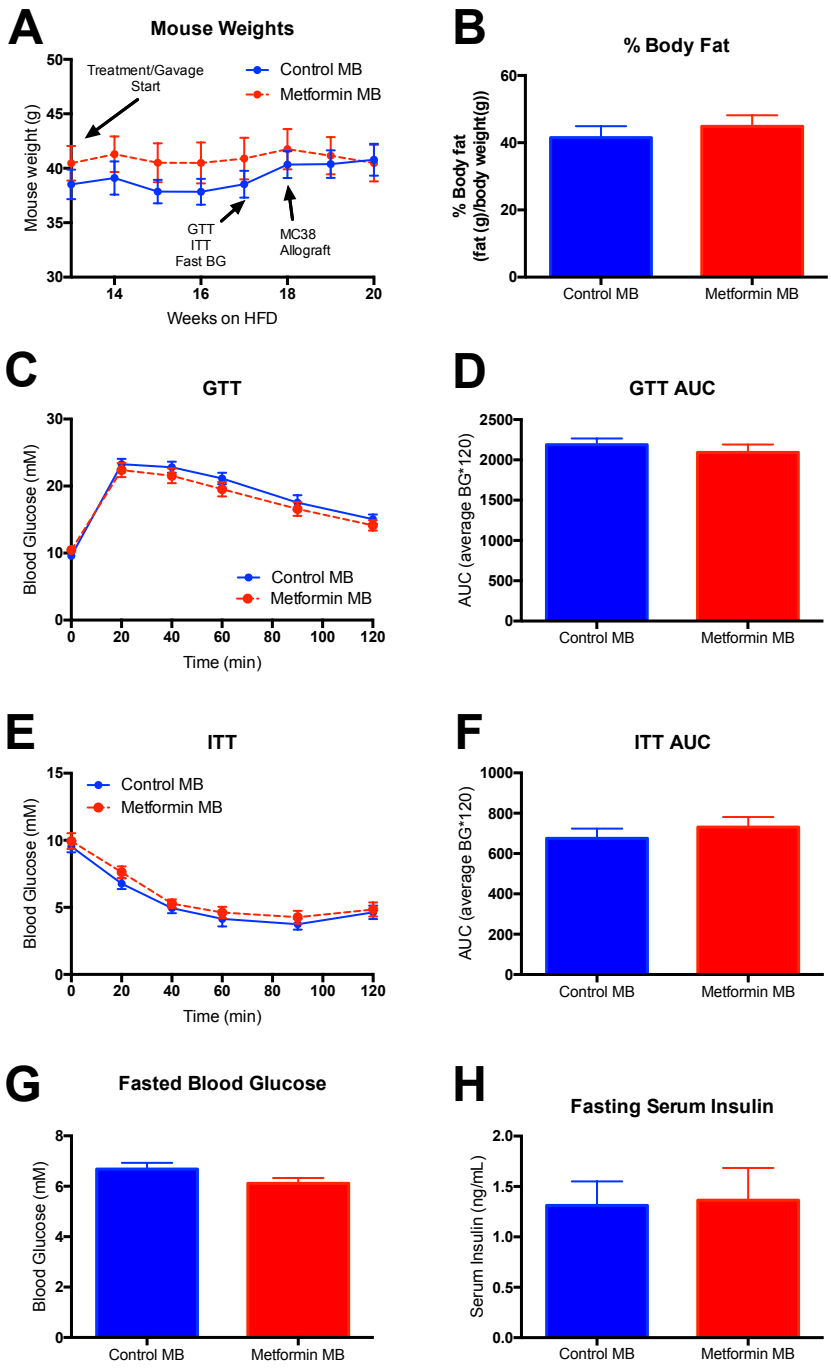

Figure 3.12: Fecal microbiome transfer effects on glucose and insulin metabolism.

Figure 3.12: Fecal microbiome transfer effects on glucose and insulin metabolism.

Mouse weights were measured during the gavage treatment period (A). Percent adiposity was measured using a Whole-Body Composition Analyzer, and percent adiposity calculated as adipose mass/total animal mass (B). Glucose tolerance testing was conducted after fasting mice for 6h, and an i.p. injection of 1g/kg of D-glucose, and blood glucose was measured over time (C). The area under the curve (AUC) was calculated to assess overall changes in glucose tolerance, calculated as the average blood glucose x 120 minutes (D). Similarly, ITT was conducted, with an i.p. injection of 1U/kg insulin (E, F). After an overnight, 12-hour fast, blood glucose and serum insulin was measured (G, H). Sample size is 9-17 per group. Repeated measures 2-Way ANOVA with post-hoc Tukey test to test for simple effects within rows was used for time-linked measurements, and unpaired t-tests were used for single variable comparisons, with $p<0.05$ considered significant.

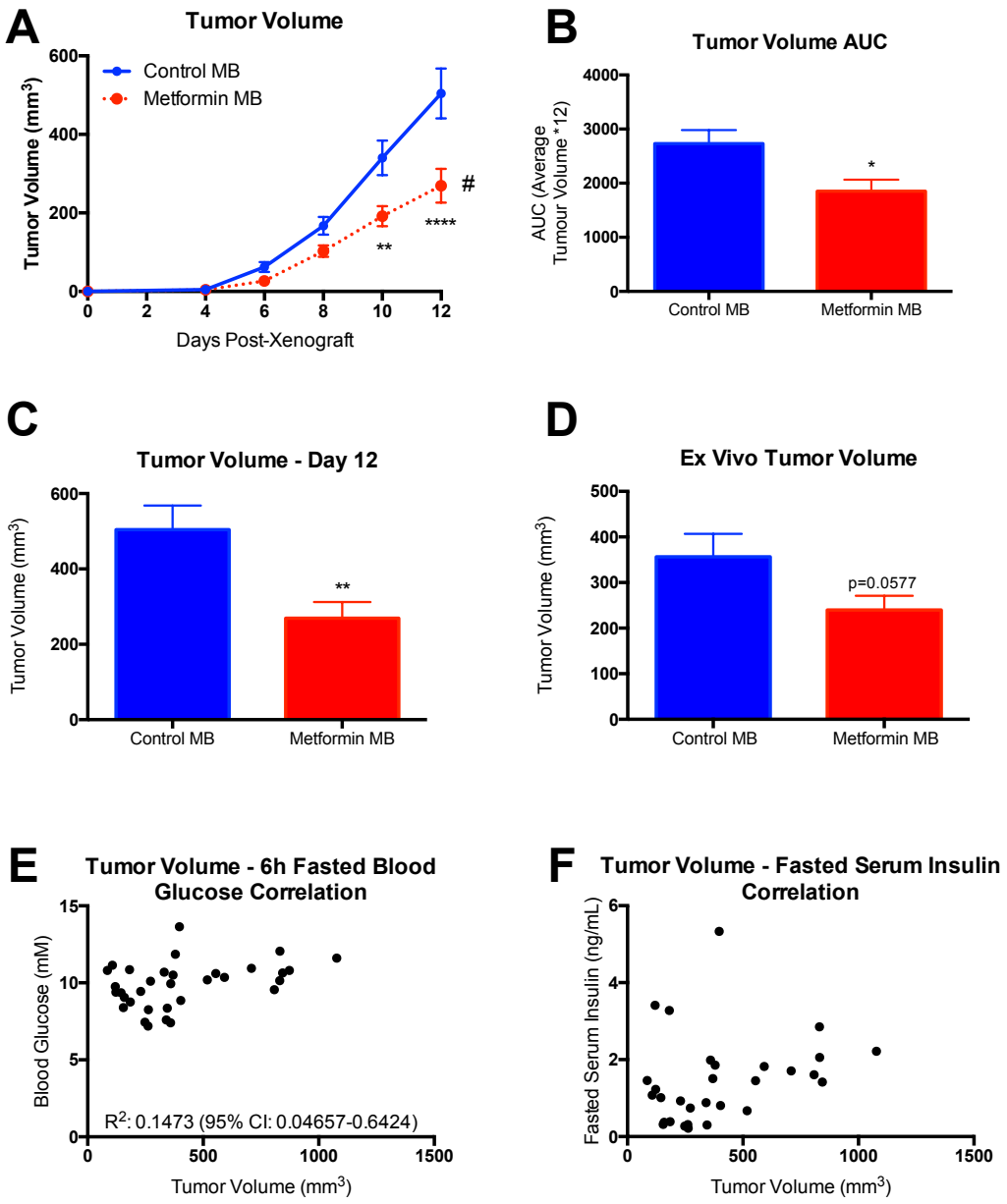

Figure 3.13: Effect of fecal microbiome transfer from metformin treated mice on MC38 allograft growth.

Figure 3.13: Effect of fecal microbiome transfer from metformin treated mice on MC38 allograft growth.

After 4 weeks of gavage from control MB or metformin MB donors, mice were subcutaneously injected with $5x10^5$ MC38 murine colon cancer cells, and allowed to grow for 12 days. Tumour volume was measured every other day starting at day 4 post-injection, and volume was calculated using an ellipsoid formula: $V = 0.5*(\text{length} \times \text{width}^2)$ (A). * indicates Control MB vs Metformin MB, and # indicates an overall treatment effect by repeated measures 2-way ANOVA with post-hoc Tukey's test. Growth rate of change was calculated as the area under the curve (AUC)=average volume*12 days (B). Final *in vivo* tumor volume in all groups plotted as a bar chart for comparison (C). *Ex vivo* tumor volume was measured (D). Pearson correlation calculations were run on matched tumor volumes to 6-hour fasted blood glucose (E) or to fasted serum insulin concentrations (F). Sample size is n=15-16 per group. T-tests were used for single-variable comparisons. $p<0.05$ was considered significant, with */# $p<0.05$, ** $p<0.01$, ****$p<0.0001$.

two (R^2=0.05689, 95%: -0.1141 to 0.5378, and R^2=0.06903, 95% CI: -0.1077 to 0.5691 comparing tumor volume to 12-hour fasting blood glucose and fasting serum insulin, respectively; Fig 3.13F).

3.10 Characterization of the gut microbiome in donor and MB recipient mice.

To characterize potential changes in the gut microbiome of donor and MB recipient mice, we conducted 16S rRNA sequencing of the V3 region of microbes present in fecal material collected at endpoint. Principle coordinate of analysis (PCoA) plots based on Bray-Curtis distances were generated to look at β-diversity among the 4 groups. Donor mice treated with metformin clustered together when the first and second greatest axes of community variation are shown (axes 1 and 2 representing 40% and 19% of total variation, respectively, on Fig 3.14A). However, control mice (donor and MB) and metformin MB animals showed no clustering in the first, second, or third axes (Fig. 3.14 A, B). PermANOVA testing of the PCoA plots found that treatment accounted for 22.5% of the variation among the samples, and was statistically significant ($p=9.99x10^{-5}$). Among control MB and metformin MB mice, treatment accounted for only 2.8% of the among-sample variation. Additionally, these data represent 2 independent cohorts of mice, and a significant cohort effect was found in both donor and MB recipients. Cohort accounted for 14.5% of the variation among the donor samples ($p = 0.007$) and 21.3% of the variation among MB recipients ($p=9.99x10^{-5}$). Taxa bar charts were generated at the phylum and family level to visualize relative

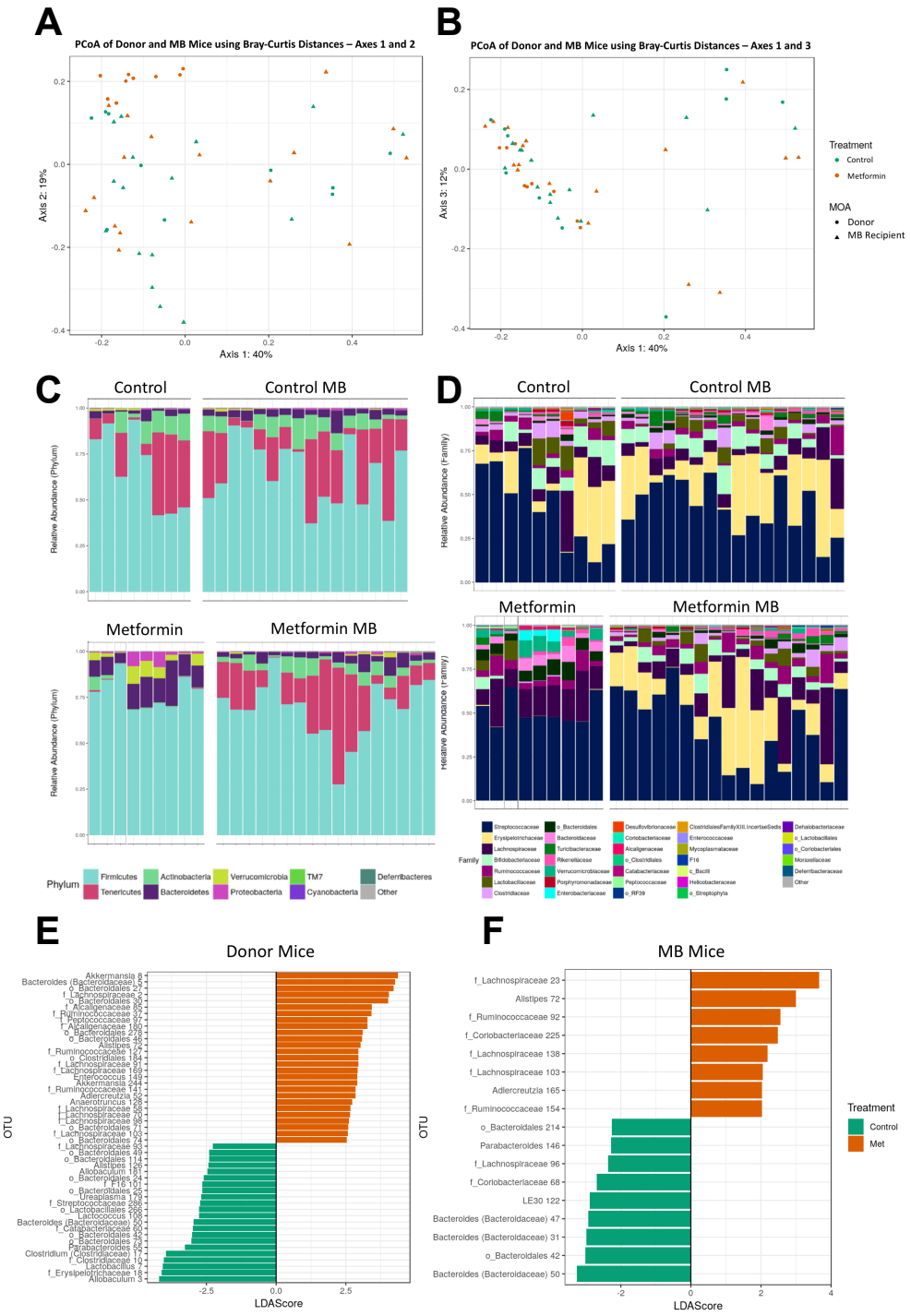

Figure 3.14: Characterization of mouse gut microbiome with exposure to 45% HFD and metformin, and the effects on microbiome with fecal transfer.

Figure 3.14: Characterization of mouse gut microbiome with exposure to 45% HFD and metformin, and the effects on microbiome with fecal transfer. Fecal material was collected at endpoint between 7-8am (after feeding cycle). Bacterial DNA was isolated, and 16S rRNA sequencing analysis run on the V3 region of the gene, using Illumina MiSeq systems. Principle coordinates of analysis (PCoA) were run on Bray-Curtis distances in fecal samples of Donor (A) and MB recipient mice (B). Relative abundance of bacteria were resolved to the Phylum (C) and Family (D) level. Each bar represents an individual mouse. Exploratory analysis of OTUs characteristic of treatment group membership in donor mice (E), and MB recipient mice (F) were conducted using LEfSe. Orange bars indicate metformin groups and green bars represent control groups.

abundances of the observed taxa. At the phylum level, *Firmicutes* were the predominant species, and metformin donors appeared to have elevated *Bacteroidetes* and *Verrucomicrobia* populations, and reduced levels of *Tenericutes* compared to all other groups (Fig 3.14C). At the family level, metformin donor mice appeared to have lower levels of *Erysipelotrichaceae* compared to control donors and control MB animals (Fig. 3.14D). Metformin donor animals also appeared to have elevated levels of *Lachnospiraceae*, *Verrucomicrobiaceae*, and *Bacteroidaceae*. *Streptococcaceae* made up the dominant family in all groups. Interestingly, it appeared that metformin MB animals do not share all the changes that metformin donor mice experience. Linear discriminate analysis (LDA) was conducted to determine which taxa are predictive of metformin treatment in donor and MB recipient mice. Donor animals had more taxa identified as predictors of group membership compared to MB recipient mice (22 and 27 taxa in donor control and donor metformin vs 9 and 8 taxa in donor MB and metformin MB recipients, respectively). *Allobaculum*, *Lactobacillus*, *Clostridiaceae*, and *Clostridium* are among the highest LDA scores in control donors, and *Akkermansia*, *Lachnospiraceae*, and *Ruminococcaceae* are among the highest LDA scores in metformin donors (Fig 3.14E). Interestingly, various *Bacteroidales* families (under the *Bacteroidetes* phylum) are identified in both control and metformin donors. Among recipient mice, *Bacteroides* received highest LDA log change values in control MB recipients, and *Lachnospiraceae*,

Allstipes, and *Ruminococcaceae* had the highest LDA scores in metformin MB recipients (Fig. 3.14F).

Next, we were interested in confirming the effect metformin treatment has on specific taxa, as reported in the literature (See Table 1.2). In the current dataset, metformin donors had significantly elevated *Klebsiella* and *Blautia*, and decreased *Clostridium*, *Lactobacillus*, and interestingly, *Akkermansia* (Fig 3.15A). In metformin MB recipients, *Klebsiella* was also elevated, and decreased *Eschericia* and *Blautia* (Fig 3.15B). Changes in the ratio of *Bacteroidetes:Firmicutes* in response to HFD-feeding and obesity has been reported in the literature (Bäckhed et al., 2004; Ley et al., 2005; Turnbaugh et al., 2006). In the current data, cohort 1 donor animals treated with metformin had a significantly higher *Bacteroidetes:Firmicutes* ratio compared to controls; however, this effect was not seen in cohort 2 donors, and a significant interaction between cohort and treatment was observed (Fig. 3.15C). In MB animals, there were no detectable changes in the *Bacteroidetes:Firmicutes* ratio between metformin and control groups (Fig. 3.15D).

3.11 Metformin microbiome transfer increases SCFA in recipient mice.

One of the main changes in the gut microbiome in response to metformin is the changes in taxa that produce SCFA, notably butyrate (Forslund et al., 2015). To examine if fecal microbiome transfer from mice treated with metformin could

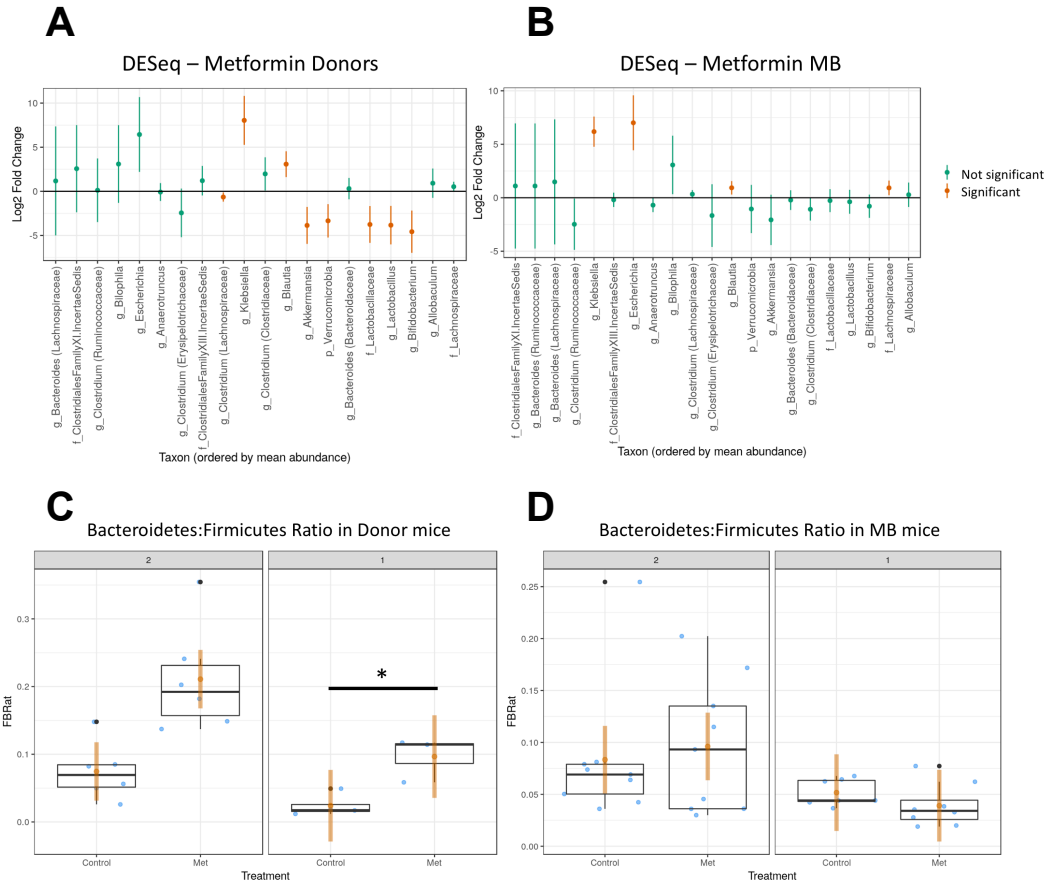

Figure 3.15: Gut microbiome changes with metformin treatment and fecal microbiome transfer.

Figure 3.15: Gut microbiome changes with metformin treatment and fecal microbiome transfer.

Hypothesis testing of differential abundance of genera, families, and phyla in donor (A) and MB recipients (B) with metformin exposure were tested using DESeq, using taxa previously recorded in the literature. Taxa in orange are significantly changed ($p<0.05$) and taxa in green are not statistically different. The ratio of *Firmicutes:Bacteroidetes* (FBRat) was calculated, and plotted by cohort (1 or 2) and by donor mice (C) and MB recipients (E). Box and whisker plots include the estimated mean (orange dot), the 95% CI of the mean (orange line) and show data points (blue dots) and outlier data points (black dots). All analyses were conducted in R with publically available packages.

cause functional changes in SCFA production in MB recipient mice, we measured SCFA concentrations in the serum of MB recipient animals. Serum acetate was not different between control MB and metformin MB animals (Fig 3.16A). However, propionate was significantly elevated (0.60μM vs 1.14μM in control MB and metformin MB, respectively), and serum butyrate levels tended to be elevated in metformin MB animals (0.43μM vs 0.917μM in control MB and metformin MB, respectively, p=0.0737) (Fig. 3.16B,D). To see if these functional outcomes could be captured by changes in the gut microbiome, we used the inferred metagenomes from the 16S rRNA sequencing, and identified the KEGG orthologs to determine the expression of genes involved in the butyrate synthesis pathway (butyrate kinase (*Buk*) acetate-CoA:acetoacetate-CoA α subunit (*AtoD*), and acetate-CoA:acetoacetate-CoA β subunit (*AtoA*)) (Fig 3.16D) and the final step in propionate synthesis, propionate-CoA transferase (*Pct*) were measured. Donor mice treated with metformin were found to have elevated levels of *Buk*, decreased levels of *AtoA*, and no measurable changes in *AtoD* (Fig 3.16E). In MB recipient mice, there were no measurable differences in any of the butyrate synthesis genes (Fig. 3.16F). Expression of *Pct* had no detectable differences between control or metformin donor, or MB recipient mice, suggesting that elevated serum propionate is resulting from the fecal transfer protocol, or from bacterial populations and genomes not detected by the current methods (Fig 3.15G).

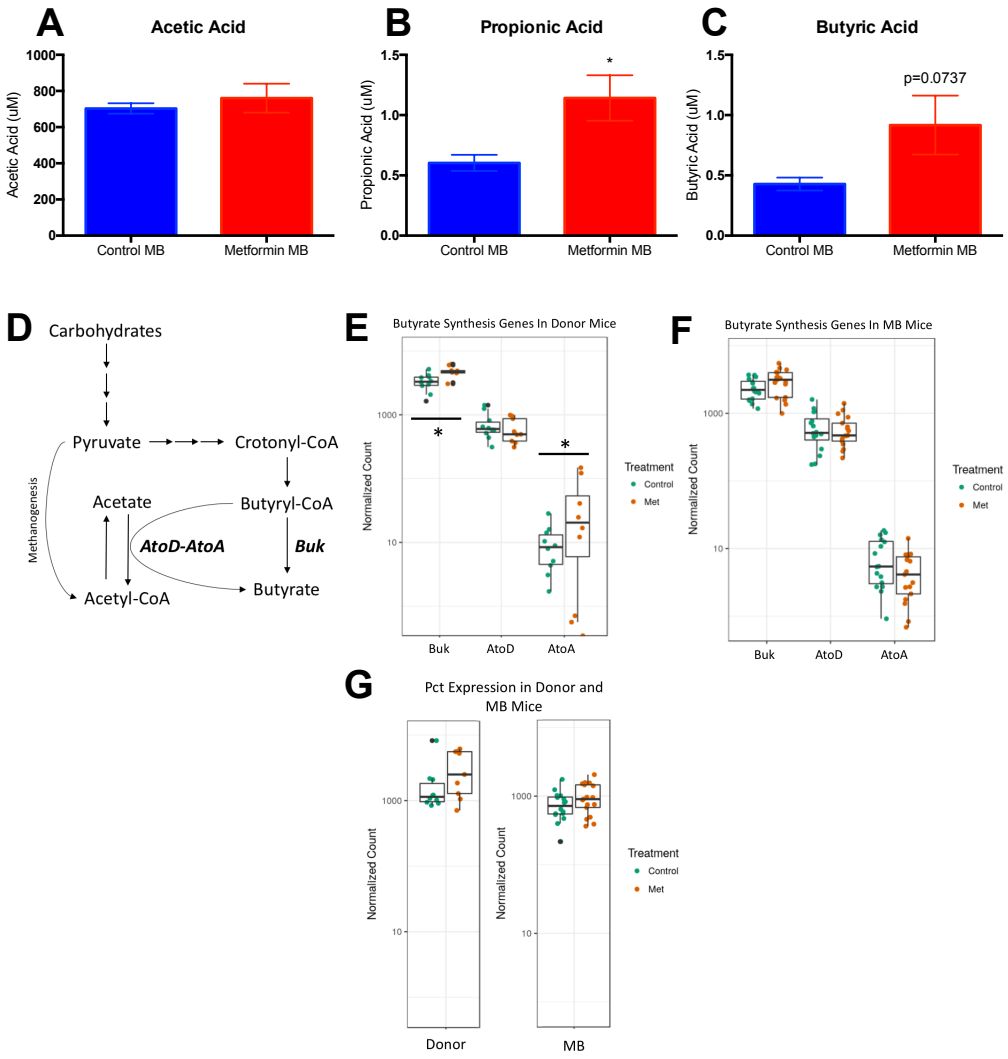

Figure 3.16: Changes in circulating SCFA concentrations in mice fed 45% HFD with fecal microbiome transfer from metformin treated mice.

Figure 3.16: Changes in circulating SCFA concentrations in mice fed 45% HFD with fecal microbiome transfer from metformin treated mice.

Serum samples were collected from mice at endpoint, after injection with ketamine and xylazine. SCFA concentrations of acetic (A), propionic (B), and butyric (C) acid were measured using UPLC-MRM/MS, with n=7 per group. The butyrate synthesis pathway is summarized (D). Gene expression was inferred from metagenomes from 16s rRNA sequencing, and KEGG orthologies were analyzed for the genes of interest using PICRUSt. The total normalized counts of butyrate synthesis genes in donor mice (E) and MB recipient mice (F) are plotted. *Buk*: butyrate kinase, and *AtoD-AtoA*: butyryl-CoA:acetate-CoA transferase (α and β subunits). A key enzyme in propionate synthesis, *Pct*: propionate-CoA transferase, was also measured in Donor and MB recipient mice (G). Box and whisker plots include the estimated mean (orange dot), the 95% CI of the mean (orange line) and show data points (blue dots) and outlier data points (black dots). T-testing was used to test for significant differences between control and metformin MB recipient serum SCFA levels. Log(2)-fold changes in gene expression, expressed as normalized counts, between control and metformin treated donors and MB recipients were analyzed using DESeq2, with $p<0.05$ considered significant.

3.12 AMPK signaling in liver and MC38 allograft tissue in donor and MB recipient mice.

Metformin is a potent activator of hepatic AMPK (Zhou et al., 2001) and so phosphorylation of AMPK and ACC were measured via immunoblotting to test for these effects in donor and MB recipient mice. To confirm MB recipient mice were not experiencing elevated hepatic AMPK activation due to potential exposure to metformin via fecal transfer, protein expression of phosphorylated AMPK and ACC were measured. Metformin-treated donor mice had significantly higher pACC-S79 compared to MB recipients (Fig. 3.17A,B) and no changes in pAMPK-T172 were measured across all groups (Fig 3.17C). With the inhibitory effects on MC38 tumor growth in metformin MB recipients, we were interested in assessing AMPK activation in this tissue as well. In the MC38 allografts, there were no measurable differences in AMPK or ACC phosphorylation (Fig 3.17D-F).

3.13 Butyrate inhibits MC38 in vitro *cell growth independent of AMPK activation.*

Butyrate is known to inhibit the growth of CRC cell lines, and in the context of clinical manifestation of CRC, the cancer cells would be in direct contact with high concentrations of butyrate in the gut (Hinnebusch et al., 2002). However, the effect of butyrate on MC38 murine colon cancer cells has not been tested. To test the direct effects of butyrate on MC38 cells, clonogenic survival to

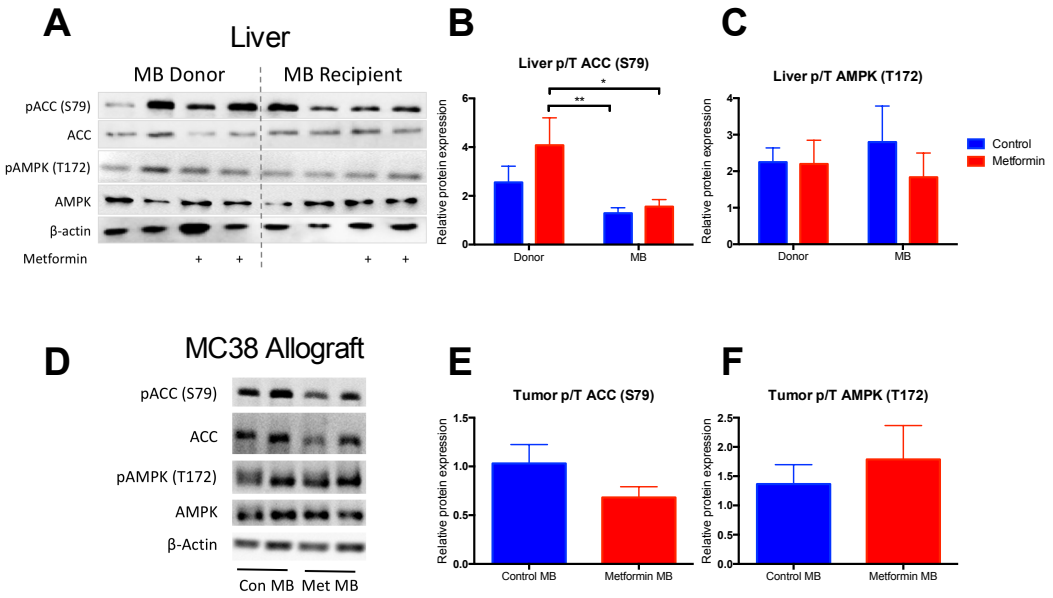

Figure 3.17: AMPK signaling in liver and tumour tissue of treated and FMT mice.

Western Blotting was used to measure AMPK signaling events by measuring levels of phosphorylated AMPK (T172) and ACC (S79) relative to their total non-phosphorylated levels in liver from donor mice (A-C) and tumours from FMT recipient mice (D-F). Tissues were collected in early morning, following the overnight feeding period. All quantifications were normalized to β-actin for loading control prior to measuring ratio of phosphorylation. 2-way ANOVA with post-hoc Tukey test, and t-tests were used for testing significant changes between treatments, with $p<0.05$ as significant.

a range of butyrate doses was tested. Butyrate was a potent inhibitor of MC38 colony formation at concentrations lower than what is achievable in the gut (Hamer et al., 2008), with an IC_{50} of 619μM (Fig. 3.18A). Additionally, evidence suggests that butyrate is an AMPK activator of gut epithelial cells, and has been shown to activate AMPK in Caco-2 CRC cells (Luying Peng, Li, Green, Holzman, & Lin, 2009). To see if AMPK could be activating AMPK in MC38 cells, a 24-hour *in vitro* treatment was applied, and AMPK and ACC phosphorylation was assessed. After 1 day of exposure to a range of doses relevant to what colonic epithelium can experience in the colon, no measurable increase in AMPK or ACC phosphorylation was found (Fig. 3.18B, C).

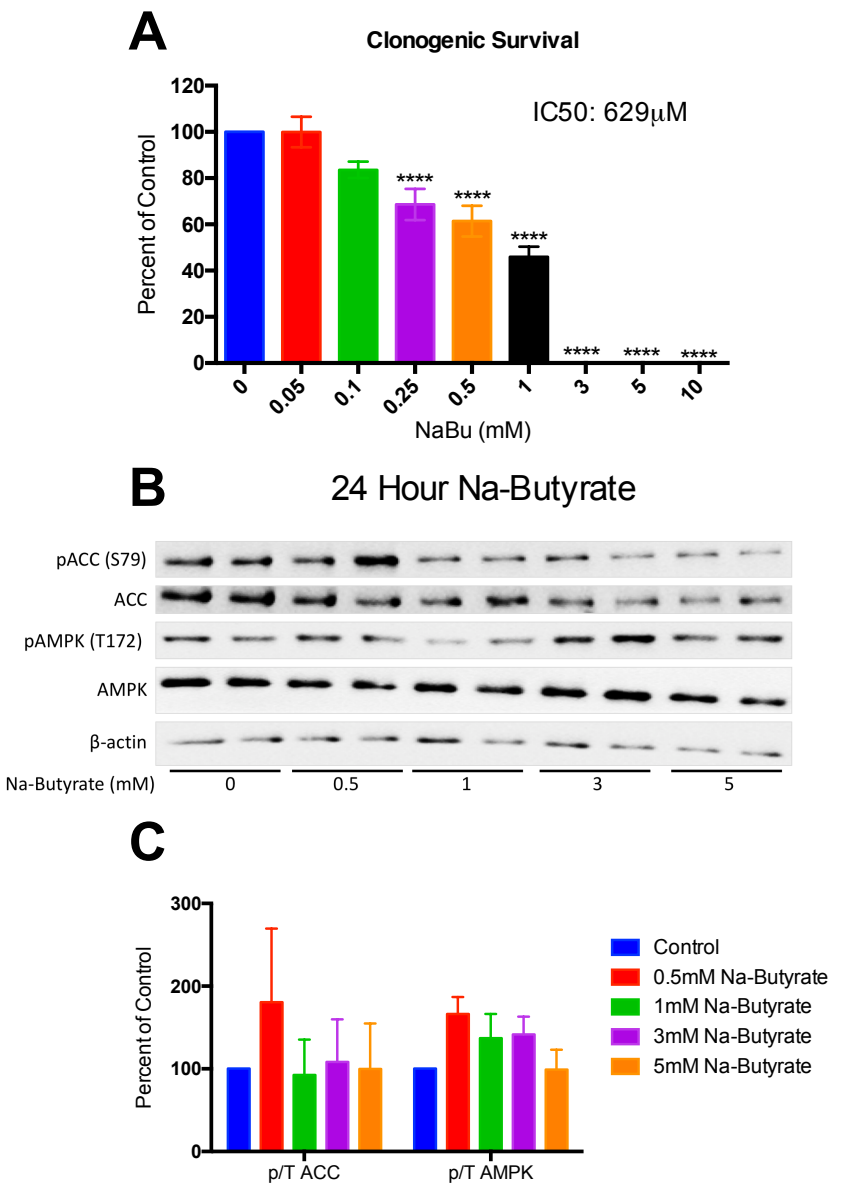

Figure 3.18: In Vitro effects of butyrate on MC38 cell clonogenic growth and AMPK signaling.

Figure 3.18: In Vitro effects of butyrate on MC38 cell clonogenic growth and AMPK signaling.

Clonogenic growth was assessed by seeding 200 cells/well in 12-well plates, treated with sodium butyrate (NaBu) (0.05-10mM), and allowed to grow for 5 days when colonies of >50 cells had grown. Colonies were stained with crystal violet, counted, normalized to untreated control (100%) and used to calculate IC_{50} concentrations, after performing a log(x) transformation and running non-linear regression analysis (A). AMPK signaling was measured in MC38 cells treated with a dose range of NaBu (B-C), and densitometry was measured. 1-way ANOVA tests were run to determine statistical significance of the treatments at $p<0.05$, and sample size is n=2, run in duplicate.

Chapter 4: Discussion

4.1 Diet effects on colorectal cancer allografts

It is well known that obesity and diabetes increase risk of certain cancer types (Giovannucci et al., 2010). The mechanisms of how adiposity and altered metabolism interact with growth and development of cancer remains unclear, and is likely complex. Using animal models that respond to environmental factors to mimic what is seen clinically is useful to understand how metabolism and cancer may interact. In the current animal model, C57BL6 mice, diet-induced obesity with impaired glucose tolerance and insulin sensitivity is known to develop with HFD-feeding (Watson et al., 2009). This provides a model in which diet and metabolism can be considered in cancer growth outcomes. Previous work has shown that the MC38 allograft model is stimulated by HFD-feeding, and results in elevated tumor growth (Algire et al., 2011; Algire et al., 2010; Nimri et al., 2015). These effects are confirmed in the current work, where chow-fed mice experience significantly lower tumor growth compared to HFD-fed mice, about 50% lower than tumors on HFD-fed animals. Additionally, HFD-feeding was confirmed to alter metabolism, as glucose tolerance testing was conducted with a glucose half that of the chow mice, and an insulin dose 60% higher than what chow-fed mice were exposed to. Fasting blood glucose levels were also significantly elevated in HFD-fed mice, and a trend for increased fed serum insulin was also present. This is important, because the inhibitory effects of metformin on the MC38 allograft model appears to rely on this stimulatory effect, and metformin had no impact on chow-fed animals with MC38 tumors (Algire et al., 2011; Algire et al., 2010). The

present work conducted on HFD and chow diets on metabolism and MC38 tumor growth provided the framework required to test the effects of metformin on these outcomes.

4.2 The role of insulin and glucose on MC38 tumor growth

Elevated circulating insulin has been associated with increased risk of CRC in clinical populations (Giovannucci, 2001; Pollak, 2012). In pre-clinical models, hyperinsulinemia was found to increase tumor growth in prostate and breast cancer models (Novosyadlyy et al., 2011; Venkateswaran et al., 2007). The MC38 allograft model is also suggested to be responsive to circulating insulin, as its growth is stimulated by both diet-induced obesity (Algire et al., 2011; Algire et al., 2010), and in response to exogenous insulin (Hvid et al., 2012). Across all cohorts in each of the three studies presented, there was a trend for a positive relationship between serum insulin and tumor volume, however this did not reach statistical significance. Previous publications on this model did not conduct statistical correlation calculations when reaching conclusions on serum insulin levels and tumor growth, but inferred these interactions through observations of elevated serum insulin and phosphorylation of Akt-Ser473 in tumor tissue (Algire et al., 2011; Algire et al., 2010). Therefore, using appropriate statistical testing, the current data was unable to confirm the connection between elevated serum insulin and tumor volume.

Fasting blood glucose is elevated with unregulated diabetes, and has also been linked to elevated CRC risk. Recent work in a large prospective cohort study found high fasting blood glucose was associated with higher CRC risk regardless of a history of T2D (Park et al., 2017). In the MC38 CRC model, metformin decreased glucose uptake into MC38 allografts only on the background of HFD (Mashhedi et al., 2011). Further work in these cells grown in high-glucose (25mM) media prior to implantation into C57BL6 mice experienced elevated growth compared to cells grown in low glucose (5mM) media, without requiring HFD-feeding (Vasconcelos-Dos-Santos et al., 2017). This study also found tumor growth was stimulated even more when grown in 25mM glucose DMEM and grafted into mice with hyperglycemia achieved via streptozotocin-induced T2D, which chemically damages the insulin-producing β-cells. Furthermore, a very recent publication revealed that a mitochondrial uncoupler that acts specifically in the liver to decrease hepatic glucose output and subsequently decreased insulin levels, resulted in reduced MC38 allografts growth and polyp formation in $APC^{Min+/-}$ mice (Wang et al., 2018). This reduced growth rate *in vivo* was not due to direct effects of the protonophore on MC38 cell growth, as growth rates were unaffected when MC38 cells were treated in vitro; supporting the concept that reductions in glucose were important (Wang et al., 2018). In the data presented here, 6-hour, and not 12-hour, fasting blood glucose was significantly correlated to tumor growth across all 3 studies. This may be due to increased variation, as 6-hour fasting occurred during daytime and 12-hour fasting occurred overnight, and

overnight fasting in mice may increase variation (Sun et al., 2016). Taken together, these data show that serum insulin does not correlate to tumor volume, but daytime 6-hour fasting blood glucose levels do.

4.3 The method of administration affects metformin's metabolic and tumor outcomes

An important consideration when studying the effects of metformin on any outcome in pre-clinical models is the method of drug administration. As such, the pharmacokinetics of metformin in mouse models has been an area of interest. In the current work, we found metformin concentrations in serum to be 23μM, 2-hours after i.p. injection of 100mg/kg metformin. In comparison, work by Wilcock and Bailey (1994) found intravenous injection of 50mg/kg metformin resulted in only 7μM metformin in the inferior vena cava at the 2-hour time point (Wilcock & Bailey, 1994). This difference in concentrations may be explained by an intraperitoneal injection, in which metformin is absorbed into the tissues and organs within the peritoneal cavity, as opposed to direct injection into circulation. In more recent work, a dose of 125mg/kg delivered by i.p. injection resulted in 42 μM in mouse plasma at the 1-hour time point, reduced from 184 μM measured at 0.5 hour (Dowling et al., 2016). Earlier work by Memmott *et al.* (2010) found that an i.p. injection of 250mg/kg resulted in 24 μM serum concentration 2-hours post-injection (Memmott et al., 2010). Therefore, the serum concentration measured in the present work appears to be in line with circulating levels reported in the

literature, given that metformin clearance is rapid, and occurs within the first hours of administration.

Despite comparable serum metformin concentrations, the current work found MC38 tumor growth and metabolic testing uninhibited by i.p. metformin in HFD-fed mice. Therefore, the role of the oral route of metformin delivery came into question. This is an area of importance, as the clinical administration of metformin is exclusively oral, and may involve the gut microbiome (Wu et al., 2017). Several recent studies have scrutinized the pharmacokinetic differences between injected and orally delivered metformin, and suggested that oral delivery results in higher tissue accumulation in both humans and mice (Chandel et al., 2016; Gormsen et al., 2016). Our data showed that oral metformin delivery improves glucose tolerance and inhibits MC38 colon cancer allografts by endpoint, and i.p. injected metformin does not. As previously discussed, MC38 allografts respond to host metabolism, as metformin seems to inhibit tumor growth exclusively on the background of diet-induced obesity, and was associated with decreased serum insulin and blood glucose levels, and this effect was found regardless of the method of administration (Algire et al., 2011; Algire et al., 2010). Overall, these data may shine some light on the clinical applications of metformin as a protective agent against cancer, suggesting that a dysregulated metabolism is required for these beneficial effects within certain cancers. With respect to the MC38 model, it also suggests that systemic effects of metformin

improving metabolism is the driving mechanism of inhibiting MC38 tumor growth, rather than metformin altering direct cell signaling effects.

4.4 MC38 cells are resistant to metformin-induced reductions in proliferation, AMPK activation, and mTOR inhibition

To consider the direct effects of metformin on the inhibition of cancer, it relies upon its ability to enter the cells. Metformin is a cation that requires transport into cells, most notably though the OCT-1 transporter. OCT-1 is highly expressed in the liver, which is metformin's primary site of action for its metabolic mechanisms relied upon for the treatment of type 2 diabetes (Wang, 2002). CRC cells have been found to express cation-selective transporters, including OCT-3 and PMAT, suggesting the potential for a direct metformin effect (Han et al., 2015). However, the status of cation-selective transporters in the MC38 cell line is currently unknown, and is an area that requires further examination. Without successful transport into the cancer cells, direct effects and modulation of AMPK and downstream pathways would not occur. To address if metformin is entering the MC38 cells, we measured its concentration in MC38 allografts treated with 100mg/kg i.p. injected metformin. Metformin concentrations in the MC38 allografts were merely ~3μM (26.9pmol/mg tissue), a fraction of the 23μM measured in serum at the same time point, 2 hours after i.p. injection. While *in vitro* tests often require higher concentrations, and do not represent processes that occur within the complexity of physiology, the

concentration differences between what is measured in the MC38 allografts, and what inhibited 50% of colony formation *in vitro* is orders of magnitude in difference (3μM in MC38 allograft tissue vs 2.4mM IC_{50} concentration to inhibit MC38 colony formation in 5mM glucose media). In an HCT116 colorectal cancer cell line xenograft, metformin concentrations were measured to be 77 μM 30 minutes after i.p. injection of 125mg/kg metformin (Dowling et al., 2016). This difference in metformin accumulation could be due to differences in timing, or due to varying levels of cation transporters present in the two cell lines. The HCT116 cell line is known to express OCT-1, and to respond to lower levels of metformin compared to MC38 cells (Wheaton et al., 2014). Additionally, further support for the hypothesis that metformin's systemic effects are driving tumor inhibition in this model comes from recent work comparing the accumulation of metformin in tumor tissue to concentrations required for direct tumour cell effects in cultured cells (Iversen et al., 2017). The authors concluded that inhibition of mitochondrial respiration as a mechanism of metformin's anti-cancer actions should only be considered in *in vitro* assays, as their *in vivo* data suggest that accumulation in xenograft tissues are unable to match those concentrations (Iversen et al., 2017). Further, when treating cancer cells *in vitro* with clinically relevant concentrations – even under low glucose and hypoxic conditions that growing tumors may experience – effects were not found (Iversen et al., 2017). The discrepancy between circulating concentrations, in μM levels, and the mM concentrations used in cell culture experiments is frequently highlighted when

observing *in vivo* effects of metformin. However, some have countered the argument that circulating metformin levels are not sufficient for direct cell effects, with evidence suggesting metformin accumulates within the mitochondria of the cells, where its inhibitory effect on complex I occurs (Andrzejewski et al., 2014; Owen et al., 2000). Again, this would require adequate uptake into the cancer cells via cation transporters. Overall, the current data found that MC38 cells are not efficient at taking up metformin, and suggests that cation-specific transporters are likely not highly expressed in this cell line.

Indirect activation of AMPK by metformin via inhibition of oxidative phosphorylation is often studied as a mechanism of action against cancer growth and development. AMPK activation in cancer tissue is often associated with the inhibition of the mTOR protein synthesis pathway. Several studies have found metformin can inhibit xenograft growth and associated mTOR signaling inhibition in various cancer types including breast, lung, and colon cancers (Algire et al., 2011; Algire et al., 2010; Cai, Zhang, Han, Everett, & Thakker, 2016; Lau et al., 2014; Memmott et al., 2010). In the present work, chronic metformin treatment did not cause measurable changes in phosphorylation of AMPK (T172) or ACC (S79), contradicting previous work (Algire et al., 2011). This lack of AMPK activation is also reflected in mTOR signaling, where phosphorylation of Raptor (S792), a known target of AMPK, and p70S6K (T389), a downstream kinase of mTOR, are unaffected by chronic metformin treatment. As the chronic exposure

samples were taken 6-hours after i.p. injection, and evidence that metformin accumulation in tumors plateaus after 1 hour, we conducted acute metformin exposure experiments to assess AMPK activation and mTOR inhibition (Iversen et al., 2017). An acute dose of 100mg/kg i.p. metformin was found to trend towards significant activation of AMPK at the 2-hour time point, however this activation was not reflected by ACC phosphorylation, a commonly used readout of AMPK activation. When considering the low metformin concentration in tumor tissue at this time point, it is possible that the drug is not reaching a critical concentration to cause sufficient AMPK activation to stimulate downstream effects. Additionally, when treating MC38 cells directly with an acute 1-hour metformin treatment, no AMPK activation was measured. These data further support the idea that the MC38 cell line is insensitive to direct metformin treatment, and that growth inhibition effects seen by oral metformin treatments are due to metabolic modulation rather than drug absorption and inhibition of oxidative phosphorylation.

4.5 Ampicillin inhibits metabolic and tumor effects of metformin

Recently, the GMB has become an area of interest in the development and pathology of T2D and obesity. The microbiome is the collective genome of the microbiota – commensal bacteria, fungi, and viruses that coexist with humans and animals. This is not limited to the gut, with microbiotas established in several areas of the body including the oral cavity, lungs, and skin. In animal and clinical

studies, differences in the gut microbiome composition and metagenome have been recorded between obese subjects and healthy weight controls (Bäckhed et al., 2004; Ley et al., 2005). Importantly, metformin has also been reported to affect the gut microbiome, with work suggesting that exposure to the drug may promote numbers of bacteria associated with a "healthy" gut microbiome (Forslund et al., 2015; Wu et al., 2017). Additionally, the gut microbiome has been found to have altered diversity with the presence of colorectal cancer (Dejea et al., 2014; Feng et al., 2015). Therefore, we aimed to study the role of the gut microbiome on metformin's anti-cancer effects, an interaction that has previously not been studied.

To try and understand the role of the GMB in metformin's anti-cancer effects, ampicillin was added to metformin in the drinking water, and metabolic and tumor outcomes were assessed. Exposure to ampicillin blunted the effects of metformin on both metabolism and tumor growth. This blunting effect further supports the systemic metformin effect hypothesis in this CRC model. However, despite the blunting effect, it cannot be ignored that metabolic changes may occur in animals exposed to antibiotics, as metabolic changes in glucose sensitivity are measurable when comparing control animals to ampicillin treated animals alone (data not shown). Therefore, further studies are required to fully isolate the role of the gut microbiome effect in mediating metformin's metabolic and anti-cancer actions. In conclusion, the present work has shown that oral metformin at

clinically relevant doses decreases tumor volume growth in murine-derived MC38 colon cancer allografts, and that the gut microbiome may be involved in these effects.

4.6 Fecal microbiome transfer from metformin treated mice inhibits MC38 tumor growth independent from metabolic changes

With the results from the ampicillin study hinting at a role for the microbiome, conducting an experiment to isolate the role of the GMB became important. Therefore, we treated C57BL/6J mice on 45% HFD with diluted feces from donor mice, also C57BL/6J and on 45% HFD, using a fecal microbiome transfer protocol. In the GMB recipient mice, feces from metformin-treated donors resulted in significantly decreased MC38 tumor volume growth. This experiment is, to our knowledge, novel, and the level of tumor growth inhibition was similar to that of oral metformin treated mice, with both groups experiencing ~30% inhibition. Interestingly, this inhibition of tumor growth in GMB recipient mice occurred independently from metabolic changes, whereas oral metformin animals experienced metabolic improvements as well as tumor growth inhibition. This is the first-time metformin effects on MC38 colon cancer growth has been uncoupled from its systemic metabolic effects. This suggests that either microbes being transferred in the fecal microbiome transfer or their active metabolites are inhibiting tumor growth in some manner. Additionally, as the allograft model

results in tumor growth subcutaneously, these results suggest that perhaps a metabolite is being released into circulation to have these effects.

Based on previous studies suggesting that metformin elevates SCFA-producing microbes, and that SCFAs, such as butyrate, can inhibit CRC growth, we measured circulating levels of acetate, propionate, and butyrate (Gijs den Besten et al., 2013; Forslund et al., 2015). Metformin GMB recipient mice had double the amount of propionate and a trend towards increased butyrate compared to control GMB mice. Previous work measuring butyrate levels found circulating concentrations of 5.7μg/mL (6.29μM) in fasting mice on 60% HFD, considerably higher than the 0.917μM measured in the current work (Gao et al., 2010). Work in humans with overweight and obesity found elevated SCFA levels, propionate specifically, compared to healthy weight controls (Schwiertz et al., 2009). In humans, a range of circulating butyrate levels have been measured, with 17-29μM measured in portal vein circulation and 2-14μM measured in venous circulation (Cummings et al., 1987; Jakobsdottir, Xu, Molin, Ahrné, & Nyman, 2013; Peters, Pomare, & Fisher, 1992; Zhao, Liu, Nyman, & Jönsson, 2007). Additionally, butyrate is associated with improved insulin sensitivity in a mouse model, although the current results did not see metabolic changes despite elevated SCFA concentrations (Gao et al., 2010). In humans, fecal transfer from healthy donors to men with metabolic syndrome, fecal butyrate levels were unchanged, however acetate was significantly elevated and propionate tended to also be elevated

(Kootte et al., 2017). Propionate is also associated with improved metabolic outcomes, primarily by interacting with lipid synthesis in the liver, and has also been shown to inhibit CRC cell growth (Hinnebusch et al., 2002; Hosseini et al., 2011). With elevated SCFAs in metformin GMB recipients, it suggests that a metformin-treated GMB can transfer either microbial populations that can elevate SCFA concentrations or that the SCFAs themselves are elevated in the fecal material used in the transfer.

To confirm if microbial species that produce SCFAs are being transferred, we measured the gene expression of butyrate and propionate synthesis enzymes, *Buk*, *AtoD/AtoA*, and *Pct*. Previous studies have found metformin enriches butyrate and propionate synthesis pathways, suggesting elevated SCFA production may be linked to metabolic outcomes with metformin treatment (Wu et al., 2017). The current work found donor animals exposed to metformin had elevated *Buk* but decreased *Pct* expression. No changes were measured from the inferred metagenomes in GMB recipient mice, suggesting there was no enhanced capacity for producing butyrate and propionate based on these gene markers. To further confirm this, more work is needed to analyze the microbiome in fecal microbiome transfer - mice, using deep sequencing rather than 16S rRNA sequencing, as the current results are inferred and rely on genome libraries (Langille et al., 2013). Taken together, transferring fecal material from metformin-treated mice into metformin-naïve mice resulted in significant tumor

growth inhibition, and elevated SCFA levels, independent from any metabolic changes.

4.7 Metformin changes composition of the gut microbiome

Metformin is now known to act on the gut microbiome, and that it may be involved in metformin's metabolic effects (Forslund et al., 2015; Wu et al., 2017). To understand how metformin may be affecting the microbiome in the present study, we employed 16S rRNA sequencing of the V3 region to explore how this treatment may affect the GMB, and whether or not it is transferrable via fecal microbiome transfer to specific-pathogen free (but not germ-free) mice. Metformin treatment resulted in a shift in beta-diversity compared to controls, and metformin GMB recipient mice did not appear to share this shift, and were not significantly different from controls. Contradictory reports exist in the literature with some reporting changes in beta-diversity, resulting in clustered shifts similar to metformin donor mice in the present work, and others finding no measurable differences (De La Cuesta-Zuluaga et al., 2017; Shin et al., 2014). It was noted by Forslund *et al.* (2017), that diversity changes with metformin treatment are not well captured by multivariate analyses (ie. permANOVA), and that differences are likely to be occurring yet undetectable (Forslund et al., 2015). Additionally, it has been noted that if a microbiome is established, it will exert a strong force to preserve its composition, and resist colonization unless an antibiotic depletion has occurred prior to colonization (Ericsson & Franklin, 2015). This may also account

for the source of variation found in metformin-MB animals, where treatment accounted for 2.8% of the variation among species, whereas there was a strong cohort effect. The differences between cohorts 1 and 2 accounted for 21.3% of variation in the microbiome of MB recipients, and this is not unexpected. It is well known that the GMB is established in early life, and predominantly determined by pup exposure to microbes in the birthing dam (Ericsson & Franklin, 2015). Considering cohorts 1 and 2 were mice ordered in at separate times, significant differences in GMB is expected. In the current study, C57BL/6J mice contained an intact microbiome, and had additional continual selection pressure from 45% HFD feeding. Therefore, it is possible that while a difference in metformin donors was not detected, there are still differences in the metformin GMB recipients that are not detectible using the current methodology and technologies available.

Recent work on metformin and the microbiome has highlighted a handful of bacteria that change with metformin treatment. As summarized in Table 1.2, a number of genera and families are increased and decreased with metformin treatment. Therefore, we tested if these taxa were changed in the microbiomes of donor and recipient mice. Our dataset confirmed increases in *Blautia* and *Klebisella*, and importantly, these effects were transferrable into metformin GMB recipient mice (Wu et al., 2017; Zhang et al., 2015). While SCFA-producing taxa exist across multiple genera, *Blautia* is one genus that is known to contain SCFA-

producing species (Zhang et al., 2015). Several studies have found the bacterial species *Akkermansia muciniphila* are elevated with metformin treatment, and exert positive effects on metabolism when directly supplemented to animals (Forslund et al., 2015; Lee & Ko, 2014; Shin et al., 2014; Wu et al., 2017; Zhang et al., 2015). However, in metformin-treated donor mice, *Akkermansia* was decreased compared to controls. Although this seems contradictory, it is possible that there is an elevation of the species *A. muciniphila* that the current 16S rRNA analysis is not sensitive to, as the current dataset was not able to identify taxa at the species level. Additionally, previous work on GMB changes with HFD and metformin exposure found no changes in *Akkermansia* numbers, and a human study found *A. muciniphila* enrichment in individuals with T2D, suggesting variation exists between studies (Bauer et al., 2018; Qin et al., 2012). Therefore, metformin causes changes at the genus level, and some changes are transferrable via fecal microbiome transfer into SPF mice, including an SCFA-producing genus.

In early studies describing changes in the gut microbiome with obesity, a change in the ratio of *Bacteroidetes*:*Firmicutes*, two of the most abundant taxa in microbiome of humans and mice, was described (Ley et al., 2005; Ley et al., 2006; Ley, Peterson, & Gordon, 2006). These studies found decreases in *Bacteroidetes* and increases in *Firmicutes* in *ob/ob* mice compared to healthy controls (Ley et al., 2005; Turnbaugh et al., 2006). These results were confirmed

in human microbiome studies, with elevated *Bacteroidetes* in study participants with overweight and obesity in some (Schwiertz et al., 2009) but not all studies (Duncan et al., 2008; Ismail et al., 2011; Zhang et al., 2015). Links between *Bacteroidetes* and CRC have also been drawn, although less work has been done in this area. While Weir *et al.* (2013) found no correlations between *Bacteroidetes* or *Firmicutes* with CRC presence in human stool samples from CRC patients and healthy controls, others suggest that *Bacteroidetes* are involved with intestinal biofilm formation associated with CRC (Drewes, Housseau, & Sears, 2016; Weir et al., 2013). Biofilms are formed when bacteria invade the mucus layer of the gastrointestinal tract, and elevate markers of inflammation. With regard to the role of the *Bacteroidtes*:*Firmicutes* ratio in response to metformin, it has been reported that metformin can restore the ratio in HFD-fed animals to that of lean animals (Lee & Ko, 2014). However, not all studies have been able to reproduce this result (Zhang et al., 2015). Therefore, we tested for a change in the ratio of *Bacteroidetes* to *Firmicutes* in the current study, and found that this ratio increased with metformin treatment, indicating the treatment may affect each of these genera populations to regulate their numbers. Our data confirms the positive effect metformin has on the ratio of these two important phyla.

4.8 Effect of butyrate on cancer cell growth and metabolism

Butyrate is a potential anti-CRC agent, and previous work suggests that it may inhibit CRC cell growth and development through various mechanisms.

Initially, the inhibition of histone deacetylases was considered to be butyrate's main mechanism of action (Archer et al., 2005; Davie, 2003). In cancer cells, this action is associated with increased apoptosis in CRC cells mediated by p21 expression and cyclin B1 inhibition (Archer et al., 2005). To our knowledge, the MC38 cell line has not been tested with butyrate treatment, so clonogenic survival was used to determine the anti-tumorigenic capacity of butyrate on this cell line. Butyrate significantly inhibited colony growth at a concentration of 250μM, with the IC_{50} concentration calculated to be just over 600μM. In mice, concentrations of butyrate in the colonic lumen have been found to range from 500-3500 μM (distal and proximal colon segments, respectively), and to be as high as 800μM at the level of the colonic crypts, suggesting the IC_{50} concentration for inhibiting MC38 is physiologically relevant (Donohoe et al., 2012). Additionally, at 3mM, a concentration of butyrate found in human feces and therefore representative of concentration that can be achieved clinically (Hamer et al., 2008), no colonies remained. In HT-29 CRC cells, 500μM butyrate inhibited proliferation, however only in the context of the Warburg effect (high glucose availability)(Donohoe et al., 2012). When the same cells were treated in low-glucose media, butyrate stimulated proliferation, suggesting its use as an energy source in glucose-limiting conditions. Additionally, butyrate has been shown to activate AMPK in colonic epithelial cells, and its activation is involved in maintaining tight-junctions in the epithelium (Yan & Ajuwon, 2017; Zhang et al., 2006). In Caco-2 CRC cells, butyrate was able to activate AMPK, however this effect was not seen with

treatment of MC38 cells (Peng et al., 2009). With the current study and previous evidence, the MC38 cell line appears to be glycolytic, and responsive to growth stimulation by glucose (Algire et al., 2011; Mashhedi et al., 2011). Additionally, it is suggested that in glycolytic cancer cells, butyrate doesn't function as a source of energy, but rather as an HDAC inhibitor (Donohoe et al., 2012). Therefore, with the inhibitory effects of butyrate on clonogenic survival, but not AMPK activation, MC38 cells may be experiencing growth inhibition due to HDAC inhibition. Further work in this area is required to confirm the mechanism of action of butyrate on MC38 cells.

4.9 Limitations

There are several limitations in the current body of work that should be considered in the interpretation and translation of the results. Regarding the model used, only one CRC cell line was tested in all studies. This is due to the requirement of a mouse that responds to HFD feeding with impaired glucose and insulin metabolism. The C57BL6 is a widely used and a well-documented mouse strain that develops diet-induced obesity and glucose intolerance with HFD (Surwit, Kuhn, Cochrane, McCubbin, & Feinglos, 1988). The C57BL6 model has an in-tact immune system (unlike the athymic Balb/c nude mice), limiting the study to rely on murine-derived cell lines. However, the experiments in this thesis could be translated to other models of CRC development that are also on the

C57BL6 background, including the genetically modified $Apc^{Min-/+}$ mouse model, and through chemical carcinogens (dimethylhydrazone or azoxymethane, for example) to induce CRC development (Karim & Huso, 2013). The measurement of MC38 allografts via hand caliper may not be very accurate, and the use of luciferase-expressing MC38 cells for volume measurement with *in vivo* fluorescent imaging systems could reduce measurement errors. The allograft model used, with a subcutaneous tumor injection, is not reflective of how CRC grows in the clinical setting. Using an orthotopic model and injecting CRC cells in the mucosa of the colon could be conducted to address the localized effects of metformin and a modified GMB on tumor growth.

Male mice were used in all the presented studies, raising the question of whether the effects found are sex-limiting. Female C57BL6 mice do not gain weight and develop glucose and insulin intolerance due to HFD-feeding to the same extent as males (Pettersson, Waldén, Carlsson, Jansson, & Phillipson, 2012). Therefore, to address the systemic mechanism of metformin's anti-cancer potential, dietary modulation of metabolism was required, thus limiting the study to using male mice. However, future work should strongly consider including females in experimental designs, to confirm metformin effects on GMB alterations and subsequent effects on cancer growth. This is especially of interest considering improvements in glucose and insulin sensitivity did not occur in fecal microbiome recipient mice. This also highlights the possibility that metformin

may affect the GMB and CRC growth without the requirement of obesity and glucose intolerance. Replicating this study on the background of a standard chow diet could help clarify this. Overall, while using a single model to test metformin's effects on the GMB and CRC cancer growth is a limiting factor, the data provide a strong basis to continue the work in varying models to further clarify these results in a wider context.

The dosing of metformin in these studies was chosen to achieve circulating serum concentrations similar to that of what has been clinically measured. While the pharmacokinetics of metformin in humans and mouse models was discussed in section 1.2.1, the oral method of administration via drinking water is unlike the clinical dosing regimen of metformin. The animals in this study were continually exposed to metformin each time they drank water, whereas patients consuming metformin typically take one or two doses a day (Graham et al., 2011). Therefore, treating animals with oral gavage would more accurately represent the clinical setting (Graham et al., 2011). The i.p. delivery method used in study 1 of this thesis mimics the spikes in drug concentration observed clinically, however this resulted in low metformin uptake into MC38 tumors. The OCT status in MC38 cells is unknown, presenting another limitation to the study. If these, or other cation transporters, are not well expressed in these cells, it could help clarify if a direct metformin effect could be reasonably considered.

The use of 16s rRNA sequencing is commonly used to characterize and assess the GMB. However, this method does not provide resolution to the species level, with the lowest taxonomic level being genera. Shotgun sequencing could be used to achieve higher resolution, and to identify specific species changing in abundance with exposure to metformin (J. Wang & Jia, 2016; H. Wu et al., 2017). This would be useful, as several studies in the field can report species associated with an observed phenotype, such as *A. muciniphila* (De La Cuesta-Zuluaga et al., 2017; Plovier et al., 2017). Additionally, recent work suggests that fat content in the diet can have large effects on GMB diversity, independent of changes in metabolism (Dalby et al., 2017). This suggests that looking at different refined fat diets with metformin could be used to observe the effects of GMB in metformin's anti-cancer effect independent from an obese phenotype. Taken together, the present work has numerous limitations, however it provide a basis of knowledge in which to further characterize how metformin, the GMB, and CRC growth may interact.

4.10 Future directions

This thesis provides the framework for a multitude of future studies on the gut microbiome and metformin effects on cancer. While the current data decisively shows that changes in the gut microbiome with metformin exposure can be isolated, transferred, and result in decreased tumor growth, much work

remains to understand how this inhibitory effect is being conferred. As mentioned, the fecal transplants could be providing SCFA-producing bacteria, resulting in the measured elevation in propionate and, to a degree, butyrate, or other fecal metabolites could be transferred. In addition to overall deep sequencing of fecal material, to provide a higher resolution of bacterial species and functional pathway changes, other experiments could be conducted to help clarify what is being transferred. To address this question, heat-deactivated fecal material could be transferred to observe metabolite-specific effects. Inactivating microbiome effects by heat treatment has been used to study pro-biotic effects on hepatocellular carcinoma, and was found to regulate T-cell differentiation, altering the cytokine and inflammation profile promoting cancer development (Li et al., 2016). Additionally, pasteurized *A. muciniphila* was found to improve insulin sensitivity and decrease fat mass and circulating lipids in HFD-fed mice (Plovier et al., 2017). Given that the MC38 model is stimulated by elevated blood glucose levels, treatment of mice with inactive *A. muciniphila*, would add more evidence that the microbiome and its interactions with host metabolism may be involved in inhibiting CRC growth. Another step would be to address the translatability aspect of a mouse study, and test human-to-mouse fecal transplants from humans exposed to metformin. This model has already confirmed the transfer of metabolic effects via fecal microbiome transfer, with improved metabolic outcomes in HFD-fed germ-free mice exposed to human fecal samples

from T2D patients with metformin treatment (Wu et al., 2017). However, this has not been carried on to look at the effects of CRC growth and development.

In addition to understanding how the gut microbiome may mediate metformin's anti-cancer effects, understanding the mechanisms underlying metformin-GMB interactions is also an area of interest. A handful of potential mechanisms are considered, including direct metformin-bacteria interactions to alter growth of certain populations, modulating bile acid secretion and altering the host environment in which the microbes live, and by affecting intestinal inflammation and altering microbiome-immune system interactions. Regarding direct metformin-bacteria interactions, Wu *et al*. (2017) observed various species grown in culture can have varied reactions to metformin treatment. This study tested *Bifidobacterium adolescentis, A. muciniphila,* and *Escherichia coli* growth response to 10mM metformin, and found increased growth of *B. adolescentis* and *A. muciniphila*, with no effect on *E. coli* (Wu et al., 2017). Metformin has been shown to increase bile salts excretion in feces (Scarpello, Hodgson, & Howlett, 1998). Bile acid secretions were also considered by Wu *et al.* (2017), finding that there were no changes in fecal bile acid content, however elevated plasma bile acids and expression of the *bsh* gene, which is responsible for bile salt hydrolase expression, occurred with metformin treatment in humans with T2D. However, the gut microbiome is also known to interact with bile acid secretion (Ridlon, Harris, Bhowmik, Kang, & Hylemon, 2016), therefore creating a chicken or the

egg problem in understanding how metformin may be involved in microbiome-mediated changes in bile acids. While further work on direct metformin-bacteria growth interactions is merited, clarifying the role of metformin on changes in bile acids provides a complex problem that will be challenging to disentangle.

The role of inflammation as a potential mediator of metformin and the micobiome effects on CRC is another topic of great interest. Inflammation is the primary link between CRC and inflammatory bowel syndrome (IBS), and both are associated with microbiome dysbiosis (Du et al., 2017; Hu et al., 2013). In a CRC-development model with alterations in the TGF-β signaling pathway, supplementing animals with the pro-CRC bacteria *Helicobacter hepaticus* resulted in the identification of LPS production as a pathway affected by microbial dysbiosis, highlighting interactions between inflammation, the gut microbiome, and CRC development (Daniel et al., 2017). Metformin has been identified as a mediator of anti-inflammatory signaling, resulting in decreased pro-inflammatory markers, including IL-6 and IL-1β, in primary hepatocytes (Cameron et al., 2016)**.** Additionally, supplementation of *A. muciniphila* in HFD-fed mice also decreased IL-6 and IL-1β levels, and led to a decrease in regulatory T-cells in adipose tissue; suggesting decreased inflammation in adipose tissue alongside with improved glucose sensitivity can be introduced via microbiome alterations (Shin et al., 2014). Butyrate has also been associated with anti-inflammatory effects, as it is important for regulating tight-junction proteins at the

intestinal barrier, thereby decreasing "leaky gut" and inflammation (Wang et al., 2009; Zhang et al., 2006; Zheng & Cantley, 2007). Given that inflammation appears to be a common thread between metformin, the gut microbiome, and CRC, understanding how they interact is potentially the next big step in this project.

In addition to inflammation, SCFA are being studied for a multitude of functions and interactions relating to metabolism and cancer. Recently the orphan nuclear receptors FFA2 and FFA3 have been shown to bind to SCFAs and exert metabolic effects, including the inhibition of gluconeogenesis in the liver (De Vadder et al., 2014; Ulven, 2012). FFA2 has immune functionality, and recent work has found that the loss of this receptor enhanced colonic adenoma formation when it was knocked out on the background of the $Apc^{Min+/-}$ mouse model (Pan et al., 2017). Additionally, SCFA interactions with FFA2 are associated with the release of the incretin glucagon-like petide-1 (GLP-1)(Tolhurst et al., 2012). GLP-1 has multiple effects that result in improved metabolic outcomes in T2D, including stimulation of insulin secretion and decreased appetite (Drucker & Nauck, 2006). However, evidence exists suggesting that GLP-1 agonists may promote colon tumorigenesis, and that the loss of the GLP-1 receptor protected $Apc^{Min+/-}$ mice from polyp formation (Koehler et al., 2015). Metformin also increases GLP-1 levels, and raises the question if this is another layer of

interactions between metformin, microbiome, SCFA, and metabolism (Mannucci et al., 2001).

Unique to this work, are the observations made regarding tumor volume growth and exposure to antibiotic treatments. While we confirmed the inhibitory effects of oral metformin, the effect of antibiotic exposure inhibiting metformin's effects is novel. Little work has been done to study the effects of antibiotics on xenograft and allograft tumor growth, with early work on acivicin showing inhibitory effects on leukemia and breast cancer models (Poster, Bruno, Penta, Neil, & McGovren, 1981). In 2002, antibiotics from the ancamysin family were found to inhibit the growth of HER-2 positive breast cancer xenografts, by degrading HER-2 and impairing P13K and Akt growth signalling (Basso, Solit, Munster, & Rosen, 2002). Additionally, proteomics-based approaches were used to discover that several antibiotics classes are inhibitors of mitochondrial biogenesis (Lamb et al., 2015). This work found that cancer stem cells, which rely on mitochondrial function and biogenesis to support growth, were negatively affected by antibiotics from the erythromycin, tetracycline, and glycylcycline families of antibiotics. These studies provide some basis for further studying the effects of antibiotics alone on cancer growth and development.

4.11 Summary

Epidemiological data in people with type 2 diabetes has provided promising insight into the potential for metformin to inhibit colon cancer (Evans et al., 2005), however, the mechanisms mediating these effects have yet to be fully elucidated. It is often thought that metformin may inhibit cancer growth by its systemic effects, improving glucose and insulin metabolism, thereby decreasing a potentially pro-cancer growth environment. Alternatively, metformin may act directly by entering the cancer cells, inhibiting energy production via complex I inhibition, activating AMPK and downregulating cellular machinery required for a proliferating cell. The three studies completed in this thesis aimed to clarify which of these mechanisms plays the largest role in a model of colorectal cancer. To this end, the effects of metformin on metabolism and tumor growth in a diet-induced obesity model with two different methods of metformin administration were tested, and expanded to explore the role of the gut microbiome in metformin's actions. In study 1, the growth-stimulatory effect of HFD feeding on the MC38 colon cancer allograft model was confirmed and found to correlate with changes in blood glucose but not serum insulin. I.p. injections of 100mg/kg metformin were found to have no impact on blood glucose, serum insulin or tumor growth. These data suggested that metformin is unlikely to suppress MC38 tumor growth through direct tumor effects and that i.p. injections of metformin are insufficient to reduce circulating blood glucose and insulin levels in high-fat diet fed mice. In study 2, the effects of oral administration of

metformin was tested, and found to improve glucose tolerance, and inhibit MC38 tumor growth. To further understand the mechanisms mediating these effects, the role of the gut microbiome was examined through the addition of the antibiotic ampicillin. This study found that the addition of ampicillin blunted the effects of metformin on reduced blood glucose and tumor growth. However, ampicillin is not localized to the gut, and this design was unable to fully tease out the role of the GMB. This led to the third study, where a fecal microbiome transfer was used to isolate out the role of the GMB in metformin's anti-cancer effects. In this study, fecal transfer from metformin-treated mice resulted in no improvements in glucose and insulin metabolism, yet inhibited MC38 tumor growth. These findings suggested metformin alters the microbiome in ways that can be transferred via fecal material to directly suppress tumor growth. Taken together, *this body of work found oral metformin reduces blood glucose and CRC tumor growth, and that the GMB is important for mediating the anti-tumor effects of metformin in a mouse model of diet-induced obesity with colon cancer.*

Bibliography

Abdulamir, A. S., Hafidh, R. R., & Bakar, F. A. (2011). The association of Streptococcus bovis/gallolyticus with colorectal tumors: The nature and the underlying mechanisms of its etiological role. *Journal of Experimental and Clinical Cancer Research*, *30*(1), 11. http://doi.org/10.1186/1756-9966-30-11

Ahn, J., Sinha, R., Pei, Z., Dominianni, C., Wu, J., Shi, J., … Yang, L. (2013). Human gut microbiome and risk for colorectal cancer. *Journal of the National Cancer Institute*, *105*(24), 1907–1911. http://doi.org/10.1093/jnci/djt300

Akram, M. (2014). Citric acid cycle and role of its intermediates in metabolism. *Cell Biochemistry and Biophysics*, *68*(3), 475–478. http://doi.org/10.1007/s12013-013-9750-1

Alessi, D. R., James, S. R., Downes, C. P., Holmes, A. B., Gaffney, P. R. J., Reese, C. B., & Cohen, P. (1997). Characterization of a 3-phosphoinositide-dependent protein kinase which phosphorylates and activates protein kinase Bα. *Current Biology*, *7*(4), 261–269. http://doi.org/10.1016/S0960-9822(06)00122-9

Algire, C., Amrein, L., Bazile, M., David, S., Zakikhani, M., & Pollak, M. (2011). Diet and tumor LKB1 expression interact to determine sensitivity to anti-neoplastic effects of metformin in vivo. *Oncogene*, *30*(10), 1174–82. http://doi.org/10.1038/onc.2010.483

Algire, C., Amrein, L., Zakikhani, M., Panasci, L., & Pollak, M. (2010). Metformin blocks the stimulative effect of a high-energy diet on colon carcinoma growth in vivo and is associated with reduced expression of fatty acid synthase. *Endocrine-Related Cancer*, *17*(2), 351–60. http://doi.org/10.1677/ERC-09-0252

Ali, S., & Fonseca, V. (2012). Overview of metformin: special focus on metformin extended release. *Expert Opinion on Pharmacotherapy*, *13*(12), 1797–805. http://doi.org/10.1517/14656566.2012.705829

Andrzejewski, S., Gravel, S.-P., Pollak, M., & St-Pierre, J. (2014). Metformin directly acts on mitochondria to alter cellular bioenergetics. *Cancer & Metabolism*, *2*(1), 12. http://doi.org/10.1186/2049-3002-2-12

Archer, S. Y., Johnson, J., Kim, H.-J., Ma, Q., Mou, H., Daesety, V., … Hodin, R. A. (2005). The histone deacetylase inhibitor butyrate downregulates cyclin B1 gene expression via a p21/WAF-1-dependent mechanism in human colon cancer cells. *American Journal of Physiology. Gastrointestinal and Liver Physiology*, *289*(4), G696-703. http://doi.org/10.1152/ajpgi.00575.2004

Arpaia, N., Campbell, C., Fan, X., Dikiy, S., Van Der Veeken, J., Deroos, P., … Rudensky, A. Y. (2013). Metabolites produced by commensal bacteria promote peripheral regulatory T-cell generation. *Nature*, *504*(7480), 451–455. http://doi.org/10.1038/nature12726

Arthur, J. C., Perez-Chanona, E., Muhlbauer, M., Tomkovich, S., Uronis, J. M., Fan, T.-J., … Jobin, C. (2012). Intestinal inflammation targets cancer-

inducing activity of the microbiota. *Science*, *338*(6103), 120–123. http://doi.org/10.1126/science.1224820

Arthur, J., Gharaibeh, R., Mühlbauer, M., Perez-Chanona, E., Uronis, J. M., McCafferty, J., … Jobin, C. (2015). Microbial genomic analysis reveals the essential role of inflammation in bacteria-induced colorectal cancer. *Nature Communications*, *5*(4724). http://doi.org/10.1002/adma.201403943.Evaluating

Aw, D. K. L., Sinha, R. A., Xie, S. Y., & Yen, P. M. (2014). Differential AMPK phosphorylation by glucagon and metformin regulates insulin signaling in human hepatic cells. *Biochemical and Biophysical Research Communications*, *447*(4), 569–573. http://doi.org/10.1016/j.bbrc.2014.04.031

Bäckhed, F., Ding, H., Wang, T., Hooper, L. V, Koh, G. Y., Nagy, A., … Gordon, J. I. (2004). The gut microbiota as an environmental factor that regulates fat storage. *Proceedings of the National Academy of Sciences of the United States of America*, *101*(44), 15718–23. http://doi.org/10.1073/pnas.0407076101

Baldeweg, S. E., Golay, A., Natali, A., Balkau, B., Del Prato, S., & Coppack, S. W. (2000). Insulin resistance, lipid and fatty acid concentrations in 867 healthy Europeans. *European Journal of Clinical Investigation*, *30*(1), 45–52. http://doi.org/10.1046/j.1365-2362.2000.00597.x

Ballestero, M. R., Monte, M. J., Briz, O., Jimenez, F., Martin, F. G., & Marin, J. J.

G. (2006). Expression of transporters potentially involved in the targeting of cytostatic bile acid derivatives to colon cancer and polyps, *72*, 729–738. http://doi.org/10.1016/j.bcp.2006.06.007

Barcenilla, A., Pryde, S. E., Martin, J. C., Duncan, H., Stewart, C. S., Henderson, C., … Flint, H. J. (2000). Phylogenetic Relationships of Butyrate-Producing Bacteria from the Human Gut. *Applied and Environmental Microbiology*, *66*(4), 1654–1661. http://doi.org/10.1128/AEM.66.4.1654-1661.2000.

Bartram, A. K., Lynch, M. D. J., Stearns, J. C., Moreno-Hagelsieb, G., & Neufeld, J. D. (2011). Generation of multimillion-sequence 16S rRNA gene libraries from complex microbial communities by assembling paired-end Illumina reads. *Applied and Environmental Microbiology*, *77*(11), 3846–3852. http://doi.org/10.1128/AEM.02772-10

Basso, A. D., Solit, D. B., Munster, P. N., & Rosen, N. (2002). Ansamycin antibiotics inhibit Akt activation and cyclin D expression in breast cancer cells that overexpress HER2. *Oncogene*, *21*(8), 1159–1166. http://doi.org/10.1038/sj/onc/1205184

Bauer, P. V, Duca, F. A., Waise, T. M. Z., Rasmussen, B. A., Abraham, M. A., Dranse, H. J., … Lam, T. K. T. (2018). Metformin alters upper small intestinal microbiota that impact a glucose-SGLT1-sensing glucoregulatory pathway. *Cell Metabolism*, p. 101–117.e5. Elsevier Inc. http://doi.org/10.1016/j.cmet.2017.09.019

Baxter, N. T., Zackular, J. P., Chen, G. Y., & Schloss, P. D. (2014). Structure of

the gut microbiome following colonization with human feces determines colonic tumor burden. *Microbiome*, *2*(1), 1–11. http://doi.org/10.1186/2049-2618-2-20

Bekusova, V. V. ., Patsanovskii, V. M., Nozdrachev, A. D., Trashkov, A. P., Artemenko, M. R., & Anisimov, V. N. (2017). Metformin prevents hormonal and metabolic disturbances and 1,2-dimethylhydrazine-induced colon carcinogenesis in non-diabetic rats. *Cancer Biology & Medicine*, *14*(1), 100–107. http://doi.org/10.20892/j.issn.2095-3941.2016.0088

Bilandzic, A., & Rosella, L. (2017). The cost of diabetes in Canada over 10 years: applying attributable health care costs to a diabetes incidence prediction model. *Health Promotion and Chronic Disease Prevention in Canada : Research, Policy and Practice*, *37*(2), 49–53. http://doi.org/10.24095/hpcdp.37.2.03

Birsoy, K., Possemato, R., Lorbeer, F. K., Bayraktar, E. C., Thiru, P., Yucel, B., … Sabatini, D. M. (2014). Metabolic determinants of cancer cell sensitivity to glucose limitation and biguanides. *Nature*, *508*(7494), 108–12. http://doi.org/10.1038/nature13110

Boleij, A., Van Gelder, M. M. H. J., Swinkels, D. W., & Tjalsma, H. (2011). Clinical importance of streptococcus gallolyticus infection among colorectal cancer patients: Systematic review and meta-analysis. *Clinical Infectious Diseases*, *53*(9), 870–878. http://doi.org/10.1093/cid/cir609

Boucher, J., Kleinridders, A., & Kahn, C. R. (2014). Insulin receptor signaling in

normal and insulin-resistant states. *Cold Spring Harb Perspect Biol 2014*, *6*, a009191. http://doi.org/10.1101/cshperspect.a009191

Boyle, T., Keegel, T., Bull, F., Heyworth, J., & Fritschi, L. (2012). Physical activity and risks of proximal and distal colon cancers: A systematic review and meta-analysis. *Journal of the National Cancer Institute*, *104*(20), 1548–1561. http://doi.org/10.1093/jnci/djs354

Brenner, H., Kloor, M., & Pox, C. P. (2014). Colorectal cancer. *The Lancet*, *383*(9927), 1490–1502. http://doi.org/10.1016/S0140-6736(13)61649-9

Brown, D. G., Rao, S., Weir, T. L., O'Malia, J., Bazan, M., Brown, R. J., & Ryan, E. P. (2016). Metabolomics and metabolic pathway networks from human colorectal cancers, adjacent mucosa, and stool. *Cancer and Metabolism*, *4*(1), 1–12. http://doi.org/10.1186/s40170-016-0151-y

Buse, J. B., DeFronzo, R. A., Rosenstock, J., Kim, T., Burns, C., Skare, S., … Fineman, M. (2016). The primary glucose-lowering effect of metformin resides in the gut, not the circulation: Results from short-term pharmacokinetic and 12-week dose-ranging studies. *Diabetes Care*, *39*(2), 198–205. http://doi.org/10.2337/dc15-0488

Buzzai, M., Jones, R. G., Amaravadi, R. K., Lum, J. J., DeBerardinis, R. J., Zhao, F., … Thompson, C. B. (2007). Systemic treatment with the antidiabetic drug metformin selectively impairs p53-deficient tumor cell growth. *Cancer Research*, *67*(14), 6745–52. http://doi.org/10.1158/0008-5472.CAN-06-4447

Cai, H., Zhang, Y., Han, T., Everett, R. S., & Thakker, D. R. (2016). Cation-

selective transporters are critical to the AMPK-mediated antiproliferative effects of metformin in human breast cancer cells. *International Journal of Cancer*, *138*(9), 2281–2292. http://doi.org/10.1002/ijc.29965

Cameron, A. R., Morrison, V., Levin, D., Mohan, M., Forteath, C., Beall, C., … Rena, G. (2016). Anti-inflammatory effects of metformin irrespective of diabetes status. *Circulation Research*, *119*(5), 652–665. http://doi.org/10.1161/CIRCRESAHA.116.308445

Canadian Cancer Society's Advisory Committee on Cancer Statistics. (2017). Canadian Cancer Statistics 2017. *Canadian Cancer Society*, 1–132. http://doi.org/0835-2976

Cani, P. D., Bibiloni, R., Knauf, C., Neyrinck, A. M., & Delzenne, N. M. (2008). Changes in gut microbiota control metabolic diet–induced obesity and diabetes in mice. *Diabetes*, *57*(6), 1470–81. http://doi.org/10.2337/db07-1403.Additional

Carling, D., Clarke, P. R., Zammit, V. A., & Hardie, D. G. (1989). Purification and characterization of the AMP-activated protein kinase. *Eur J Biochemistry*, *136*, 129–136. http://doi.org/10.1111/j.1432-1033.1989.tb15186.x

Castaño-Milla, C., Chaparro, M., & Gisbert, J. P. (2014). Systematic review with meta-analysis: The declining risk of colorectal cancer in ulcerative colitis. *Alimentary Pharmacology and Therapeutics*, *39*(7), 645–659. http://doi.org/10.1111/apt.12651

Chan, D. S. M., Lau, R., Aune, D., Vieira, R., Greenwood, D. C., Kampman, E., & Norat, T. (2011). Red and processed meat and colorectal cancer incidence: Meta-analysis of prospective studies. *PLoS ONE*, *6*(6). http://doi.org/10.1371/journal.pone.0020456

Chandel, N. S., Avizonis, D., Reczek, C. R., Weinberg, S. E., Menz, S., Neuhaus, R., … Pollak, M. (2016). Are metformin doses used in murine cancer models clinically relevant? *Cell Metabolism*, *23*(4), 569–570. http://doi.org/10.1016/j.cmet.2016.03.010

Chang, Y. T., Tsai, H. L., Kung, Y. T., Yeh, Y. S., Huang, C. W., Ma, C. J., … Wang, J. Y. (2018). Dose-dependent relationship between metformin and colorectal cancer occurrence among patients with Type 2 Diabetes—A nationwide cohort study. *Translational Oncology*, *11*(2), 535–541. http://doi.org/10.1016/j.tranon.2018.02.012

Chauvin, C., Koka, V., Nouschi, A., Mieulet, V., Hoareau-Aveilla, C., Dreazen, A., … Pende, M. (2014). Ribosomal protein S6 kinase activity controls the ribosome biogenesis transcriptional program. *Oncogene*, *33*(4), 474–483. http://doi.org/10.1038/onc.2012.606

Choi, C. S., Savage, D. B., Abu-Elheiga, L., Liu, Z.-X., Kim, S., Kulkarni, A., … Shulman, G. I. (2007). Continuous fat oxidation in acetyl-CoA carboxylase 2 knockout mice increases total energy expenditure, reduces fat mass, and improves insulin sensitivity. *Proceedings of the National Academy of Sciences of the United States of America*, *104*(42), 16480–5.

http://doi.org/10.1073/pnas.0706794104

Chung, H., Pamp, S. J., Hill, J. A., Surana, N. K., Sanna, M., Troy, E. B., … Kasper, D. L. (2012). Gut immune maturation depends on colonization with a host-specific microbiotia. *Cell*, *149*(7), 1578–1593. http://doi.org/10.1016/j.cell.2012.04.037.Gut

Clausen, M. R., & Mortensen, P. B. (1995). Kinetic studies on colonocyte metabolism of short chain fatty acids and glucose in ulcerative colitis. *Gut*, *37*(5), 684–689. http://doi.org/10.1136/gut.37.5.684

Cook, G. A., Otto, D. A., & Cornell, N. W. (1983). Malonyl-CoA inhibition of carnitine palmitoyltransferase: interpretation of I50 and K1 values. *The Biochemical Journal*, *212*(2), 525–7. http://doi.org/10.1042/bj2120525

Copps, K. ., & White, M. F. (2012). Regulation of insulin sensitivity by serine or threonine phosphorylation of insulin receptor substrate proteins IRS1 and IRS2. *Diabetologia*, *55*(10), 2565–2582. http://doi.org/10.1007/s00125-012-2644-8.Regulation

Corradetti, M. N., Inoki, K., Bardeesy, N., DePinho, R. A., & Guan, K. L. (2004). Regulation of the TSC pathway by LKB1: Evidence of a molecular link between tuberous sclerosis complex and Peutz-Jeghers syndrome. *Genes and Development*, *18*(13), 1533–1538. http://doi.org/10.1101/gad.1199104

Creamer, B., Shorter, R. G., & Bamforth, J. (1961). The turnover and shedding of epithelial cells. I. The turnover in the gastro-intestinal tract. *Gut*, *2*, 110–118. http://doi.org/10.1136/gut.2.2.110

Cufí, S., Corominas-Faja, B., Lopez-Bonet, E., Bonavia, R., Pernas, S., López, I. Á., … Menendez, J. A. (2013). Dietary restriction-resistant human tumors harboring the PIK3CA-activating mutation H1047R are sensitive to metformin. *Oncotarget*, *4*(9), 1484–95. http://doi.org/10.18632/oncotarget.1234

Cummings, J. H., Pomare, E. W., Branch, H. W. J., Naylor, C. P. E., & Macfarlane, T. (1987). Short chain fatty acids in human large intestine , portal , hepatic and venous blood. *Gut*, *28*, 1221–1227.

Cunningham, D., Atkin, W., Lenz, H. J., Lynch, H. T., Minsky, B., Nordlinger, B., & Starling, N. (2010). Colorectal cancer. *The Lancet*, *375*(9719), 1030–1047. http://doi.org/10.1016/S0140-6736(10)60353-4

Currie, C. J., Poole, C. D., & Gale, E. A. M. (2009). The influence of glucose-lowering therapies on cancer risk in type 2 diabetes. *Diabetologia*, *52*(9), 1766–77. http://doi.org/10.1007/s00125-009-1440-6

Currie, E., Schulze, A., Zechner, R., Walther, T. C., & Farese, R. V. (2013). Cellular fatty acid metabolism and cancer. *Cell Metabolism*, *18*(2), 153–61. http://doi.org/10.1016/j.cmet.2013.05.017

Dalby, M. J., Ross, A. W., Walker, A. W., & Morgan, P. J. (2017). Dietary uncoupling of gut microbiota and energy harvesting from obesity and glucose tolerance in mice. *Cell Reports*, *21*(6), 1521–1533. http://doi.org/10.1016/j.celrep.2017.10.056

Daniel, S. G., Ball, C. L., Besselsen, D. G., Doetschman, T., & Hurwitz, B. L.

(2017). Functional changes in the gut microbiome contribute to transforming growth factor beta-deficient colon cancer. *MSystems*, *2*(5), e00065-17.

Davie, J. R. (2003). Inhibition of histone deacetylase activity by butyrate. *The Journal of Nutrition*, *133*(7 Suppl), 24785S–2493S.

Davies, S. P., Helps, N. R., Cohen, P. T. W., & Hardie, D. G. (1995). 5′-AMP inhibits dephosphorylation, as well as promoting phosphorylation, of the AMP-activated protein kinase. Studies using bacterially expressed human protein phosphatase-2Cα and native bovine protein phosphatase-2Ac. *FEBS Letters*, *377*(3), 421–425. http://doi.org/10.1016/0014-5793(95)01368-7

De Jong, R. G., Burden, A. M., De Kort, S., Van Herk-Sukel, M. P., Vissers, P. A., Janssen, P. K., … Janssen-Heijnen, M. L. (2017). No decreased risk of gastrointestinal cancers in users of metformin in the Netherlands; A time-varying analysis of metformin exposure. *Cancer Prevention Research*, *10*(5), 290–297. http://doi.org/10.1158/1940-6207.CAPR-16-0277

De La Cuesta-Zuluaga, J., Mueller, N. T., Corrales-Agudelo, V., Velásquez-Mejía, E. P., Carmona, J. A., Abad, J. M., & Escobar, J. S. (2017). Metformin is associated with higher relative abundance of mucin-degrading akkermansia muciniphila and several short-chain fatty acid-producing microbiota in the gut. *Diabetes Care*, *40*(1), 54–62. http://doi.org/10.2337/dc16-1324

De Vadder, F., Kovatcheva-Datchary, P., Goncalves, D., Vinera, J., Zitoun, C., Duchampt, A., … Mithieux, G. (2014). Microbiota-generated metabolites

promote metabolic benefits via gut-brain neural circuits. *Cell*, *156*(1–2), 84–96. http://doi.org/10.1016/j.cell.2013.12.016

DeFronzo, R. A. (2009). From the triumvirate to the ominous octet: A new paradigm for the treatment of type 2 diabetes mellitus. *Diabetes*, *58*(4), 773–795. http://doi.org/10.2337/db09-9028

Dejea, C. M., Wick, E. C., Hechenbleikner, E. M., White, J. R., Mark Welch, J. L., Rossetti, B. J., … Sears, C. L. (2014). Microbiota organization is a distinct feature of proximal colorectal cancers. *Proceedings of the National Academy of Sciences*, *111*(51), 18321–18326. http://doi.org/10.1073/pnas.1406199111

Demigné, C., Morand, C., Levrat, M.-A., Besson, C., Moundras, C., & Rémésy, C. (1995). Effect of propionate on fatty acid and cholesterol synthesis and on acetate metabolism in isolated rat hepatocytes. *The British Journal of Nutrition*, *74*(2), 209–219. http://doi.org/10.1079/BJN19950124

Den Besten, G., Bleeker, A., Gerding, A., Van Eunen, K., Havinga, R., Van Dijk, T. H., … Bakker, B. M. (2015). Short-chain fatty acids protect against high-fat diet-induced obesity via a pparg-dependent switch from lipogenesis to fat oxidation. *Diabetes*, *64*(7), 2398–2408. http://doi.org/10.2337/db14-1213

den Besten, G., Lange, K., Havinga, R., van Dijk, T. H., Gerding, A., van Eunen, K., … Reijngoud, D.-J. (2013). Gut-derived short-chain fatty acids are vividly assimilated into host carbohydrates and lipids. *AJP: Gastrointestinal and Liver Physiology*, *305*(12), G900–G910.

http://doi.org/10.1152/ajpgi.00265.2013

den Besten, G., van Eunen, K., Groen, A. K., Venema, K., Reijngoud, D.-J., & Bakker, B. M. (2013). The role of short-chain fatty acids in the interplay between diet, gut microbiota, and host energy metabolism. *Journal of Lipid Research*, *54*(9), 2325–2340. http://doi.org/10.1194/jlr.R036012

Dong, Y., Zhou, J., Zhu, Y., Luo, L., He, T., Hu, H., … Teng, Z. (2017). Abdominal obesity and colorectal cancer risk: systematic review and meta-analysis of prospective studies. *Bioscience Reports*, *37*(6), BSR20170945. http://doi.org/10.1042/BSR20170945

Donohoe, D. R., Collins, L. B., Wali, A., Bigler, R., Sun, W., & Bultman, S. J. (2012). The warburg effect dictates the mechanism of butyrate-mediated histone acetylation and cell proliferation. *Molecular Cell*, *48*(4), 612–626. http://doi.org/10.1016/j.molcel.2012.08.033

Donohoe, D. R., Garge, N., Zhang, X., Sun, W., O'Connell, T. M., Bunger, M. K., & Bultman, S. K. (2011). The microbiome and butyrate regulate energy metabolism and autophagy in the mammalian colon. *Cell Metabolism*, *13*(5), 517–526. http://doi.org/10.1016/j.cmet.2011.02.018.The

Donohoe, D. R., Holley, D., Collins, L. B., Montgomery, S. A., Whitmore, A. C., Hillhouse, A., … Bultman, S. J. (2014). A gnotobiotic mouse model demonstrates that dietary fiber protects against colorectal tumorigenesis in a microbiota- and butyrate-dependent manner. *Cancer Discovery*, *4*(12), 1387–1397. http://doi.org/10.1158/2159-8290.CD-14-0501

Dorsey, J. L., & Becker, M. H. (2018). American Diabetes Association Standards of Medical care in Diabetes - 2018. *Diabetes Care*, *41*(Supplement 1), S55–S64. http://doi.org/10.2337/dc18-S006

Dowling, R. J. O., Lam, S., Bassi, C., Mouaaz, S., Aman, A., Kiyota, T., … Stambolic, V. (2016). Metformin pharmacokinetics in mouse tumors: Implications for human therapy. *Cell Metabolism*, *23*(4), 567–568. http://doi.org/10.1016/j.cmet.2016.03.006

Drewes, J. L., Housseau, F., & Sears, C. L. (2016). Sporadic colorectal cancer: Microbial contributors to disease prevention, development and therapy. *British Journal of Cancer*, *115*(3), 273–280. http://doi.org/10.1038/bjc.2016.189

Drucker, D. J., & Nauck, M. A. (2006). The incretin system: glucagon-like peptide-1 receptor agonists and dipeptidyl peptidase-4 inhibitors in type 2 diabetes. *Lancet*, *368*(9548), 1696–1705. http://doi.org/10.1016/S0140-6736(06)69705-5

Du, L., Kim, J. J., Shen, J., Chen, B., & Dai, N. (2017). KRAS and TP53 mutations in inflammatory bowel disease-associated colorectal cancer: a meta-analysis. *Oncotarget*, *8*(13), 22175–22186. http://doi.org/10.18632/oncotarget.14549

Ducker, G. S., Atreya, C. E., Simko, J. P., Hom, Y. K., Matli, M. R., Benes, C. H., … Warren, R. S. (2014). Incomplete inhibition of phosphorylation of 4E-BP1 as a mechanism of primary resistance to ATP-competitive mTOR

inhibitors. *Oncogene*, *33*(12), 1590–1600. http://doi.org/10.1038/onc.2013.92

Duncan, S. H., Holtrop, G., Lobley, G. E., Calder, A. G., Stewart, C. S., & Flint, H. J. (2004). Contribution of acetate to butyrate formation by human faecal bacteria. *British Journal of Nutrition*, *91*(06), 915. http://doi.org/10.1079/BJN20041150

Duncan, S. H., Lobley, G. E., Holtrop, G., Ince, J., Johnstone, A. M., Louis, P., & Flint, H. J. (2008). Human colonic microbiota associated with diet, obesity and weight loss. *International Journal of Obesity*, *32*(11), 1720–1724. http://doi.org/10.1038/ijo.2008.155

Eastwood, G. L. (1977). Gastrointestinal epithelial renewal. *Gastroenterology*, *72*(5), 962–975. http://doi.org/10.1016/S0016-5085(77)80221-7

Eisenberg, M. L., Maker, A. V, Slezak, L. A., Nathan, J. D., Sritharan, K. C., Jena, B. P., … Andersen, D. K. (2005). Insulin receptor (IR) and glucose transporter 2 (GLUT2) proteins form a complex on the rat hepatocyte membrane. *Original Paper Cell Physiol Biochem*, *15*, 51–58.

El-Mir, M.-Y., Nogueira, V., Fontaine, E., Averet, N., Rigoulet, M., & Leverve, X. (2000). Dimethylbiguanide inhibits cell respiration via an indirect effect targeted on the respiratory chain complex I. *Journal of Biological Chemistry*, *275*(1), 223–228. http://doi.org/10.1074/jbc.275.1.223

Ellison, L. F., & Wilkins, K. (2012). Canadian trends in cancer prevalence. *Health Reports / Statistics Canada, Canadian Centre for Health Information*, *23*(1),

7–16.

Ericsson, A. C., & Franklin, C. L. (2015). Manipulating the gut microbiota: Methods and challenges. *ILAR Journal*, *56*(2), 205–217. http://doi.org/10.1093/ilar/ilv021

Evans, J. M. M., Donnelly, L. A., Emslie-Smith, A. M., Alessi, D. R., & Morris, A. D. (2005). Metformin and reduced risk of cancer in diabetic patients. *BMJ (Clinical Research Ed.)*, *330*(7503), 1304–5. http://doi.org/10.1136/bmj.38415.708634.F7

Everard, A., Belzer, C., Geurts, L., Ouwerkerk, J. P., Druart, C., Bindels, L. B., & Guiot, Y. (2013). Cross-talk between *Akkermansia muciniphila* and intestinal epithelium controls diet-induced obesity. *Proc. Nati. Acad. Sci. USA*, *110*(22), 9066–9071. http://doi.org/10.1073/pnas.1219451110/-/DCSupplemental.www.pnas.org/cgi/doi/10.1073/pnas.1219451110

Fabbrini, E., Magkos, F., Mohammed, B. S., Pietka, T., Abumrad, N. A., Patterson, B. W., … Klein, S. (2009). Intrahepatic fat, not visceral fat, is linked with metabolic complications of obesity. *Proceedings of the National Academy of Sciences*, *106*(36), 15430–15435. http://doi.org/10.1073/pnas.0904944106

Faubert, B., Boily, G., Izreig, S., Griss, T., Samborska, B., Dong, Z., … Jones, R. G. (2013). AMPK is a negative regulator of the Warburg effect and suppresses tumor growth in vivo. *Cell Metabolism*, *17*(1), 113–24. http://doi.org/10.1016/j.cmet.2012.12.001

Fedirko, V., Tramacere, I., Bagnardi, V., Rota, M., Scotti, L., Islami, F., … Jenab, M. (2011). Alcohol drinking and colorectal cancer risk: An overall and dose-Response meta-analysis of published studies. *Annals of Oncology*, *22*(9), 1958–1972. http://doi.org/10.1093/annonc/mdq653

Feng, Q., Liang, S., Jia, H., Stadlmayr, A., Tang, L., Lan, Z., … Wang, J. (2015). Gut microbiome development along the colorectal adenoma–carcinoma sequence. *Nature Communications*, *6*, 6528. http://doi.org/10.1038/ncomms7528

Ford, R. J., Fullerton, M. D., Pinkosky, S. L., Day, E. A., Scott, J. W., Oakhill, J. S., … Steinberg, G. R. (2015). Metformin and salicylate synergistically activate liver AMPK, inhibit lipogenesis and improve insulin sensitivity. *Biochemical Journal*, *468*(1), 125–132. http://doi.org/10.1042/BJ20150125

Foretz, M., Guigas, B., Bertrand, L., Pollak, M., & Viollet, B. (2014). Metformin: From mechanisms of action to therapies. *Cell Metabolism*, *20*(6), 953–966. http://doi.org/10.1016/j.cmet.2014.09.018

Foretz, M., Hébrard, S., Leclerc, J., Zarrinpashneh, E., Soty, M., Mithieux, G., … Viollet, B. (2010). Metformin inhibits hepatic gluconeogenesis in mice independently of the LKB1/AMPK pathway via a decrease in hepatic energy state. *The Journal of Clinical Investigation*, *120*(7), 2355–2369. http://doi.org/10.1172/JCI40671DS1

Forslund, K., Hildebrand, F., Nielsen, T., & Falony, G. (2015). Disentangling the effects of type 2 diabetes and metformin on the human gut microbiota.

Nature, *528*(7581), 262–266. http://doi.org/10.1038/nature15766.Disentangling

Foster, K. G., & Fingar, D. C. (2010). Mammalian target of rapamycin (mTOR): Conducting the cellular signaling symphony. *Journal of Biological Chemistry*, *285*(19), 14071–14077. http://doi.org/10.1074/jbc.R109.094003

Franciosi, M., Lucisano, G., Lapice, E., Strippoli, G. F. M., Pellegrini, F., & Nicolucci, A. (2013). Metformin therapy and risk of cancer in patients with type 2 diabetes: systematic review. *PloS One*, *8*(8), e71583. http://doi.org/10.1371/journal.pone.0071583

Francipane, M. G., & Lagasse, E. (2013). mTOR pathway in colorectal cancer: an update. *Oncotarget*, *5*(1), 49–66. http://doi.org/10.18632/oncotarget.1548

Fritsche-Guenther, R., Zasada, C., Mastrobuoni, G., Royla, N., Roßner, F., Pietzke, M., … Kempa, S. (2018). Alterations of mTOR signaling impact metabolic stress resistance in colorectal carcinomas with BRAF and KRAS mutations. *Scientific Reports*, *8*(January), 9204. http://doi.org/10.1038/s41598-018-27394-1

Fujisaka, S., Ussar, S., Clish, C., Devkota, S., Dreyfuss, J. M., Sakaguchi, M., … Kahn, C. R. (2016). Antibiotic effects on gut microbiota and metabolism are host dependent. *The Journal of Clinical Investigation*, *126*(12), 4330–4443. http://doi.org/10.1172/JCI86674.resistance

Fullerton, M. D., Galic, S., Marcinko, K., Sikkema, S., Pulinilkunnil, T., Chen, Z.-P., … Steinberg, G. R. (2013). Single phosphorylation sites in Acc1 and

Acc2 regulate lipid homeostasis and the insulin-sensitizing effects of metformin. *Nature Medicine*, *19*(12), 1649–1654. http://doi.org/10.1038/nm.3372

Gan, X., Wang, J., Su, B., & Wu, D. (2011). Evidence for direct activation of mTORC2 kinase activity by phosphatidylinositol 3,4,5-trisphosphate. *Journal of Biological Chemistry*, *286*(13), 10998–11002. http://doi.org/10.1074/jbc.M110.195016

Gandini, S., Puntoni, M., Heckman-Stoddard, B. M., Dunn, B. K., Ford, L., DeCensi, A., & Szabo, E. (2014). Metformin and cancer risk and mortality: A systematic review and meta-analysis taking into account biases and confounders. *Cancer Prevention Research*, *7*(9), 867–885. http://doi.org/10.1158/1940-6207.CAPR-13-0424

Gao, Z., Yin, J., Zhang, J., Ward, R. E., Martin, R. J., Lefevre, M., … Ye, J. (2010). Butyrate improves insulin sensitivity and increases energy expenditure in mice. *Diabetes*, *58*(8), 1–14. http://doi.org/10.2337/db08-1637.

Gilbert, J. A., Quinn, R. A., Debelius, J., Xu, Z. Z., Morton, J., Garg, N., … Knight, R. (2016). Microbiome-wide association studies link dynamic microbial consortia to disease. *Nature*, *535*(7610), 94–103. http://doi.org/10.1038/nature18850

Giovannucci, E. (2001). Insulin, insulin-like growth factors and colon cancer: A review of the evidence. *The Journal of Nutrition*, *131*(11), 3109–3120.

Giovannucci, E., Harlan, D. M., Archer, M. C., Bergenstal, R. M., Gapstur, S. M., Habel, L. A., … Yee, D. (2010). Diabetes and cancer: A consensus report. *Diabetes Care*, *33*(7), 1674–85. http://doi.org/10.2337/dc10-0666

GLOBOCAN. (2012). Fact Sheets by Cancer. Colorectal Cancer: estimated incidence, mortality and prevalence worldwide in 2012. Retrieved May 24, 2018, from http://globocan.iarc.fr/Pages/fact_sheets_cancer.aspx

GLOBOCAN 2012. (2018). Population Fact Sheets: World. Retrieved July 17, 2018, from http://globocan.iarc.fr/Pages/fact_sheets_population.aspx

Gómez-Rubio, V. (2017). ggplot2 - Elegant Graphics for Data Analysis (2nd Edition). *Journal of Statistical Software*, *77*(Book Review 2), 3–5. http://doi.org/10.18637/jss.v077.b02

Gonzalez-Garcia, R., McCubbin, T., Navone, L., Stowers, C., Nielsen, L., & Marcellin, E. (2017). Microbial propionic acid production. *Fermentation*, *3*(2), 21. http://doi.org/10.3390/fermentation3020021

González, N., Prieto, I., Puerto-Nevado, L. del, Portal-Nuñez, S., Ardura, J. A., Corton, M., … Consortium, D. C. C. (2017). 2017 update on the relationship between diabetes and colorectal cancer: Epidemiology, potential molecular mechanisms and therapeutic implications. *Oncotarget*, *8*(11), 18456–18485. http://doi.org/10.18632/oncotarget.14472

Goodwin, A. C., Shields, C. E. D., Wu, S., Huso, D. L., Wu, X., Murray-Stewart, T. R., … Casero, R. A. (2011). Polyamine catabolism contributes to enterotoxigenic Bacteroides fragilis-induced colon tumorigenesis.

Proceedings of the National Academy of Sciences, *108*(37), 15354–15359. http://doi.org/10.1073/pnas.1010203108

Gormsen, L. C., Sundelin, E. I., Jensen, J. B., Vendelbo, M. H., Jakobsen, S., Munk, O. L., … Jessen, N. (2016). In vivo imaging of human 11C-metformin in peripheral organs: Dosimetry, biodistribution, and kinetic analyses. *Journal of Nuclear Medicine*, *57*(12), 1920–1926. http://doi.org/10.2967/jnumed.116.177774

Government of Canada, P. (2011). Diabetes in Canada: Facts and figures from a public health perspective - Public Health Agency of Canada.

Gowans, G. J., Hawley, S. A., Ross, F. A., & Hardie, D. G. (2013). AMP is a true physiological regulator of amp-activated protein kinase by both allosteric activation and enhancing net phosphorylation. *Cell Metabolism*, *18*(4), 556–566. http://doi.org/10.1016/j.cmet.2013.08.019

Graham, G. G., Punt, J., Arora, M., Day, R. O., Doogue, M. P., Duong, J. K., … Williams, K. M. (2011). Clinical pharmacokinetics of metformin. *Clinical Pharmacokinetics*, *50*(2), 81–98. http://doi.org/10.2165/11534750-000000000-00000

Grenham, S., Clarke, G., Cryan, J. F., & Dinan, T. G. (2011). Brain-gut-microbe communication in health and disease. *Frontiers in Physiology*, *2*(Dec), 1–15. http://doi.org/10.3389/fphys.2011.00094

Griss, T., Vincent, E. E., Egnatchik, R., Chen, J., Ma, E. H., Faubert, B., … Jones, R. G. (2015). Metformin antagonizes cancer cell proliferation by suppressing

mitochondrial-dependent biosynthesis. *PLOS Biology*, *13*(12), e1002309. http://doi.org/10.1371/journal.pbio.1002309

Grover, M., & Kashyap, P. C. (2014). Germ free mice as a model to study effect of gut microbiota on host physiology. *Neurogastroenterology Motility*, *26*(6), 745–748. http://doi.org/10.1111/nmo.12366.Germ

Guariguata, L., Whiting, D. R., Hambleton, I., Beagley, J., Linnenkamp, U., & Shaw, J. E. (2014). Global estimates of diabetes prevalence for 2013 and projections for 2035. *Diabetes Research and Clinical Practice*, *103*(2), 137–149. http://doi.org/10.1016/j.diabres.2013.11.002

Gulhati, P., Cai, Q., Li, J., Liu, J., Rychahou, P. G., Lee, E. Y., … Mark, B. (2009). Targeted inhibition of mTOR signaling inhibits tumorigenesis of colorectal cancer. *Clinical Cancer Research*, *15*(23), 7207–7216. http://doi.org/10.1158/1078-0432.CCR-09-1249.TARGETED

Gunton, J. E., Delhanty, P. J. D., Takahashi, S. I., & Baxter, R. C. (2003). Metformin rapidly increases insulin receptor activation in human liver and signals preferentially through insulin-receptor substrate-2. *Journal of Clinical Endocrinology and Metabolism*, *88*(3), 1323–1332. http://doi.org/10.1210/jc.2002-021394

Gwinn, D. M., Shackelford, D. B., Egan, D. F., Mihaylova, M. M., Mery, A., Vasquez, D. S., … Shaw, R. J. (2008). AMPK phosphorylation of raptor mediates a metabolic checkpoint. *Molecular Cell*, *30*(2), 214–226. http://doi.org/10.1016/j.molcel.2008.03.003

Ha, J., Daniel, S., Broyles, S. S., & Kim, K. H. (1994). Critical phosphorylation sites for acetyl-CoA carboxylase activity. *The Journal of Biological Chemistry*, *269*(35), 22162–8.

Hahn-Windgassen, A., Nogueira, V., Chen, C. C., Skeen, J. E., Sonenberg, N., & Hay, N. (2005). Akt activates the mammalian target of rapamycin by regulating cellular ATP level and AMPK activity. *Journal of Biological Chemistry*, *280*(37), 32081–32089. http://doi.org/10.1074/jbc.M502876200

Hamer, H. M., Jonkers, D., Venema, K., Vanhoutvin, S., Troost, F. J., & Brummer, R. J. (2008). Review article: The role of butyrate on colonic function. *Alimentary Pharmacology and Therapeutics*, *27*(2), 104–119. http://doi.org/10.1111/j.1365-2036.2007.03562.x

Han, T. K., Proctor, W. R., Costales, C. L., Cai, H., Everett, R. S., & Thakker, D. R. (2015). Four cation-selective transporters contribute to apical uptake and accumulation of metformin in Caco-2 cell monolayers. *J Pharmacol Exp Ther*, *352*(3), 519–528. http://doi.org/10.1124/jpet.114.220350

Hanahan, D., & Weinberg, R. A. (2011). Hallmarks of cancer: the next generation. *Cell*, *144*(5), 646–74. http://doi.org/10.1016/j.cell.2011.02.013

Hardie, D. G., Ross, F. A., & Hawley, S. A. (2012). AMPK: a nutrient and energy sensor that maintains energy homeostasis. *Nature Reviews. Molecular Cell Biology*, *13*(4), 251–62. http://doi.org/10.1038/nrm3311

Hawley, S. A., Pan, D. A., Mustard, K. J., Ross, L., Bain, J., Edelman, A. M., … Hardie, D. G. (2005). Calmodulin-dependent protein kinase kinase-β is an

alternative upstream kinase for AMP-activated protein kinase. *Cell Metabolism*, *2*(1), 9–19. http://doi.org/10.1016/j.cmet.2005.05.009

Hawley, S. A., Selbert, M. A., Goldstein, E. G., Edelman, A. M., Carling, D., & Hardie, D. G. (1995). 5′-AMP activates the AMP-activated protein kinase cascade, and Ca2+/calmodulin the calmodulin-dependent protein kinase I cascade, via three independent mechanisms. *J. Biol. Chem.*, *270*(45), 27186–27191.

He, L., Sabet, A., Djedjos, S., Miller, R., Sun, X., Mehboob, A., … Wondisford, F. E. (2009). Metformin and insulin suppress hepatic gluconeogenesis by inhibiting cAMP signaling through phosphorylation of CREB binding protein (CBP). *Cell*, *137*(4), 635–646. http://doi.org/10.1016/j.cell.2009.03.016.Metformin

Hemminki, A., Markie, D., Tomlinson, I., Avizienyte, E., Roth, S., Loukola, A., … Aaltonen, L. A. (1998). A serine/threonine kinase gene defective in Peutz-Jeghers syndrome. *Nature*, *391*(6663), 184–187. http://doi.org/10.1038/34432

Herzig, S., Long, F., Jhala, U. S., Hedrick, S., Quinn, R., Bauer, A., … Montminy, M. (2001). CREB regulates hepatic gluconeogenesis through the coactivator PGC-1. *Nature*, *413*(6852), 179–183. http://doi.org/10.1038/35093131

Hinnebusch, B. F., Meng, S., Wu, J. T., Archer, S. Y., & Hodin, R. A. (2002). The effects of short-chain fatty acids on human colon cancer cell phenotype are

associated with histone hyperacetylation. *The Journal of Nutrition*, *132*(5), 1012–1017. http://doi.org/10.1038/nrc3610

Hong, S., Zhao, B., Lombard, D. B., Fingar, D. C., & Inoki, K. (2014). Cross-talk between sirtuin and mammalian target of rapamycin complex 1 (mTORC1) signaling in the regulation of S6 kinase 1 (S6K1) phosphorylation. *Journal of Biological Chemistry*, *289*(19), 13132–13141. http://doi.org/10.1074/jbc.M113.520734

Hosono, K., Endo, H., Takahashi, H., Sugiyama, M., Sakai, E., Uchiyama, T., … Nakajima, A. (2010). Metformin suppresses colorectal aberrant crypt foci in a short-term clinical trial. *Cancer Prevention Research*, *3*(9), 1077–1083. http://doi.org/10.1158/1940-6207.CAPR-10-0186

Hosono, K., Endo, H., Takahashi, H., Sugiyama, M., Uchiyama, T., Suzuki, K., … Nakajima, A. (2010). Metformin suppresses azoxymethane-induced colorectal aberrant crypt foci by activating AMP-activated protein kinase. *Molecular Carcinogenesis*, *49*(7), 662–671. http://doi.org/10.1002/mc.20637

Hossain, P., Kawar, B., & El Nahas, M. (2007). Obesity and diabetes in the developing world — A growing challenge. *New England Journal of Medicine*, *356*(3), 213–215. http://doi.org/10.1056/NEJMp068177

Hosseini, E., Grootaert, C., Verstraete, W., & Van de Wiele, T. (2011). Propionate as a health-promoting microbial metabolite in the human gut. *Nutrition Reviews*, *69*(5), 245–258. http://doi.org/10.1111/j.1753-4887.2011.00388.x

Hu, B., Elinav, E., Huber, S., Strowig, T., Hao, L., Hafemann, A., … Flavell, R. A. (2013). Microbiota-induced activation of epithelial IL-6 signaling links inflammasome-driven inflammation with transmissible cancer. *Proceedings of the National Academy of Sciences*, *110*(24), 9862–9867. http://doi.org/10.1073/pnas.1307575110

Hundal, R. S., Krssak, M., Dufour, S., Laurent, D., Lebon, V., Chandramouli, V., … Shulman, G. I. (2000). Mechanism by which metformin reduces glucose production in type 2 diabetes. *Diabetes*, *49*(12), 2063–2069. http://doi.org/10.1109/TMI.2012.2196707.Separate

Hvid, H., Fendt, S.-M., Blouin, M.-J., Birman, E., Voisin, G., Svendsen, A. M., … Pollak, M. (2012). Stimulation of MC38 tumor growth by insulin analog X10 involves the serine synthesis pathway. *Endocrine-Related Cancer*, *19*(4), 557–74. http://doi.org/10.1530/ERC-12-0125

Inoki, K., Zhu, T., & Guan, K.-L. (2003). TSC2 mediates cellular energy response to control cell growth and survival. *Cell*, *115*(5), 577–590. http://doi.org/10.1016/S0092-8674(03)00929-2

Inzucchi, S. E., Bergenstal, R. M., Buse, J. B., Diamant, M., Ferrannini, E., Nauck, M., … Matthews, D. R. (2015). Management of hyperglycemia in type 2 diabetes, 2015: A patient-centered approach. Update to a position statement of the american diabetes association and the european association for the study of diabetes. *Diabetes Care*, *38*(1), 140–149. http://doi.org/10.2337/dc14-2441

Ismail, N. A., Ragab, S. H., ElBaky, A. A., Shoeib, A. R. S., Alhosary, Y., & Fekry, D. (2011). Frequency of firmicutes and bacteroidetes in gut microbiota in obese and normal weight Egyptian children and adults. *Archives of Medical Science*, *7*(3), 501–507. http://doi.org/10.5114/aoms.2011.23418

Iversen, A. B., Horsman, M. R., Jakobsen, S., Jensen, J. B., Garm, C., Jessen, N., … Busk, M. (2017). Results from 11C-metformin-PET scans, tissue analysis and cellular drug-sensitivity assays questions the view that biguanides affects tumor respiration directly. *Scientific Reports*, *7*(1), 9436. http://doi.org/10.1038/s41598-017-10010-z

Jacinto, E., Loewith, R., Schmidt, A., Lin, S., Rüegg, M. A., Hall, A., & Hall, M. N. (2004). Mammalian TOR complex 2 controls the actin cytoskeleton and is rapamycin insensitive. *Nature Cell Biology*, *6*(11), 1122–1128. http://doi.org/10.1038/ncb1183

Jakobsdottir, G., Xu, J., Molin, G., Ahrné, S., & Nyman, M. (2013). High-fat diet reduces the formation of butyrate, but increases succinate, inflammation, liver fat and cholesterol in rats, while dietary fibre counteracts these effects. *PLoS ONE*, *8*(11), 1–15. http://doi.org/10.1371/journal.pone.0080476

Jia, Y., Ma, Z., Liu, X., Zhou, W., He, S., Xu, X., … Tian, K. (2015). Metformin prevents DMH-induced colorectal cancer in diabetic rats by reversing the warburg effect. *Cancer Medicine*, *4*(11), 1730–1741. http://doi.org/10.1002/cam4.521

Jiang, G., & Zhang, B. B. (2003). Glucagon and regulation of glucose metabolism. *American Journal of Physiology - Endocrinology And Metabolism*, *284*(4), E671–E678. http://doi.org/10.1152/ajpendo.00492.2002

Jiang, Y., Ben, Q., Shen, H., Lu, W., Zhang, Y., & Zhu, J. (2011). Diabetes mellitus and incidence and mortality of colorectal cancer: A systematic review and meta-analysis of cohort studies. *European Journal of Epidemiology*, *26*(11), 863–876. http://doi.org/10.1007/s10654-011-9617-y

Kahn, S. E., Cooper, M. E., & Del Prato, S. (2014). Pathophysiology and treatment of type 2 diabetes: Perspectives on the past, present and future. *Lancet*, *383*(9922), 1068–1083. http://doi.org/10.1016/S0140-6736(13)62154-6.PATHOPHYSIOLOGY

Kalender, A., Selvaraj, A., Kim, S. Y., Gulati, P., Brûlé, S., Viollet, B., … Thomas, G. (2010). Metformin, independent of AMPK, inhibits mTORC1 in a rag GTPase-dependent manner. *Cell Metabolism*, *11*(5), 390–401. http://doi.org/10.1016/j.cmet.2010.03.014

Karim, B. O., & Huso, D. L. (2013). Mouse models for colorectal cancer. *American Journal of Cancer Research*, *3*(3), 240–50. http://doi.org/10.1038/sj.onc.1203036

Kim, J. H., Lee, K. J., Seo, Y., Kwon, J., Yoon, J. P., Kang, J. Y., … II Kim, T. (2018). Effects of metformin on colorectal cancer stem cells depend on alterations in glutamine metabolism. *Scientific Reports*, *8*(1), 409. http://doi.org/10.1038/s41598-017-18762-4

Klip, A., & Leiter, L. A. (1990). Cellular mechanism of action of metformin. *Diabetes Care*, *13*(6), 696–704. http://doi.org/10.2337/diacare.13.6.696

Koehler, J. A., Baggio, L. L., Yusta, B., Longuet, C., Rowland, K. J., Cao, X., … Drucker, D. J. (2015). GLP-1R agonists promote normal and neoplastic intestinal growth through mechanisms requiring Fgf7. *Cell Metabolism*, *21*(3), 379–391. http://doi.org/10.1016/j.cmet.2015.02.005

Koenuma, M., Yamori, T., & Tsuruo, T. (1989). Insulin and insulin-like growth factor 1 stimulate proliferation of metastatic variangs of colon carcinoma 26. *Japan Journal of Cancer Research*, *80*, 51–58.

Koo, S. H., Flechner, L., Qi, L., Zhang, X., Screaton, R. A., Jeffries, S., … Montminy, M. (2005). The CREB coactivator TORC2 is a key regulator of fasting glucose metabolism. *Nature*, *437*(7062), 1109–1111. http://doi.org/10.1038/nature03967

Kootte, R. S., Levin, E., Salojärvi, J., Smits, L. P., Hartstra, A. V., Udayappan, S. D., … Nieuwdorp, M. (2017). Improvement of insulin sensitivity after lean donor feces in metabolic syndrome is driven by baseline intestinal microbiota composition. *Cell Metabolism*, *26*(4), 611–619.e6. http://doi.org/10.1016/j.cmet.2017.09.008

Kulecka, M., Paziewska, A., Zeber-Lubecka, N., Ambrozkiewicz, F., Kopczynski, M., Kuklinska, U., … Ostrowski, J. (2016). Prolonged transfer of feces from the lean mice modulates gut microbiota in obese mice. *Nutrition and Metabolism*, *13*(1), 1–9. http://doi.org/10.1186/s12986-016-0116-8

Lalau, J.-D., Arnouts, P., Sharif, A., & De Broe, M. E. (2015). Metformin and other antidiabetic agents in renal failure patients. *Kidney International*, *87*(2), 308–322. http://doi.org/10.1038/ki.2014.19

Lamb, R., Ozsvari, B., Lisanti, C. L., Tanowitz, H. B., Howell, A., Martinez-Outschoorn, U. E., … Lisanti, M. P. (2015). Antibiotics that target mitochondria effectively eradicate cancer stem cells, across multiple tumor types: Treating cancer like an infectious disease. *Oncotarget*, *6*(7), 4569–4584. http://doi.org/10.18632/oncotarget.3174

Langille, M. G. I., Zaneveld, J., Caporaso, J. G., McDonald, D., Knights, D., Reyes, J. A., … Huttenhower, C. (2013). Predictive functional profiling of microbial communities using 16S rRNA marker gene sequences. *Nature Biotechnology*, *31*(9), 814–821. http://doi.org/10.1038/nbt.2676

Larsson, S. C., Orsini, N., & Wolk, A. (2005). Diabetes mellitus and risk of colorectal cancer: a meta-analysis. *Journal of the National Cancer Institute*, *97*(22), 1679–87. http://doi.org/10.1093/jnci/dji375

Lau, Y.-K. I., Du, X., Rayannavar, V., Hopkins, B., Shaw, J., Bessler, E., … Maurer, M. A. (2014). Metformin and erlotinib synergize to inhibit basal breast cancer. *Oncotarget*, *5*(21), 10503–10517.

Lawler, M., Alsina, D., Adams, R. A., Anderson, A. S., Brown, G., Fearnhead, N. S., … Tomlinson, I. (2018). Critical research gaps and recommendations to inform research prioritisation for more effective prevention and improved outcomes in colorectal cancer. *Gut*, *67*, 179–193.

http://doi.org/10.1136/gutjnl-2017-315333

Layden, B. T., Yalamanchi, S. K., Wolever, T. M., Dunaif, A., & Lowe Jr., W. L. (2012). Negative association of acetate with visceral adipose tissue and insulin levels. *Diabetes Metab Syndr.Obes.*, *5*, 49–55. http://doi.org/10.2147/DMSO.S29244

Lee, G., Malietzis, G., Askari, A., Bernardo, D., Al-Hassi, H. O., & Clark, S. K. (2015). Is right-sided colon cancer different to left-sided colorectal cancer? - A systematic review. *European Journal of Surgical Oncology*, *41*(3), 300–308. http://doi.org/10.1016/j.ejso.2014.11.001

Lee, H., & Ko, G. (2014). Effect of metformin on metabolic improvement and gut microbiota. *Applied and Environmental Microbiology*, *80*(19), 5935–5943. http://doi.org/10.1128/AEM.01357-14

Lee, W.-J., & Hase, K. (2014). Gut microbiota-generated metabolites in animal health and disease. *Nature Chemical Biology*, *10*(6), 416–24. http://doi.org/10.1038/nchembio.1535

Lewis, G., Carpentier, A., Adeli, K., & Giacca, A. (2002). Disordered fat storage and mobilization in the pathogenesis of insulin resistance and type 2 diabetes. *Endocrine Reviews*, *23*(2), 201. http://doi.org/10.1210/edrv.23.2.0461

Ley, R. E., Backhed, F., Turnbaugh, P., Lozupone, C. A., Knight, R. D., & Gordon, J. I. (2005). Obesity alters gut microbial ecology. *Proceedings of the National Academy of Sciences*, *102*(31), 11070–11075.

http://doi.org/10.1073/pnas.0504978102

Ley, R. E., Peterson, D. A., & Gordon, J. I. (2006). Ecological and evolutionary forces shaping microbial diversity in the human intestine. *Cell*, *124*(4), 837–848. http://doi.org/10.1016/j.cell.2006.02.017

Ley, R., Turnbaugh, P., Klein, S., & Gordon, J. (2006). Microbial ecology: human gut microbes associated with obesity. *Nature*, *444*(7122), 1022–3. http://doi.org/10.1038/nature4441021a

Li, B., Li, X., Ni, Z., Zhang, Y., Zeng, Y., Yan, X., … He, F. (2016). Dichloroacetate and metformin synergistically suppress the growth of ovarian cancer cells. *Oncotarget*, 1–13. http://doi.org/10.18632/oncotarget.10694

Li, J., Sung, C. Y. J., Lee, N., Ni, Y., Pihlajamäki, J., Panagiotou, G., & El-Nezami, H. (2016). Probiotics modulated gut microbiota suppresses hepatocellular carcinoma growth in mice. *Proceedings of the National Academy of Sciences*, *113*(9), E1306–E1315. http://doi.org/10.1073/pnas.1518189113

Li, W., Hua, B., Saud, S. M., Lin, H., Hou, W., Matthias, S., … Young, M. R. (2015). Berberine regulates AMP-activated protein kinase signaling pathways and inhibits colon tumorigenesis in mice. *Molecular Carcinogenesis*, *54*(10), 1096–1109. http://doi.org/10.1002/mc.22179.Berberine

Li, Y., Xu, S., Mihaylova, M., Zheng, B., Hou, X., Jiang, B., … Zang, M. (2011).

AMPK phosphorylates and inhibits SREBP activity to attenuate hepatic steatosis and atherosclerosis in diet-induced dnsulin resistant mice. *Cell Metabolism*, *13*(4), 617–638. http://doi.org/10.1016/j.cmet.2011.03.009.AMPK

Liang, P. S., Chen, T.-Y., & Giovannucci, E. (2009). Cigarette smoking and colorectal cancer incidence and mortality: Systematic review and meta-analysis. *International Journal of Cancer*, *124*(10), 2406–2415. http://doi.org/10.1002/ijc.24191

Lichtenstein, P., Holm, N., Verkasalo, P., Iliadou, A., Kaprio, J., Koskenvuo, M., … Hemminki, K. (2000). Environmental and heritable factors in the causation of cancer - Analyses of cohorts of twins from Sweden, Denmar, and Finland. *The New England Journal of Medicine*, *343*(2), 78–85.

Lin, P., Kent, D. M., Winn, A. N., Cohen, J. T., & Neumann, P. J. (2015). Multiple chronic conditions in type 2 siabetes mellitus: Prevalence and sonsequences. *American Journal of Managed Care*, *21*(1), e23–e34.

Louis, P., & Flint, H. J. (2009). Diversity, metabolism and microbial ecology of butyrate-producing bacteria from the human large intestine. *FEMS Microbiology Letters*, *294*(1), 1–8. http://doi.org/10.1111/j.1574-6968.2009.01514.x

Love, M. I., Huber, W., & Anders, S. (2014). Moderated estimation of fold change and dispersion for RNA-seq data with DESeq2. *Genome Biology*, *15*(12), 1–21. http://doi.org/10.1186/s13059-014-0550-8

Ludwig, D. S., Pereira, M., Kroenke, C., Hilner, J., Van Horn, L., Slattery, M., & Jacobs, D. (1999). Dietary fiber, weight gain, and cardiovascular disease risk factors in young adults. *JAMA*, *282*(16), 1539. http://doi.org/10.1001/jama.282.16.1539

Lundberg, R., Toft, M. F., August, B., Hansen, A. K., & Hansen, C. H. F. (2016). Antibiotic-treated versus germ-free rodents for microbiota transplantation studies. *Gut Microbes*, *7*(1), 68–74. http://doi.org/10.1080/19490976.2015.1127463

Ma, Y., Yang, Y., Wang, F., Zhang, P., Shi, C., Zou, Y., & Qin, H. (2013). Obesity and risk of colorectal cancer: A systematic review of prospective studies. *PLoS ONE*, *8*(1), e53916. http://doi.org/10.1371/journal.pone.0053916

Mackenzie, R. W. A., & Elliott, B. T. (2014). Akt / PKB activation and insulin signaling : a novel insulin signaling pathway in the treatment of type 2 diabetes. *Diabetes Metab Syndr Obes*, *7*, 55–64.

Madiraju, A. K., Erion, D. M., Rahimi, Y., Zhang, X.-M., Braddock, D. T., Albright, R. A., … Shulman, G. I. (2014). Metformin suppresses gluconeogenesis by inhibiting mitochondrial glycerophosphate dehydrogenase. *Nature*, *510*(7506), 542–546. http://doi.org/10.1038/nature13270

Madiraju, A. K., Qiu, Y., Perry, R. J., Rahimi, Y., Zhang, X.-M., Zhang, D., … Shulman, G. I. (2018). Metformin inhibits gluconeogenesis via a redox-

dependent mechanism in vivo. *Nature Medicine*, Epub ahead of print. http://doi.org/10.1038/s41591-018-0125-4

Madsen, A., Bozickovic, O., Bjune, J., Mellgren, G., & Sagen, J. V. (2015). Metformin inhibits hepatocellular glucose , lipid and cholesterol biosynthetic pathways by transcriptionally suppressing steroid receptor coactivator 2. *Scientific Reports*, *5*, 16430. http://doi.org/10.1038/srep16430

Mamane, Y., Petroulakis, E., Rong, L., Yoshida, K., Ler, L. W., & Sonenberg, N. (2004). eIF4E--from translation to transformation. *Oncogene*, *23*(18), 3172–9. http://doi.org/10.1038/sj.onc.1207549

Mannucci, E., Ognibene, a, Cremasco, F., Bardini, G., Mencucci, a, Pierazzuoli, E., … Rotella, C. M. (2001). Effect of metformin on glucagon-like peptide 1 (GLP-1) and leptin levels in obese nondiabetic subjects. *Diabetes Care*, *24*(3), 489–494. http://doi.org/10.2337/diacare.24.3.489

Marble, A. (1934). Diabetes and cancer. *New England Journal of Medicine*, *211*(8), 339–349. http://doi.org/10.1056/NEJM193408232110801

Marini, C., Bianchi, G., Buschiazzo, A., Ravera, S., Martella, R., Bottoni, G., … Sambuceti, G. (2016). Divergent targets of glycolysis and oxidative phosphorylation result in additive effects of metformin and starvation in colon and breast cancer. *Scientific Reports*, *6*, 19569. http://doi.org/10.1038/srep19569

Maruthur, N. M., Tseng, E., Hutfless, S., Wilson, L. M., Suarez-Cuervo, C., Berger, Z., … Bolen, S. (2016). Diabetes medications as monotherapy or

metformin-based combination therapy for type 2 diabetes: A systematic review and meta-analysis. *Annals of Internal Medicine*, *164*(11), 740–751. http://doi.org/10.7326/M15-2650

Mashhedi, H., Blouin, M. J., Zakikhani, M., David, S., Zhao, Y., Bazile, M., … Pollak, M. (2011). Metformin abolishes increased tumor 18F-2-fluoro-2-deoxy-d- glucose uptake associated with a high-energy diet. *Cell Cycle*, *10*(16), 2770–2778. http://doi.org/10.4161/cc.10.16.16219

McMurdie, P. J., & Holmes, S. (2013). Phyloseq: An R package for reproducible interactive analysis and graphics of microbiome census data. *PLoS ONE*, *8*(4), e61217. http://doi.org/10.1371/journal.pone.0061217

Membrez, M., Blancher, F., Jaquet, M., Bibiloni, R., Cani, P. D., Burcelin, R. G., … Chou, C. J. (2008). Gut microbiota modulation with norfloxacin and ampicillin enhances glucose tolerance in mice. *The FASEB Journal*, *22*(7), 2416–2426. http://doi.org/10.1096/fj.07-102723

Memmott, R. M., Mercado, J. R., Maier, C. R., Kawabata, S., Fox, S. D., & Dennis, P. A. (2010). Metformin prevents tobacco carcinogen-induced lung tumorigenesis. *Cancer Prevention Research*, *3*(9), 1066–1076. http://doi.org/10.1158/1940-6207.CAPR-10-0055

Merlano, M. C., Granetto, C., Fea, E., Ricci, V., & Garrone, O. (2017). Heterogeneity of colon cancer: From bench to bedside. *ESMO Open*, *2*(3), e000218. http://doi.org/10.1136/esmoopen-2017-000218

Microbiome Project Consortium, H. (2012). A framework for human microbiome

research. *Nature*, *486*(7402), 215–221. http://doi.org/10.1038/nature11209

Microbiome Project Consortium, H. (2013). Structure, Function and Diversity of the Healthy Human Microbiome. *Nature*, *486*(7402), 207–214. http://doi.org/10.1038/nature11234.Structure

Miller, R. A., Chu, Q., Xie, J., Foretz, M., Viollet, B., & Birnbaum, M. J. (2013). Biguanides suppress hepatic glucagon signalling by decreasing production of cyclic AMP. *Nature*, *494*(7436), 256–60. http://doi.org/10.1038/nature11808

Miyo, M., Konno, M., Nishida, N., Sueda, T., Noguchi, K., Matsui, H., … Zhou, J. (2016). Metabolic adaptation to nutritional stress in human colorectal cancer. *Scientific Reports*, *6*, 38415. http://doi.org/10.1038/srep38415

Mogavero, A., Maiorana, M. V., Zanutto, S., Varin, L., Bozzi, F., Belfi, A., … Pierotti, M. A. (2017). Metformin transiently inhibits colorectal cancer cell proliferation as a result of either AMPK activation or increased ROS production. *Scientific Reports*, *7*, 15992. http://doi.org/10.1038/s41598-017-16149-z

Mollica, M. P., Raso, G. M., Cavaliere, G., Trinchese, G., De Filippo, C., Aceto, S., … Meli, R. (2017). Butyrate regulates liver mitochondrial function, efficiency, and dynamics in insulin-resistant obese mice. *Diabetes*, *66*(5), 1405–1418. http://doi.org/10.2337/db16-0924

Moore, M. C., Coate, K. C., J, W. J., An, Z., Cherrrington, A. D., Winnick, J. J., & Cherrington, A. D. (2012). Regulation of hepatic glucose uptake and storage in vivo. *Advances in Nutrition*, *3*, 286–294.

http://doi.org/10.3945/an.112.002089.hand

Murugan, A. K., Alzahrani, A., & Xing, M. (2013). Mutations in critical domains confer the human mTOR gene strong tumorigenicity. *Journal of Biological Chemistry*, *288*(9), 6511–6521. http://doi.org/10.1074/jbc.M112.399485

Neuwirth, E. (2014). RColorBrewer: ColorBrewer Palettes. Retrieved July 29, 2018, from https://cran.r-project.org/web/packages/RColorBrewer/index.html

Nimri, L., Saadi, J., Peri, I., Yehuda-Shnaidman, E., & Schwartz, B. (2015). Mechanisms linking obesity to altered metabolism in mice colon carcinogenesis. *Oncotarget*, *6*(35), 38195–209. http://doi.org/10.18632/oncotarget.5561

Nolan, C. J., Madiraju, M. S. R., Delghingaro-Augusto, V., Peyot, M.-L., & Prentki, M. (2006). Fatty acid signaling in the beta-cell and insulin secretion. *Diabetes*, *55*(Supplement 2), S16–S23. http://doi.org/10.2337/db06-S003

Novosyadlyy, R., Lann, D. E., Vijayakumar, A., Rowzee, A., Lazzarino, D. A., Fierz, Y., … Leroith, D. (2011). Insulin-mediated acceleration of breast cancer development and progression in a non-obese model of type 2 diabetes. *Cancer Research*, *70*(2), 741–751. http://doi.org/10.1158/0008-5472.CAN-09-2141.Insulin-mediated

Ohigashi, S., Sudo, K., Kobayashi, D., Takahashi, O., Takahashi, T., Asahara, T., … Onodera, H. (2013). Changes of the intestinal microbiota, short chain fatty acids, and fecal pH in patients with colorectal cancer. *Digestive*

Diseases and Sciences, *58*(6), 1717–1726. http://doi.org/10.1007/s10620-012-2526-4

Owen, M., Doran, E., & Halestrap, A. (2000). Evidence that metformin exerts its anti-diabetic effects through inhibition of complex 1 of the mitochondrial respiratory chain. *Biochem. J*, *614*, 607–614.

Pan, P., W Skaer, C., Wang, H. T., Oshima, K., Huang, Y. W., Yu, J., … Wang, L. S. (2017). Loss of free fatty acid receptor 2 enhances colonic adenoma development and reduces the chemopreventive effects of black raspberries in ApcMin/+ mice. *Carcinogenesis*, *38*(1), 86–93. http://doi.org/10.1093/carcin/bgw122

Park, H., Cho, S., Woo, H., Park, S. K., Shin, H., Chang, H., … Shin, A. (2017). Fasting glucose and risk of colorectal cancer in the Korean Multi-center Cancer Cohort. *Plos One*, 1–12. http://doi.org/10.1371/journal.pone.0188465

Park, M.-Y., Kim, M. Y., Seo, Y. R., Kim, J.-S., & Sung, M.-K. (2016). High-fat diet accelerates intestinal tumorigenesis through disrupting intestinal cell membrane integrity. *Journal of Cancer Prevention*, *21*(2), 95–103. http://doi.org/10.15430/JCP.2016.21.2.95

Pedersen, H. K., Gudmundsdottir, V., Nielsen, H. B., Hyotylainen, T., Nielsen, T., Jensen, B. A. H., … Pedersen, O. (2016). Human gut microbes impact host serum metabolome and insulin sensitivity. *Nature*, *535*(7612), 376–381. http://doi.org/10.1038/nature18646

Peng, L., Li, Z.-R., Green, R. S., Holzman, I. R., & Lin, J. (2009). Butyrate

enhances the intestinal barrier by facilitating tight junction assembly via activation of AMP-activated protein kinase in Caco-2 cell monolayers. *Journal of Nutrition*, *139*(9), 1619–1625. http://doi.org/10.3945/jn.109.104638

Peng, L., Li, Z., Green, R. S., Holzman, I. R., & Lin, J. (2009). Butyrate enhances the intestinal barrier by facilitating tight junction assembly via activation of AMP-activated protein kinase. *The Journal of Nutrition*, *139*, 1619–1625. http://doi.org/10.3945/jn.109.104638.1619

Perry, R. J., Peng, L., Barry, N. A., Cline, G. W., Zhang, D., Cardone, R. L., … Goodman, A. L. (2016). Acetate mediates a microbiome-brain-beta cell axis promoting metabolic syndrome. *Nature*, *534*(7606), 213–217. http://doi.org/10.1038/nature18309.Acetate

Peters, S. G., Pomare, E. W., & Fisher, C. A. (1992). Portal and peripheral blood short chain fatty acid concentrations after caecal lactulose instillation at surgery. *Gut*, *33*(9), 1249–1252. http://doi.org/10.1136/gut.33.9.1249

Peters, U., Bien, S., & Zubair, N. (2016). Genetic architechture of colorectal cancer. *Gut*, *70*(12), 773–779. http://doi.org/10.1097/OGX.0000000000000256.Prenatal

Pettersson, U. S., Waldén, T. B., Carlsson, P.-O., Jansson, L., & Phillipson, M. (2012). Female Mice are Protected against High-Fat Diet Induced Metabolic Syndrome and Increase the Regulatory T Cell Population in Adipose Tissue. *PLoS ONE*, *7*(9), e46057. http://doi.org/10.1371/journal.pone.0046057

Plovier, H., Everard, A., Druart, C., Depommier, C., Van Hul, M., Geurts, L., … Cani, P. D. (2017). A purified membrane protein from Akkermansia muciniphila or the pasteurized bacterium improves metabolism in obese and diabetic mice. *Nature Medicine*, *23*(1), 107–113. http://doi.org/10.1038/nm.4236

Pollak, M. (2012). The insulin and insulin-like growth factor receptor family in neoplasia: an update. *Nature Reviews. Cancer*, *12*(3), 159–69. http://doi.org/10.1038/nrc3215

Pollak, M. N., Perdue, J. F., Margolese, R. G., Baer, K., & Richard, M. (1987). Presence of Somatomedin Receptors on Primary. *Cancer Letters*, *38*, 223–230.

Poster, D. S., Bruno, S., Penta, J., Neil, G. L., & McGovren, J. P. (1981). Acivicin: An antitumor antibiotic. *Cancer Clinical Trials*, *4*, 327–330.

Puigserver, P., Rhee, J., Donovan, J., Kitamura, Y., Altomonte, J., & Dong, H. (2003). Insulin-regulated hepatic gluconeogenesis through FOXO1 – PGC-1 a interaction. *Nature*, *423*(May), 550–555. http://doi.org/10.1038/nature01606.1.

Puppa, M. J., White, J. P., Sato, S., Cairns, M., Baynes, J. W., & Carson, J. A. (2011). Gut barrier dysfunction in the Apc Min/+ mouse model of colon cancer cachexia. *Biochimica et Biophysica Acta - Molecular Basis of Disease*, *1812*(12), 1601–1606. http://doi.org/10.1016/j.bbadis.2011.08.010

Qin, J., Li, R., Raes, J., Arumugam, M., Burgdorf, K. S., Manichanh, C., …

Zoetendal, E. (2010). A human gut microbial gene catalogue established by metagenomic sequencing. *Nature*, *464*(7285), 59–65. http://doi.org/10.1038/nature08821

Qin, J., Li, Y., Cai, Z., Li, S., Zhu, J., Zhang, F., … Wang, J. (2012). A metagenome-wide association study of gut microbiota in type 2 diabetes. *Nature*, *490*(7418), 55–60. http://doi.org/10.1038/nature11450

R Core Team. (2013). R: A language and environment for statistical Computing. Retrieved July 29, 2018, from https://www.r-project.org/

Rath, E., Moschetta, A., & Haller, D. (2018). Mitochondrial function — gatekeeper of intestinal epithelial cell homeostasis. *Nature Reviews Gastroenterology & Hepatology*, 1. http://doi.org/10.1038/s41575-018-0021-x

Rawson, R. B. (2003). The SREBP pathway--insights from insigs and insects. *Nature Reviews. Molecular Cell Biology*, *4*(8), 631–640. http://doi.org/10.1038/nrm1174

Reddy, B. S., Narisawa, T., & Weisburger, J. H. (1976). Colon carcinogenesis in germ-free rats with intrarectal 1,2-Dimethylhydrazine and subcutaneous azoxymethane. *Cancer Research*, *36*, 2874–2876.

Reddy, B. S., Narisawa, T., Wright, P., Vukusich, D., Weisburger, J. H., & Wynder, E. L. (1975). Colon carcinogenesis with azoxymethane and dimethylhydrazine in germ-free rats. *Cancer Research*, *35*(2), 287–290.

Reynolds, I. S., O'Toole, A., Deasy, J., McNamara, D. A., & Burke, J. P. (2017).

A meta-analysis of the clinicopathological characteristics and survival outcomes of inflammatory bowel disease associated colorectal cancer. *International Journal of Colorectal Disease*, *32*(4), 443–451. http://doi.org/10.1007/s00384-017-2754-3

Ridlon, J. M., Harris, S. C., Bhowmik, S., Kang, D. J., & Hylemon, P. B. (2016). Consequences of bile salt biotransformations by intestinal bacteria. *Gut Microbes*, *7*(1), 22–39. http://doi.org/10.1080/19490976.2015.1127483

Roediger, W. E. (1980). Role of anaerobic bacteria in the metabolic welfare of the colonic mucosa in man. *Gut*, *21*(9), 793–798. http://doi.org/10.1136/gut.21.9.793

Röhrig, F., & Schulze, A. (2016). The multifaceted roles of fatty acid synthesis in cancer. *Nature Reviews Cancer*, *16*(11), 732–749. http://doi.org/10.1038/nrc.2016.89

Roulin, D., Cerantola, Y., Dormond-Meuwly, A., Demartines, N., & Dormond, O. (2010). Targeting mTORC2 inhibits colon cancer cell proliferation in vitro and tumor formation in vivo. *Molecular Cancer*, *9*, 2–5. http://doi.org/10.1186/1476-4598-9-57

Rune, I., Hansen, C. H. F., Ellekilde, M., Nielsen, D. S., Skovgaard, K., Rolin, B. C., … Hansen, A. K. (2013). Ampicillin-improved glucose tolerance in diet-induced obese C57BL/6NTac mice is age dependent. *Journal of Diabetes Research*, *2013*. http://doi.org/10.1155/2013/319321

Salani, B., Maffioli, S., Hamoudane, M., Parodi, a., Ravera, S., Passalacqua, M.,

… Maggi, D. (2012). Caveolin-1 is essential for metformin inhibitory effect on IGF1 action in non-small-cell lung cancer cells. *The FASEB Journal*, *26*(2), 788–798. http://doi.org/10.1096/fj.11-192088

Saltiel, A. R., & Kahn, C. R. (2001). Insulin signalling and the regulation of glucose and lipid metabolism. *Nature*, *414*(6865), 799–806. http://doi.org/10.1038/414799a

Sambol, N. C., Brookes, L. G., Chiang, J., Goodman, A. M., Lin, E. T., Liu, C. Y., & Benet, L. Z. (1996). Food intake and dosage level, but not tablet vs solution dosage form, affect the absorption of metformin HCl in man. *British Journal of Clinical Pharmacology*, *42*(4), 510–512. http://doi.org/10.1111/j.1365-2125.1996.tb00017.x

Samuel, V. T., & Shulman, G. I. (2012). Integrating mechanisms for insulin resistance: Common threads and missing links. *Cell*, *148*(5), 852–871. http://doi.org/10.1016/j.cell.2012.02.017.Integrating

Samuels, Y., Wang, Z., Bardelli, A., Silliman, N., Ptak, J., Szabo, S., … Velculescu, V. E. (2004). High frequency of mutations of the PIK3CA gene in human cancers. *Science*, *304*(5670), 554. http://doi.org/10.1126/science.1096502

Sánchez-martínez, R., Cruz-gil, S., Cedrón, M. G. De, Vargas, T., Molina, S., García, B., … Molina, A. R. De. (2015). A link between lipid metabolism and epithelial-mesenchymal transition provides a target for colon cancer therapy. *Oncotarget*.

Sato, T., Nakashima, A., Guo, L., & Tamanoi, F. (2009). Specific activation of mTORC1 by Rheb G-protein in vitro involves enhanced recruitment of its substrate protein. *Journal of Biological Chemistry*, *284*(19), 12783–12791. http://doi.org/10.1074/jbc.M809207200

Scarpello, J. H., Hodgson, E., & Howlett, H. C. (1998). Effect of metformin on bile salt circulation and intestinal motility in type 2 diabetes mellitus. *Diabetic.Medicine : A Journal of the.British.Diabetic.Association.*, *15*(Figure 1), 651–656.

Schwartz, S., Fonseca, V., Berner, B., Cramer, M., Chiang, Y.-K., & Lewin, A. (2006). Efficacy, tolerability, and safety of a novel once-daily extended-release metformin in patients with type 2 diabetes. *Diabetes Care*, *29*(4), 759–764. http://doi.org/10.2337/diacare.29.04.06.dc05-1967

Schwiertz, A., Taras, D., Schäfer, K., Beijer, S., Bos, N. a, Donus, C., & Hardt, P. D. (2009). Microbiota and SCFA in lean and overweight healthy subjects. *Obesity*, *18*, 190–195. http://doi.org/10.1038/oby.2009.167

Scott, J. W., Ling, N., Issa, S. M. A., Dite, T. A., O'Brien, M. T., Chen, Z. P., … Oakhill, J. S. (2014). Small molecule drug A-769662 and AMP synergistically activate naive AMPK independent of upstream kinase signaling. *Chemistry and Biology*, *21*(5), 619–627. http://doi.org/10.1016/j.chembiol.2014.03.006

Segata, N., Izard, J., Waldron, L., Gevers, D., Miropolsky, L., Garrett, W. S., & Huttenhower, C. (2011). Metagenomic biomarker discovery and explanation.

Genome Biology, *12*(6). http://doi.org/10.1186/gb-2011-12-6-r60

Sharma, M., Nazareth, I., & Petersen, I. (2016). Trends in incidence, prevalence and prescribing in type 2 diabetes mellitus between 2000 and 2013 in primary care: A retrospective cohort study. *BMJ Open*, *6*(1), e010210. http://doi.org/10.1136/bmjopen-2015-010210

Shaw, R. J., Kosmatka, M., Bardeesy, N., Hurley, R. L., Witters, L. a, DePinho, R. a, & Cantley, L. C. (2004). The tumor suppressor LKB1 kinase directly activates AMP-activated kinase and regulates apoptosis in response to energy stress. *Proceedings of the National Academy of Sciences of the United States of America*, *101*(10), 3329–35. http://doi.org/10.1073/pnas.0308061100

Shaw, R. J., Lamia, K. a, Vasquez, D., Koo, S.-H., Bardeesy, N., Depinho, R. a, … Cantley, L. C. (2005). The kinase LKB1 mediates glucose homeostasis in liver and therapeutic effects of metformin. *Science*, *310*(5754), 1642–6. http://doi.org/10.1126/science.1120781

Shimobayashi, M., & Hall, M. N. (2014). Making new contacts: the mTOR network in metabolism and signalling crosstalk. *Nature Reviews. Molecular Cell Biology*, *15*(3), 155–62. http://doi.org/10.1038/nrm3757

Shin, N.-R., Lee, J.-C., Lee, H.-Y., Kim, M.-S., Whon, T. W., Lee, M.-S., & Bae, J.-W. (2014). An increase in the Akkermansia spp. population induced by metformin treatment improves glucose homeostasis in diet-induced obese mice. *Gut*, *63*(5), 727–35. http://doi.org/10.1136/gutjnl-2012-303839

Shu, Y., Sheardown, S. a S., Brown, C., Owen, R. P., Zhang, S., Castro, R. a, …

Giacomini, K. M. (2007). Effect of genetic variation in the organic cation transporter 1 (OCT1) on metformin action. *Journal of Clinical …*, *117*(5), 1422–31. http://doi.org/10.1172/JCI30558DS1

Siddle, K. (2011). Signalling by insulin and IGF receptors: Supporting acts and new players. *Journal of Molecular Endocrinology*, *47*(1). http://doi.org/10.1530/JME-11-0022

Simon, K. (2016). Colorectal cancer development and advances in screening. *Clinical Interventions in Aging*, *11*, 967–976. http://doi.org/10.2147/CIA.S109285

Stapleton, D., Mitchelhill, K. I., Gao, G., Widmer, J., Michell, B. J., Teh, T., … Kemp, B. E. (1996). Mammalian AMP-activated protein kinase subfamily. *Journal of Biological Chemistry*, *271*(2), 611–614. http://doi.org/10.1074/jbc.271.2.611

Statistics Canada. (2015). Table 102-0561 - Leading causes of death, total population, by age group and sex, Canada, annual. Retrieved May 23, 2018, from http://www5.statcan.gc.ca/cansim/a26?lang=eng&id=1020561

Statistics Canada, G. of C. (2017). *Health Fact Sheets: Diabetes, 2016*. *Statistics Canada* (Vol. 82–625–X).

Steinberg, G., & Kemp, B. (2009). AMPK in health and disease. *Physiological Reviews*, *89*, 1025–1078. http://doi.org/10.1152/physrev.00011.2008.

Stewart, B., & Wild, C. P. (2014). World Cancer Report 2014. *International Agency for Research on Cancer*.

Suissa, S., & Azoulay, L. (2012). Metformin and the risk of cancer: time-related biases in observational studies. *Diabetes Care*, *35*(12), 2665–73. http://doi.org/10.2337/dc12-0788

Sun, C., Li, X., Liu, L., Canet, M. J., Guan, Y., Fan, Y., & Zhou, Y. (2016). Effect of fasting time on measuring mouse blood glucose level. *International Journal of Clinical and Experimental Medicine*, *9*(2), 4186–4189.

Sun, J., & Jin, T. (2008). Both Wnt and mTOR signaling pathways are involved in insulin-stimulated proto-oncogene expression in intestinal cells. *Cellular Signalling*, *20*(1), 219–229. http://doi.org/10.1016/j.cellsig.2007.10.010

Surwit, R. S. S., Kuhn, C. M. M., Cochrane, C., McCubbin, J. a., & Feinglos, M. N. (1988). Diet-induced type II diabetes in C57BL/6J mice. *Diabetes*, *37*(9), 1163–1167. http://doi.org/10.2337/diabetes.37.9.1163

Suzuki, T., Bridges, D., Nakada, D., Skiniotis, G., Morrison, S. J., Lin, J., … Inoki, K. (2013). Inhibition of AMPK catabolic action by GSK3. *Molecular Cell*, *50*(3), 407–419. http://doi.org/10.1109/TMI.2012.2196707.Separate

Takahashi, H., Hosono, K., Endo, H., & Nakajima, A. (2013). Colon epithelial proliferation and carcinogenesis in diet-induced obesity. *Journal of Gastroenterology and Hepatology*, *28 Suppl 4*, 41–7. http://doi.org/10.1111/jgh.12240

Tang, Y., Chen, Y., Jiang, H., & Nie, D. (2011). The role of short-chain fatty acids in orchestrating two types of programmed cell death in colon cancer. *Autophagy*, *7*(2), 235–237. http://doi.org/10.4161/auto.7.2.14277

Tavares, M. R., Pavan, I. C. B., Amaral, C. L., Meneguello, L., Luchessi, A. D., & Simabuco, F. M. (2015). The S6K protein family in health and disease. *Life Sciences*, *131*, 1–10. http://doi.org/10.1016/j.lfs.2015.03.001

Taylor, D., Burt, B., Williams, M., Haug, P., & Cannon-Albright, L. (2010). Population-based family-history-specific risks for colorectal cancer: a constellation approach. *Gastroenterology*, *138*(3), 877–885. http://doi.org/10.1053/j.gastro.2009.11.044.Population-based

Thakkar, B., Aronis, K. N., Vamvini, M. T., Shields, K., & Mantzoros, C. S. (2013). Metformin and sulfonylureas in relation to cancer risk in type II diabetes patients: A meta-analysis using primary data of published studies. *Metabolism: Clinical and Experimental*, *62*(7), 922–934. http://doi.org/10.1016/j.metabol.2013.01.014

The ORIGIN Trial. (2012). Basal insulin and cardiovascular and other outcomes in dysglycemia. *New England Journal of Medicine*, *367*(4), 319–328. http://doi.org/10.1056/NEJMoa1203858

Toda, K., Kawada, K., Iwamoto, M., Inamoto, S., Sasazuki, T., Shirasawa, S., … Sakai, Y. (2016). Metabolic alterations caused by KRAS mutations in colorectal cancer contribute to cell adaptation to glutamine depletion by upregulation of asparagine synthetase. *Neoplasia*, *18*(11), 654–665. http://doi.org/10.1016/j.neo.2016.09.004

Tolhurst, G., Heffron, H., Lam, Y. S., Parker, H. E., Habib, A. M., Diakogiannaki, E., … Gribble, F. M. (2012). Short-chain fatty acids stimulate glucagon-like

peptide-1 secretion via the G-protein-coupled receptor FFAR2. *Diabetes*, *61*(2), 364–371. http://doi.org/10.2337/db11-1019

Tomimoto, A., Endo, H., Sugiyama, M., Fujisawa, T., Hosono, K., Takahashi, H., … Nakajima, A. (2008). Metformin suppresses intestinal polyp growth in ApcMin/+ mice. *Cancer Science*, *99*(11), 2136–2141. http://doi.org/10.1111/j.1349-7006.2008.00933.x

Tucker, G. T., Casey, C., Phillips, P. J., Connor, H., Ward, J. D., & Woods, H. F. (1981). Metformin kinetics in healthy subjects and in patients with diabetes mellitus. *British Journal of Clinical Pharmacology*, *12*(2), 235–246. http://doi.org/10.1111/j.1365-2125.1981.tb01206.x

Turnbaugh, P. J., Ley, R. E., Mahowald, M. A., Magrini, V., Mardis, E. R., & Gordon, J. I. (2006). An obesity-associated gut microbiome with increased capacity for energy harvest. *Nature*, *444*(7122), 1027–1031. http://doi.org/10.1038/nature05414

UKPDS, U. P. D. S. G. (1998). Effect of intensive blood-glucose control with metformin on complications in overweight patients with type 2 diabetes (UKPDS 34). *Lancet*, *352*(9131), 854–865. http://doi.org/10.1016/S0140-6736(98)07037-8

Ulven, T. (2012). Short-chain free fatty acid receptors FFA2/GPR43 and FFA3/GPR41 as new potential therapeutic targets. *Front Endocrinol (Lausanne)*, *3*(October), 111. http://doi.org/10.3389/fendo.2012.00111

Unger, R. H. (2003). Weapons of lean body mass destruction: The role of ectopic

lipids in the metabolic syndrome. *Endocrinology*, *144*(12), 5159–5165. http://doi.org/10.1210/en.2003-0870

Vadlakonda, L., Dash, A., Pasupuleti, M., Anil Kumar, K., & Reddanna, P. (2013). The paradox of Akt-mTOR interactions. *Frontiers in Oncology*, *3*(June), 1–9. http://doi.org/10.3389/fonc.2013.00165

Valvezan, A. J., Zhang, F., Diehl, J. A., & Klein, P. S. (2012). Adenomatous Polyposis Coli (APC) regulates multiple signaling pathways by enhancing glycogen synthase kinase-3 (GSK-3) activity. *Journal of Biological Chemistry*, *287*(6), 3823–3832. http://doi.org/10.1074/jbc.M111.323337

Vander Haar, E., Lee, S.-I., Bandhakavi, S., Griffin, T. J., & Kim, D.-H. (2007). Insulin signalling to mTOR mediated by the Akt/PKB substrate PRAS40. *Nature Cell Biology*, *9*(3), 316–23. http://doi.org/10.1038/ncb1547

Vasconcelos-Dos-Santos, A., Loponte, H. F. B. R., Mantuano, N. R., Oliveira, I. A., De Paula, I. F., Teixeira, L. K., … Todeschini, A. R. (2017). Hyperglycemia exacerbates colon cancer malignancy through hexosamine biosynthetic pathway. *Oncogenesis*, *6*(3). http://doi.org/10.1038/oncsis.2017.2

Venkateswaran, V., Haddad, A. Q., Fleshner, N. E., Fan, R., Sugar, L. M., Nam, R., … Pollak, M. (2007). Association of diet-induced hyperinsulinemia with accelerated growth of prostate cancer (LNCaP) xenografts. *Journal of the National Cancer Institute*, *99*(23), 1793–1800. http://doi.org/10.1093/jnci/djm231

Vetrano, S., & Danese, S. (2013). Colitis, microbiota, and colon cancer: An infernal triangle. *Gastroenterology*, *144*(2), 461–463. http://doi.org/10.1053/j.gastro.2012.12.016

Vital, M., Howe, A., & Tiedje, J. (2014). Revealing the bacterial synthesis pathways by analyzing (meta) genomic data. *MBio*, *5*(2), e00889. http://doi.org/10.1128/mBio.00889-14.Editor

Vogtmann, E., Hua, X., Zeller, G., Sunagawa, S., Voigt, A. Y., Hercog, R., … Sinha, R. (2016). Colorectal cancer and the human gut microbiome: Reproducibility with whole-genome shotgun sequencing. *PLoS ONE*, *11*(5), 1–13. http://doi.org/10.1371/journal.pone.0155362

Wang, C., Xu, C., Sun, M., Luo, D., & Liao, D. (2009). Acetyl-CoA carboxylase-α inhibitor TOFA induces human cancer cell apoptosis. *Biochemical and Biophysical Research Communications*, *385*(3), 302–306. http://doi.org/10.1016/j.bbrc.2009.05.045.Acetyl-CoA

Wang, D.-S. (2002). Involvement of organic cation transporter 1 in hepatic and intestinal distribution of metformin. *Journal of Pharmacology and Experimental Therapeutics*, *302*(2), 510–515. http://doi.org/10.1124/jpet.102.034140

Wang, H. B., Wang, P. Y., Wang, X., Wan, Y. L., & Liu, Y. C. (2012). Butyrate enhances intestinal epithelial barrier function via up-regulation of tight junction protein claudin-1 transcription. *Digestive Diseases and Sciences*, *57*(12), 3126–3135. http://doi.org/10.1007/s10620-012-2259-4

Wang, J., & Jia, H. (2016). Metagenome-wide association studies: fine-mining the microbiome. *Nat Rev Microbiol*, *Accepted i*(8), 508–522. http://doi.org/10.1038/nrmicro.2016.83

Wang, P., Zou, F., Zhang, X., Li, H., Dulak, A., Tomko, R. J., … Yu, J. (2009). microRNA-21 negatively regulates Cdc25A and cell cycle progression in colon cancer cells. *Cancer Research*, *69*(20), 8157–8165. http://doi.org/10.1158/0008-5472.CAN-09-1996

Wang, X. W., & Zhang, Y. J. (2014). Targeting mTOR network in colorectal cancer therapy. *World Journal of Gastroenterology*, *20*(15), 4178–4188. http://doi.org/10.3748/wjg.v20.i15.4178

Wang, Y., Nasiri, A. R., Damsky, W. E., Perry, C. J., Zhang, X. M., Rabin-Court, A., … Perry, R. J. (2018). Uncoupling hepatic oxidative phosphorylation reduces tumor growth in two murine models of colon cancer. *Cell Reports*, *24*(1), 47–55. http://doi.org/10.1016/j.celrep.2018.06.008

Warren, R. S., Yuan, H., Matli, M. R., Ferrara, N., & Donner, D. B. (1996). Induction of vascular endothelial growth factor by insulin-like growth factor 1 in colorectal carcinoma. *J Biol Chem*, *271*(46), 29483–29488. http://doi.org/10.1074/jbc.271.46.29483

Watkins, L. F., Lewis, L. R., & Levine, A. E. (1990). Characterization of the synergistic effect of insulin and transferrin and the regulation of their receptors on a human colon carcinoma cell line. *International Journal of Cancer*, *45*, 372–375.

Watson, P. M., Commins, S. P., Beiler, R. J., Hatcher, H. C., Gettys, T. W., M, P., & J, R. (2009). Differential regulation of leptin expression and function in A/J vs. C57BL/6J mice during diet-induced obesity. *American Journal of Physiology - Endocrinology And Metabolism*, 356–365.

Weinberg, S. E., & Chandel, N. S. (2014). Targeting mitochondria metabolism for cancer therapy. *Nature Chemical Biology*, *11*(1), 9–15. http://doi.org/10.1038/nchembio.1712

Weir, T. L., Manter, D. K., Sheflin, A. M., Barnett, B. A., Heuberger, A. L., & Ryan, E. P. (2013). Stool microbiome and metabolome differences between colorectal cancer patients and healthy adults. *PLoS ONE*, *8*(8). http://doi.org/10.1371/journal.pone.0070803

Wheaton, W. W., Weinberg, S. E., Hamanaka, R. B., Soberanes, S., Sullivan, L. B., Anso, E., … Chandel, N. S. (2014). Metformin inhibits mitochondrial complex I of cancer cells to reduce tumorigenesis. *ELife*, *3*, e02242. http://doi.org/10.7554/eLife.02242

Whelan, F. J., & Surette, M. G. (2017). A comprehensive evaluation of the sl1p pipeline for 16S rRNA gene sequencing analysis. *Microbiome*, *5*, 1–13. http://doi.org/10.1186/s40168-017-0314-2

WHO. (2006). Definition and diagnosis of diabetes mellitus and intermediate hyperglycemia. *Who2*, 50. http://doi.org/ISBN 92 4 159493 4

Wickham, H. (2017). Tidyverse packages - Tidyverse. Retrieved July 29, 2018, from https://www.tidyverse.org/packages/

Wilcock, C., & Bailey, C. J. (1994). Accumulation of metformin by tissues of the normal and diabetic mouse. *Xenobiotica; the Fate of Foreign Compounds in Biological Systems*, *24*(1), 49–57. http://doi.org/10.3109/00498259409043220

World Cancer Research Fund/American Institute for Cancer Research, T. (2018). Diet , nutrition, physical activity and colorectal cancer. Retrieved from www.dietandcancerreport.org

Wu, H., Esteve, E., Tremaroli, V., Khan, M. T., Caesar, R., Mannerås-Holm, L., … Bäckhed, F. (2017). Metformin alters the gut microbiome of individuals with treatment-naive type 2 diabetes, contributing to the therapeutic effects of the drug. *Nature Medicine*, *23*(7), 850–858. http://doi.org/10.1038/nm.4345

Wu, N., Yang, X., Zhang, R., Li, J., Xiao, X., Hu, Y., … Zhu, B. (2013). Dysbiosis signature of fecal microbiota in colorectal cancer patients. *Microbial Ecology*, *66*(2), 462–470. http://doi.org/10.1007/s00248-013-0245-9

Yan, H., & Ajuwon, K. M. (2017). Butyrate modifies intestinal barrier function in IPEC-J2 cells through a selective upregulation of tight junction proteins and activation of the Akt signaling pathway. *PLoS ONE*, *12*(6), 1–20. http://doi.org/10.1371/journal.pone.0179586

Yang, Y.-X., Hennessy, S., & Lewis, J. D. (2004). Insulin therapy and colorectal cancer risk among type 2 diabetes mellitus patients: A systemic review and

meta-analysis. *Gastroenterology*, *127*, 1044–1050. http://doi.org/10.1186/1746-1596-9-91

Yao, C.-A., Ortiz-Vega, S., Sun, Y.-Y., Chien, C.-T., Chuang, J.-H., Lin, Y., … Rico, P. (2017). Association of mSin1 with mTORC2 Ras and Akt reveals a crucial domain on mSin1 involved in Akt phosphorylation, *8*(38), 63392–63404. http://doi.org/10.18632/oncotarget.18818

Yap, F., Craddock, L., & Yang, J. (2011). Mechanism of AMPK suppression of LXR-dependent Srebp-1c transcription. *International Journal of Biological Sciences*, *7*(5), 645–650. http://doi.org/10.7150/ijbs.7.645

Ye, J. (2013). Improving insulin sensitivity with HDAC inhibitor. *Diabetes*, *62*(3), 685–687. http://doi.org/10.2337/db12-1354

Yoon, J. C., Puigserver, P., Chen, G., Donovan, J., Wu, Z., Rhee, J., … Spiegelman, B. M. (2001). Control of hepatic gluconeogenesis through the transcriptional coactivator PGC-1. *Nature*, *413*(6852), 131–138. http://doi.org/10.1038/35093050

Yu, J., Feng, Q., Wong, S. H., Zhang, D., Yi Liang, Q., Qin, Y., … Wang, J. (2017). Metagenomic analysis of faecal microbiome as a tool towards targeted non-invasive biomarkers for colorectal cancer. *Gut*, *66*(1), 70–78. http://doi.org/10.1136/gutjnl-2015-309800

Zaafar, D. K., Zaitone, S. A., & Moustafa, Y. M. (2014). Role of metformin in suppressing 1,2-dimethylhydrazine-induced colon cancer in diabetic and non-diabetic mice: Effect on tumor angiogenesis and cell proliferation. *PLoS*

ONE, *9*(6), 1–12. http://doi.org/10.1371/journal.pone.0100562

Zeller, G., Tap, J., Voigt, A. Y., Sunagawa, S., Kultima, J. R., Costea, P. I., … Bork, P. (2014). Potential of fecal microbiota for early-stage detection of colorectal cancer. *Molecular Systems Biology*, *10*(11), 766–766. http://doi.org/10.15252/msb.20145645

Zhan, Y., Ginanni, N., Tota, M. R., Wu, M., Bays, N. W., Richon, V. M., … Krauss, S. (2008). Control of cell growth and survival by enzymes of the fatty acid synthesis pathway in HCT-116 colon cancer cells. *Human Cancer Biology*, *14*(18), 5735–5743. http://doi.org/10.1158/1078-0432.CCR-07-5074

Zhang, L., Li, J., Young, L. H., & Caplan, M. J. (2006). AMP-activated protein kinase regulates the assembly of epithelial tight junctions. *Proceedings of the National Academy of Sciences*, *103*(46), 17272–17277. http://doi.org/10.1073/pnas.0608531103

Zhang, X., Zhao, Y., Xu, J., Xue, Z., Zhang, M., Pang, X., … Zhao, L. (2015). Modulation of gut microbiota by berberine and metformin during the treatment of high-fat diet-induced obesity in rats. *Scientific Reports*, *5*(August), 14405. http://doi.org/10.1038/srep14405

Zhang, Z.-J., Zheng, Z.-J., Kan, H., Song, Y., Cui, W., Zhao, G., & Kip, K. E. (2011). Reduced risk of colorectal cancer with metformin therapy in patients with type 2 diabetes: a meta-analysis. *Diabetes Care*, *34*(10), 2323–8. http://doi.org/10.2337/dc11-0512

Zhao, G., Liu, J. fu, Nyman, M., & Jönsson, J. Å. (2007). Determination of short-chain fatty acids in serum by hollow fiber supported liquid membrane extraction coupled with gas chromatography. *Journal of Chromatography B: Analytical Technologies in the Biomedical and Life Sciences*, *846*(1–2), 202–208. http://doi.org/10.1016/j.jchromb.2006.09.027

Zheng, B., & Cantley, L. C. (2007). Regulation of epithelial tight junction assembly and disassembly by AMP-activated protein kinase. *Proceedings of the National Academy of Sciences*, *104*(3), 819–822. http://doi.org/10.1073/pnas.0610157104

Zhou, D., Pan, Q., Shen, F., Cao, H. X., Ding, W. J., Chen, Y. W., & Fan, J. G. (2017). Total fecal microbiota transplantation alleviates high-fat diet-induced steatohepatitis in mice via beneficial regulation of gut microbiota. *Scientific Reports*, *7*(1), 1–11. http://doi.org/10.1038/s41598-017-01751-y

Zhou, G., Myers, R., Li, Y., Chen, Y., Shen, X., Fenyk-Melody, J., … Moller, D. E. (2001). Role of AMP-activated protein kinase in mechanism of metformin action. *Journal of Clinical Investigation*, *108*(8), 1167–1174. http://doi.org/10.1172/JCI200113505

Zhou, M., Xia, L., & Wang, J. (2007). Metformin transport by a newly clonsed proton-stimulated organic cation transporter (plasma membrane monoamine transporter) expresed in human intestine. *Drug Metabolism and Disposition: The Biological Fate of Chemicals*, *35*(10), 1956–1962. http://doi.org/10.1111/j.1743-6109.2008.01122.x.Endothelial